

# Evidence for unresolved point sources in the GeV gamma-ray excess

Tracy Slatyer

based on arXiv:1506.05124 (submitted to Science)

with Samuel Lee, Mariangela Lisanti, Ben Safdi and Wei Xue



Accurate Astrophysics, Correct Cosmology

London, England

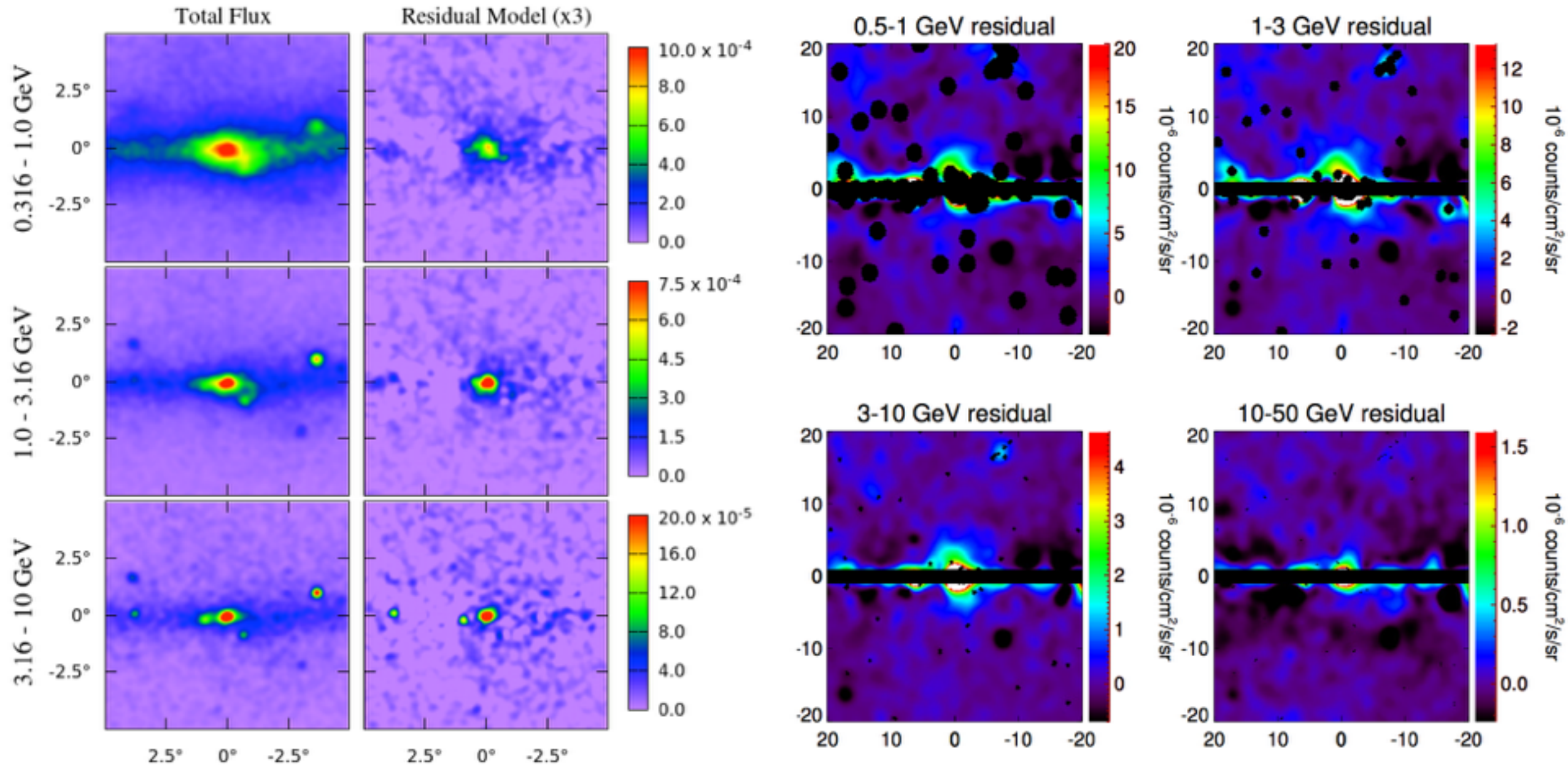
14 July 2015

# Outline

- **BACKGROUND:** a primer on the GeV gamma-ray excess
  - Properties that suggest a dark matter origin
  - Astrophysical alternatives
- **METHOD:** template fitting for models with non-Poissonian statistics
- **RESULTS:** evidence for a (peculiar?) point source population largely responsible for the excess

# The GeV gamma-ray excess

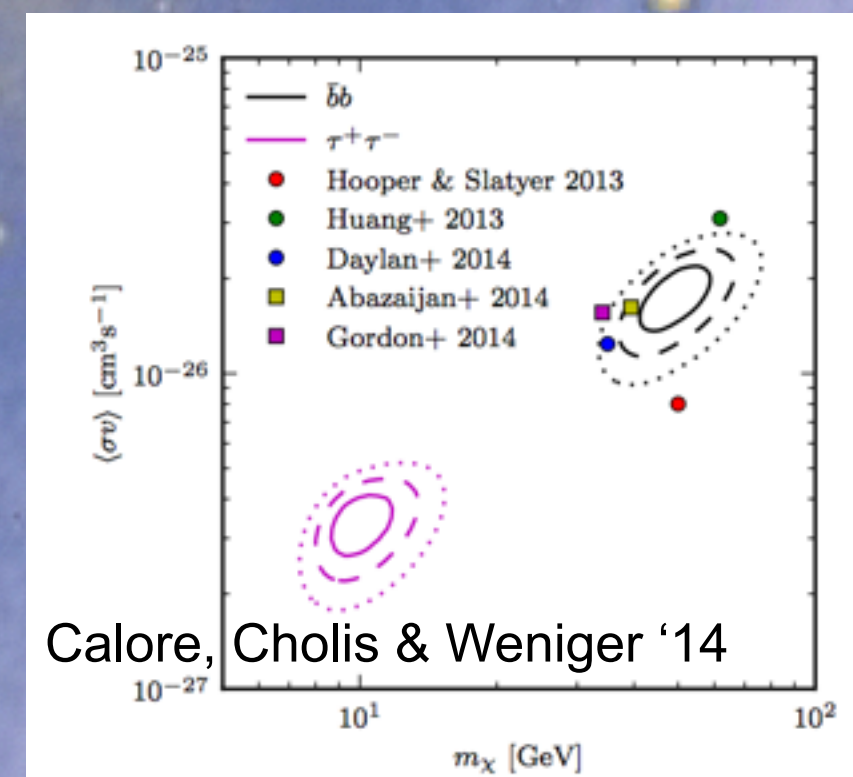
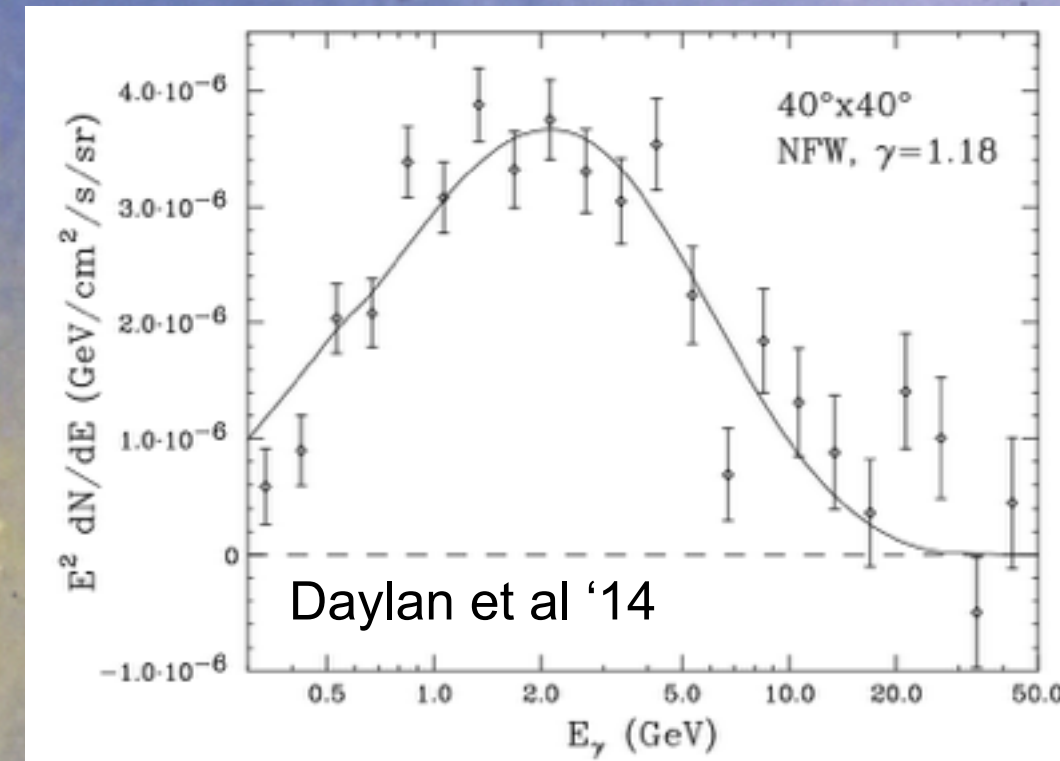
- Excess of  $\sim 1\text{-}3$  GeV gamma rays in the (extended) central region of the Milky Way, spatially concentrated at the Galactic Center, identified as a possible signature of dark matter annihilation.
- Discovered in public data from the Fermi Gamma-Ray Space Telescope
  - First in the Galactic Center (Goodenough & Hooper 09).
  - Later extending to higher latitudes (Hooper & TRS 13).
  - Existence and properties have been confirmed in both regions by multiple independent groups.
- Highly significant, not a statistical fluctuation.
  - Tens of thousands of photons
  - Can contribute up to  $\sim 30\%$  of the total photon flux (at the peak of the excess, and near the Galactic Center)



- Generally consistent with spherical symmetry around the Galactic Center (can exclude stretches by more than  $\sim 20\%$  along the Galactic plane).
- Power-law slope (in inferred flux per unit volume, assuming spherical symmetry)  $\sim r^{-2.2-2.8}$ . If photons originate from DM annihilation (scaling as density squared), corresponds to a small- $r$  DM density profile slightly steeper than standard Navarro-Frenk-White (NFW) profile, proportional to  $r^{-1.1-1.4}$  (compared to  $1/r$  for standard NFW).
- Appears centered on Sgr A\*, the black hole at the center of the Milky Way.
- Extends out to at least 10 degrees ( $\sim 1.5$  kpc) from the GC.

# Dark matter...

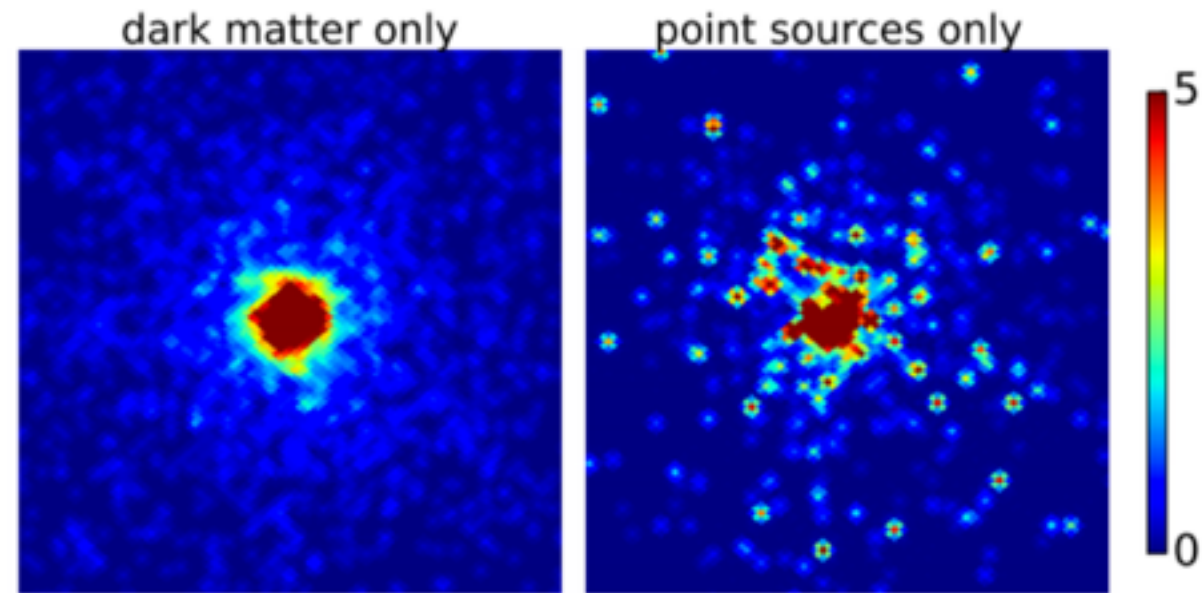
- Naturally explains:
  - The shape of the spectrum - well fit by fairly light DM ( $\sim 100$  GeV or less) annihilating to a range of Standard Model particles.
  - Apparent absence of spatial variation in the spectrum of the excess.
  - The  $\sim$ spherical morphology of the signal.
  - The profile: steeply peaked at the Galactic Center but extending out to (at least) 10 degrees.
- Required annihilation cross section lines up with long-standing predictions for the “thermal relic” scenario.



# ... or astrophysics?

- MILLISECOND PULSARS (first proposed by Abazajian 1011.4275):
  - Spectrum of observed MSPs matches excess well at energies  $> 1$  GeV.
  - MSPs originate from binary systems, can naturally explain steep slope of profile.
  - BUT: sphericity unexpected, and required luminosity function different than inferred elsewhere in the Galaxy.
- COSMIC RAY OUTFLOWS:
  - Almost certainly have occurred in the past - but challenges in simultaneously matching morphology + spectrum for excess (Carlson & Profumo 1405.7685, Petrovic, Serpico & Zaharijas 1411.2980, Cholis et al 1506.05119).

# Point sources vs diffuse emission



- Setting aside questions of theoretical plausibility, what can the data tell us?
- Central question: can we distinguish smooth diffuse emission from a population of point sources?
- The hope: spatial distribution of photons should be different (in detail) between these two cases.
- Of course, depends on luminosity function of sources. Very large number of very faint sources = diffuse emission.

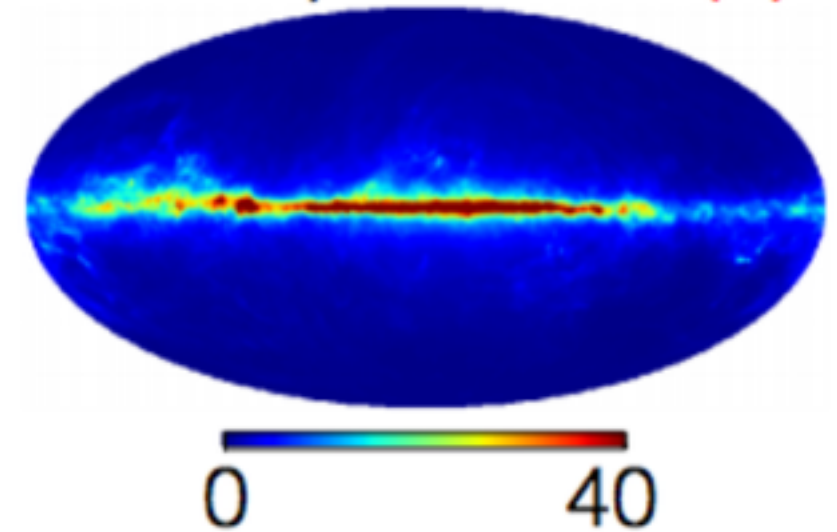
# Template fitting

- Model the photon counts (within some energy bin) as a linear combination of background and signal spatial templates  $\mu_{p,l}$ .
- Templates obtained by taking physical models or simple ansatzes, applying exposure and smoothing by Fermi point spread function (PSF).
- Given model (as a function of coefficients  $\theta=\{\alpha_l\}$ ), overall likelihood is given by the product of the Poisson likelihoods for each (spatial) pixel.
- Maximize likelihood with respect to  $\theta$  parameters (frequentist) or compute posterior probabilities (Bayesian).

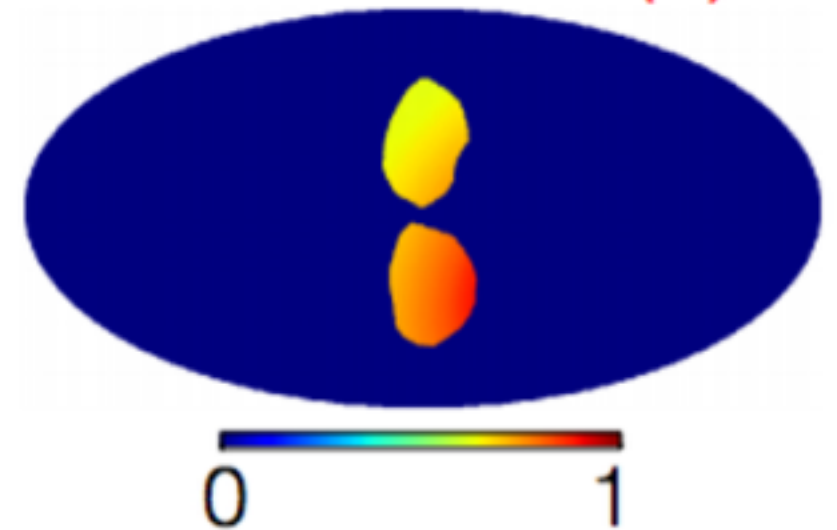
$$\mu_p = \sum_l \alpha_l \mu_{p,l} \quad p_k^{(p)} = \frac{(\mu_p)^k e^{-\mu_p}}{k!}$$

$$p(d|\theta, \mathcal{M}) = \prod_p p_{n_p}^{(p)}(\theta)$$

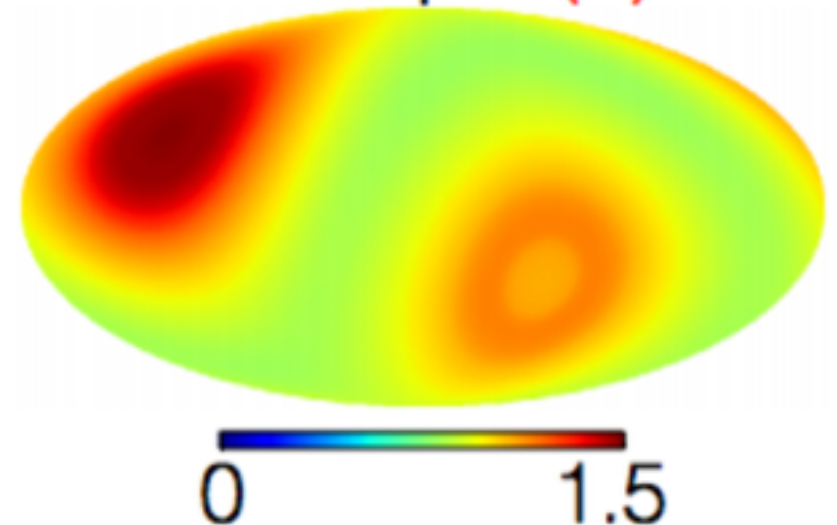
Fermi p6 diffuse (1)

 $\mu_{p,1}$ 

Fermi bubbles (1)

 $\mu_{p,2}$ 

Isotropic (1)

 $\mu_{p,3}$ 

# Non-Poissonian templates

- Known sources - can model them, or mask their locations.
- Unknown sources - remain agnostic as to their location, create likelihood including non-Poissonian statistics for photon counts, i.e. Non-Poissonian Template Fitting (NPTF).
- Method worked out and applied to gamma-ray data by Malyshev & Hogg '11, focusing on isotropically distributed PSs. Need to compute:

expected number  
of m-photon  
sources in a pixel

$$x_m = \frac{\Omega_{\text{pix}}}{4\pi} \int_0^\infty dS \frac{dN}{dS}(S) \int df \rho(f) \frac{(fS)^m}{m!} e^{-fS}.$$

generating function  
for point source  
population

$$\sum_{k=0}^{\infty} p_k t^k = \exp \left[ \sum_{m=1}^{\infty} x_m (t^m - 1) \right] \equiv P(t)$$

For comparison, in Poisson case:

$$\mathcal{P}^{(p)}(t) = \exp[\mu_p(t - 1)]$$

Overall generating function  $\mathcal{P}^{(p)}(t)$  is given by product of generating functions for each template. Then:

pixel likelihood

$$p_k^{(p)} = \frac{1}{k!} \left. \frac{d^k \mathcal{P}^{(p)}}{dt^k} \right|_{t=0}$$

# Non-Poissonian templates

- Known sources - can model them, or mask their locations.
- Unknown sources - remain agnostic as to their location, create likelihood including non-Poissonian statistics for photon counts, i.e. Non-Poissonian Template Fitting (NPTF).
- Method worked out and applied to gamma-ray data by Malyshev & Hogg '11, focusing on isotropically distributed PSs. Need to compute:

expected number  
of m-photon  
sources in a pixel

$$x_m = \frac{\Omega_{\text{pix}}}{4\pi} \int_0^\infty dS \frac{dN}{dS}(S) \int df \rho(f) \frac{(fS)^m}{m!} e^{-fS}.$$

Number of sources providing S counts,  
including position-dependent normalization

generating function  
for point source  
population

$$\sum_{k=0}^{\infty} p_k t^k = \exp \left[ \sum_{m=1}^{\infty} x_m (t^m - 1) \right] \equiv P(t)$$

For comparison, in Poisson case:

$$\mathcal{P}^{(p)}(t) = \exp[\mu_p(t - 1)]$$

Overall generating function  $\mathcal{P}^{(p)}(t)$  is given by product of generating functions for each template. Then:

pixel likelihood

$$p_k^{(p)} = \frac{1}{k!} \left. \frac{d^k \mathcal{P}^{(p)}}{dt^k} \right|_{t=0}$$

# Non-Poissonian templates

- Known sources - can model them, or mask their locations.
- Unknown sources - remain agnostic as to their location, create likelihood including non-Poissonian statistics for photon counts, i.e. Non-Poissonian Template Fitting (NPTF).
- Method worked out and applied to gamma-ray data by Malyshev & Hogg '11, focusing on isotropically distributed PSs. Need to compute:

expected number  
of m-photon  
sources in a pixel

$$x_m = \frac{\Omega_{\text{pix}}}{4\pi} \int_0^\infty dS \frac{dN}{dS}(S) \int df \rho(f) \frac{(fS)^m}{m!} e^{-fS}.$$

df integral accounts for PSF, weighting function determined by Monte Carlo

Number of sources providing S counts,  
including position-dependent normalization

generating function  
for point source  
population

$$\sum_{k=0}^{\infty} p_k t^k = \exp \left[ \sum_{m=1}^{\infty} x_m (t^m - 1) \right] \equiv P(t)$$

For comparison, in Poisson case:

$$\mathcal{P}^{(p)}(t) = \exp[\mu_p(t - 1)]$$

Overall generating function  $\mathcal{P}^{(p)}(t)$  is given by product of generating functions for each template. Then:

pixel likelihood

$$p_k^{(p)} = \frac{1}{k!} \left. \frac{d^k \mathcal{P}^{(p)}}{dt^k} \right|_{t=0}$$

# Non-Poissonian templates

- Known sources - can model them, or mask their locations.
- Unknown sources - remain agnostic as to their location, create likelihood including non-Poissonian statistics for photon counts, i.e. Non-Poissonian Template Fitting (NPTF).
- Method worked out and applied to gamma-ray data by Malyshev & Hogg '11, focusing on isotropically distributed PSs. Need to compute:

df integral accounts for PSF, weighting function determined by Monte Carlo

expected number of m-photon sources in a pixel

$$x_m = \frac{\Omega_{\text{pix}}}{4\pi} \int_0^\infty dS \frac{dN}{dS}(S) \int df \rho(f) \frac{(fS)^m}{m!} e^{-fS}.$$

Number of sources providing S counts, including position-dependent normalization

Poisson draw for actual number of photons, given f S expected

generating function for point source population

$$\sum_{k=0}^{\infty} p_k t^k = \exp \left[ \sum_{m=1}^{\infty} x_m (t^m - 1) \right] \equiv P(t)$$

For comparison, in Poisson case:

$$\mathcal{P}^{(p)}(t) = \exp[\mu_p(t - 1)]$$

Overall generating function  $\mathcal{P}^{(p)}(t)$  is given by product of generating functions for each template. Then:

pixel likelihood

$$p_k^{(p)} = \frac{1}{k!} \left. \frac{d^k \mathcal{P}^{(p)}}{dt^k} \right|_{t=0}$$

# Fitting procedure

- Use energy range ~2-12 GeV - good angular resolution (degrades at lower energies), includes peak of GeV excess.
- Use data with a quality cut to improve angular resolution.
- Use Fermi Pass 7 data up to December 2013 (results confirmed with both up-to-date Pass 7 and Pass 8 data, which have different event reconstruction pipelines).
- Where required, model source count function as a broken power law - four parameters, including overall normalization.

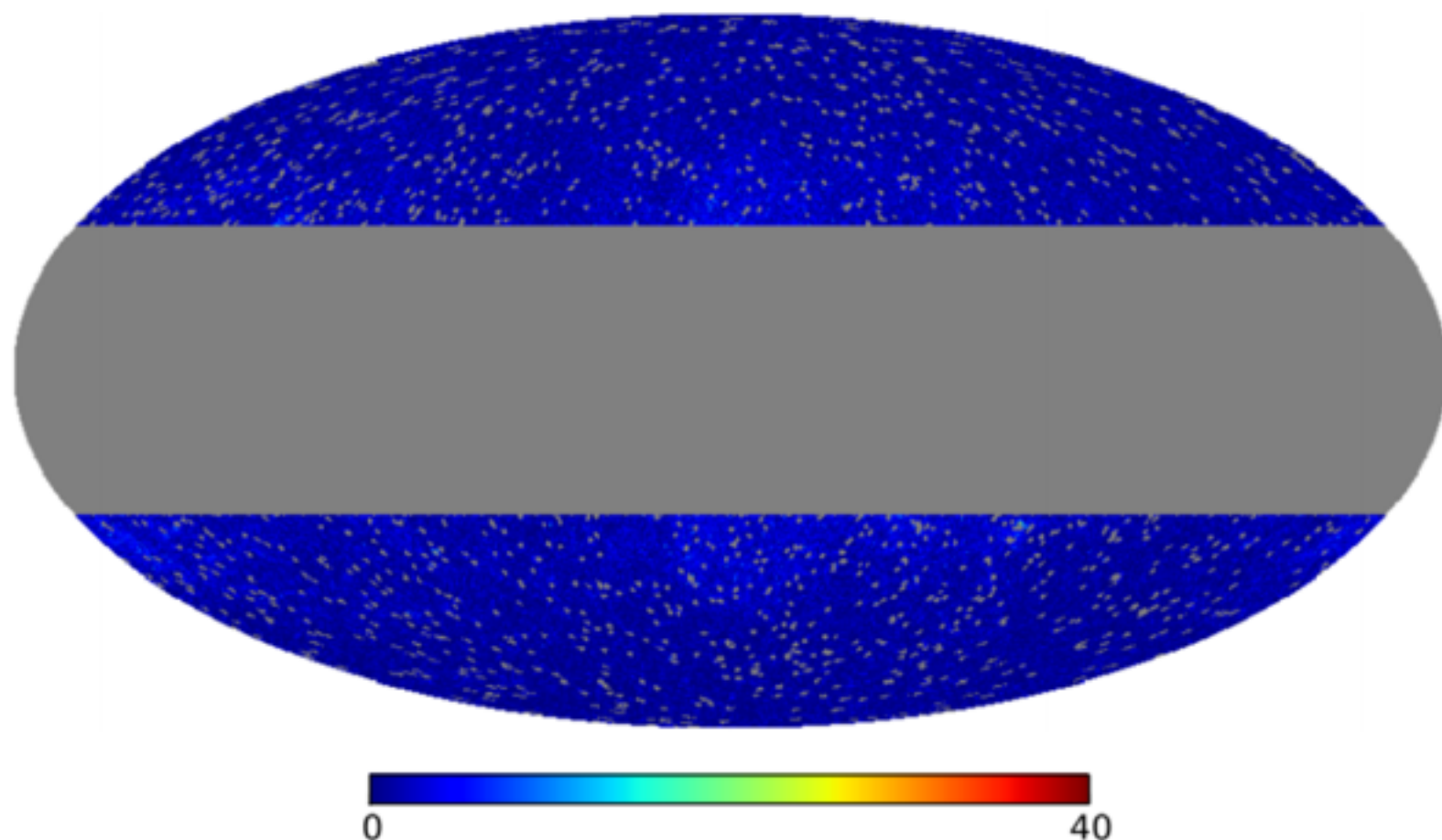
follows a spatial template

$$\frac{dN_p(S)}{dS} = A_p \begin{cases} \left(\frac{S}{S_b}\right)^{-n_1} & S \geq S_b \\ \left(\frac{S}{S_b}\right)^{-n_2} & S < S_b \end{cases}$$

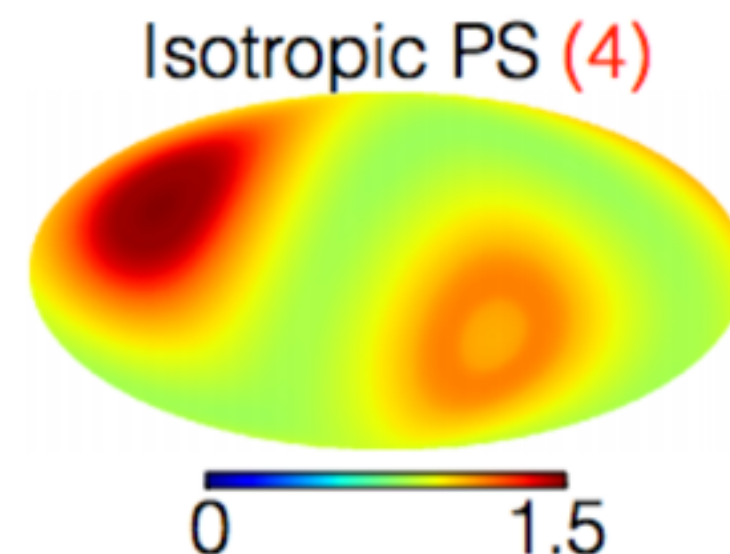
- Fits always include diffuse model, Fermi Bubbles and isotropic diffuse templates, + other templates as appropriate.
- In some analyses we mask the known point sources (based on the Fermi LAT 4-Year Point Source Catalog, 3FGL); where this is done, the mask radius is just under 1 degree (formally,  $5\sigma$  where  $\sigma$  is the approximate Gaussian width of the PSF for the lowest-energy photons in the bin).

# High-latitude analysis

mask region within 30 degrees of Galactic plane



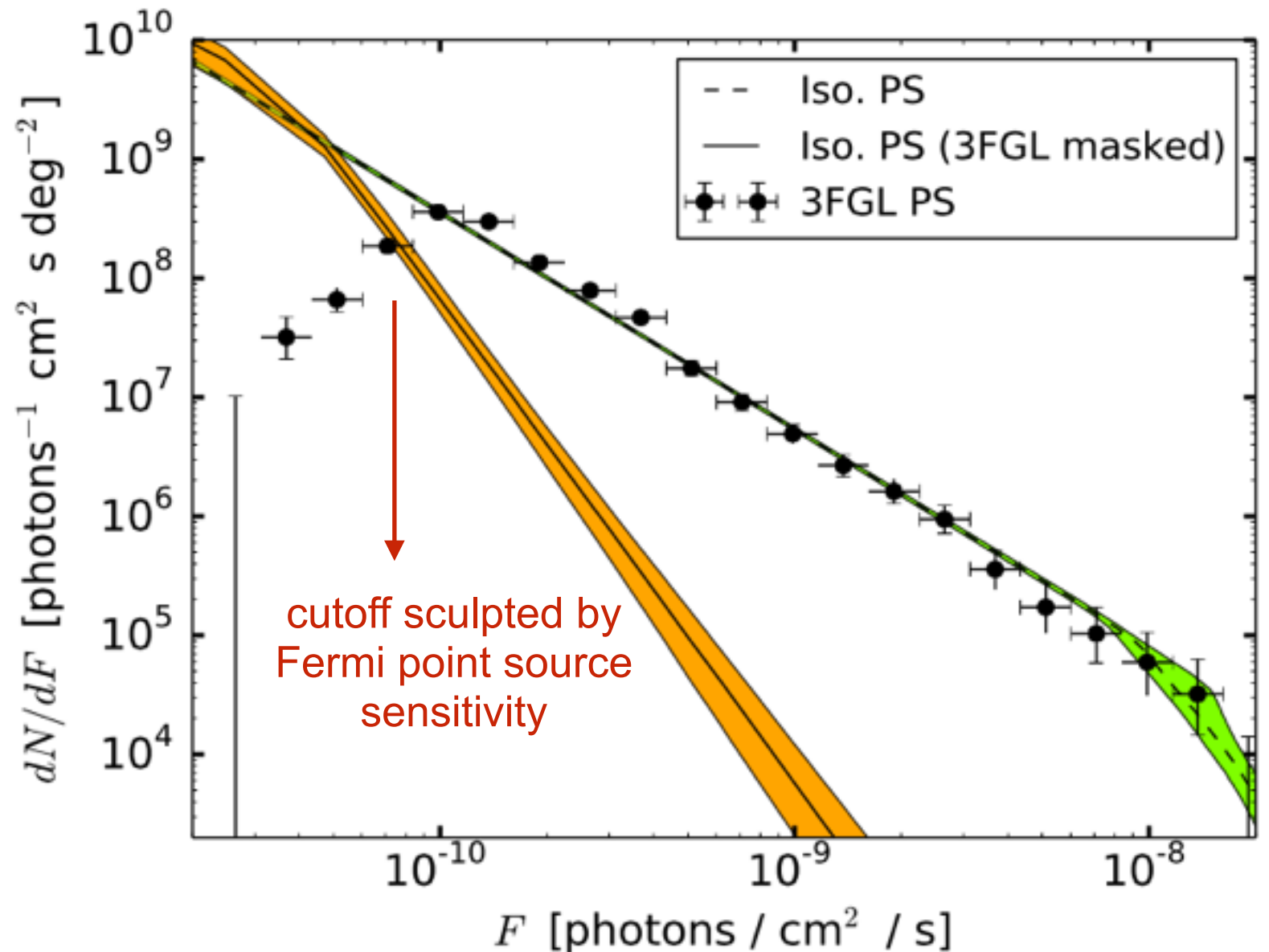
add isotropic non-Poissonian point source template (4 d.o.f)



- Test method first at high latitude ( $|b| > 30^\circ$ ), searching for unresolved uniformly distributed (isotropic) sources.
- Previously studied by Malyshev & Hogg '11 using a similar approach (unbinned likelihood rather than pixel-based likelihood); we find consistent results, also consistent with estimate of isotropic diffuse background from Ackermann et al 1410.3696.

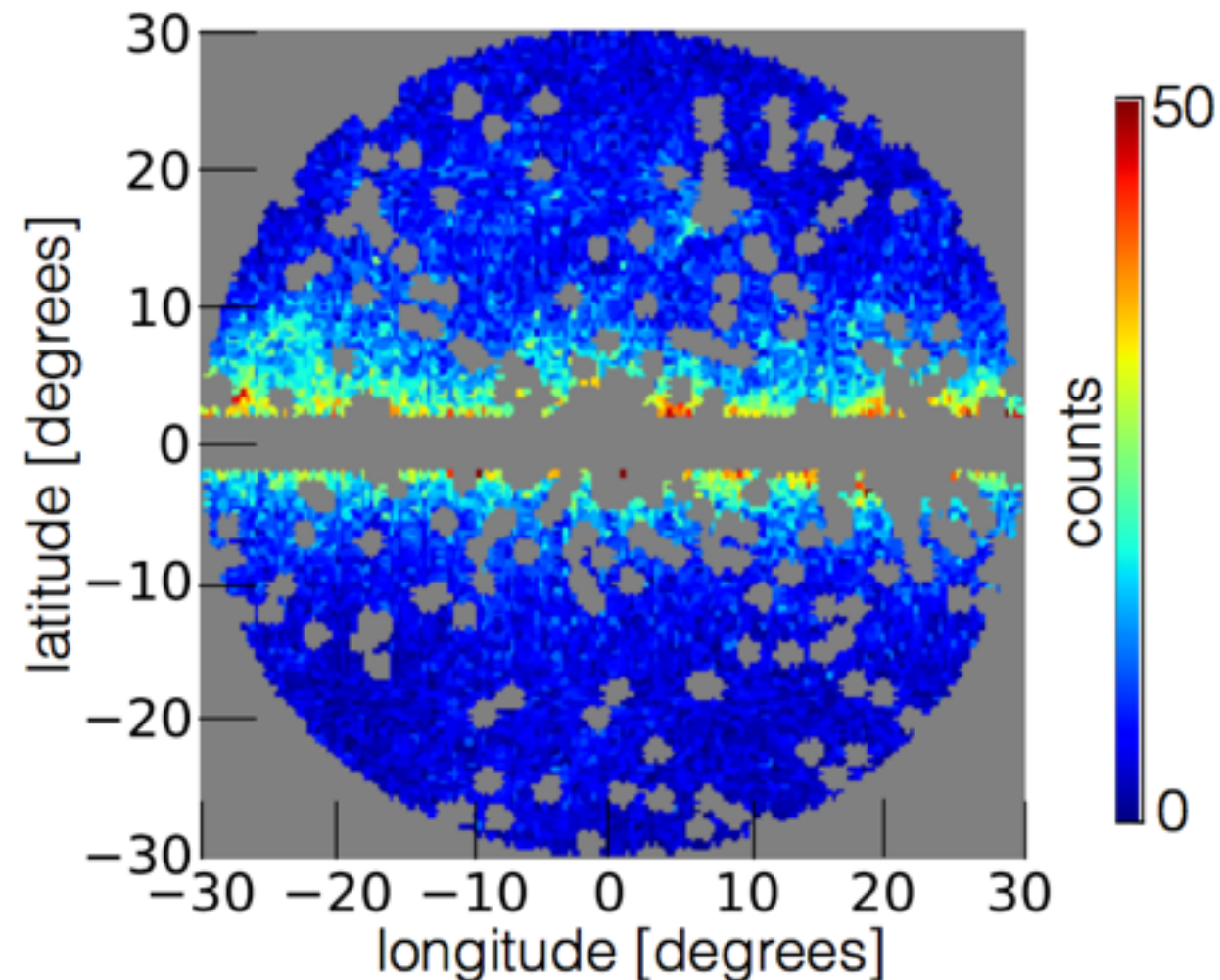
# High-latitude results

- 3FGL PS = known sources in this region.
- Green line = reconstructed source count function without masking sources.
- Orange line = source count function when all known sources are masked.
- Low-luminosity slope of source count function is recovered even when all sources are masked.



Masked (unmasked) analysis finds that 47% (55%) of the isotropic gamma-ray background is due to (resolved and unresolved) point sources.

# Inner Galaxy (IG) analysis



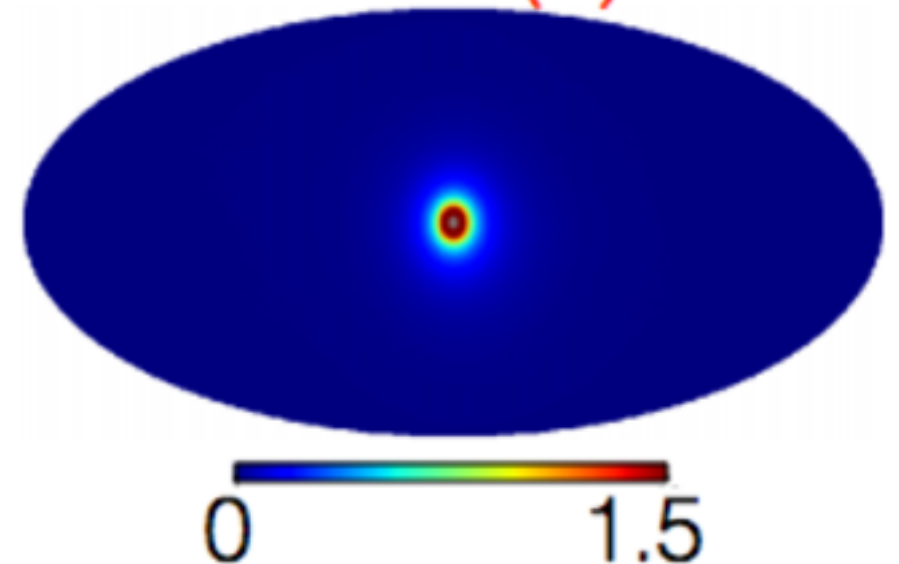
- Fit region is within 30 degree radius of Galactic Center, masking the region within 2 degrees of the plane.
- Results shown in terms of smaller region, within 10 degree radius of the center.

# Signal templates

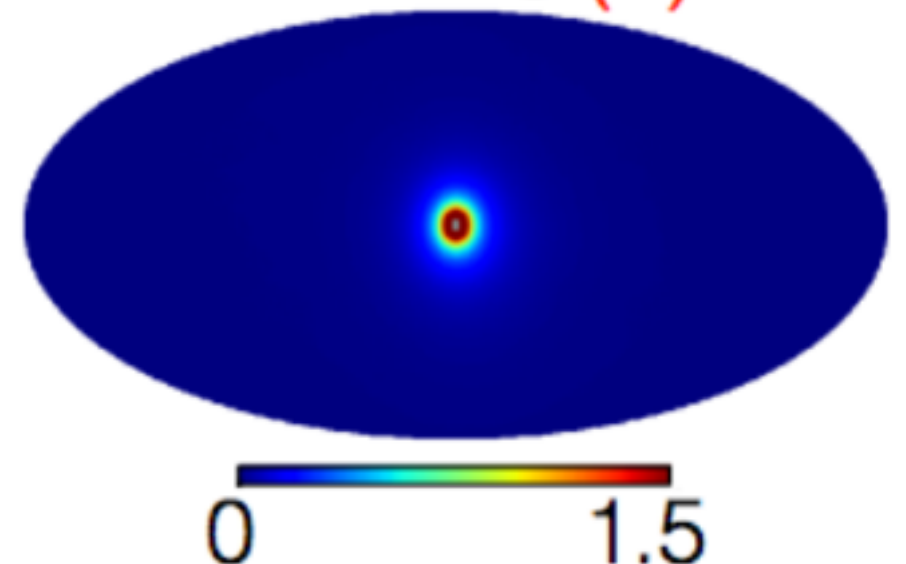
- In addition to high-latitude templates, include:
  - DM annihilation template corresponding to a modified NFW profile scaling as  $r^{-1.25}$  at small  $r$ , squared and projected along the line of sight. Labeled “NFW DM”. 1 extra parameter (normalization).
  - Point source (PS) template with the same overall spatial distribution as “NFW DM” template, but non-Poissonian statistics. Labeled “NFW PS”. 4 extra parameters (normalization + source count function).

new templates

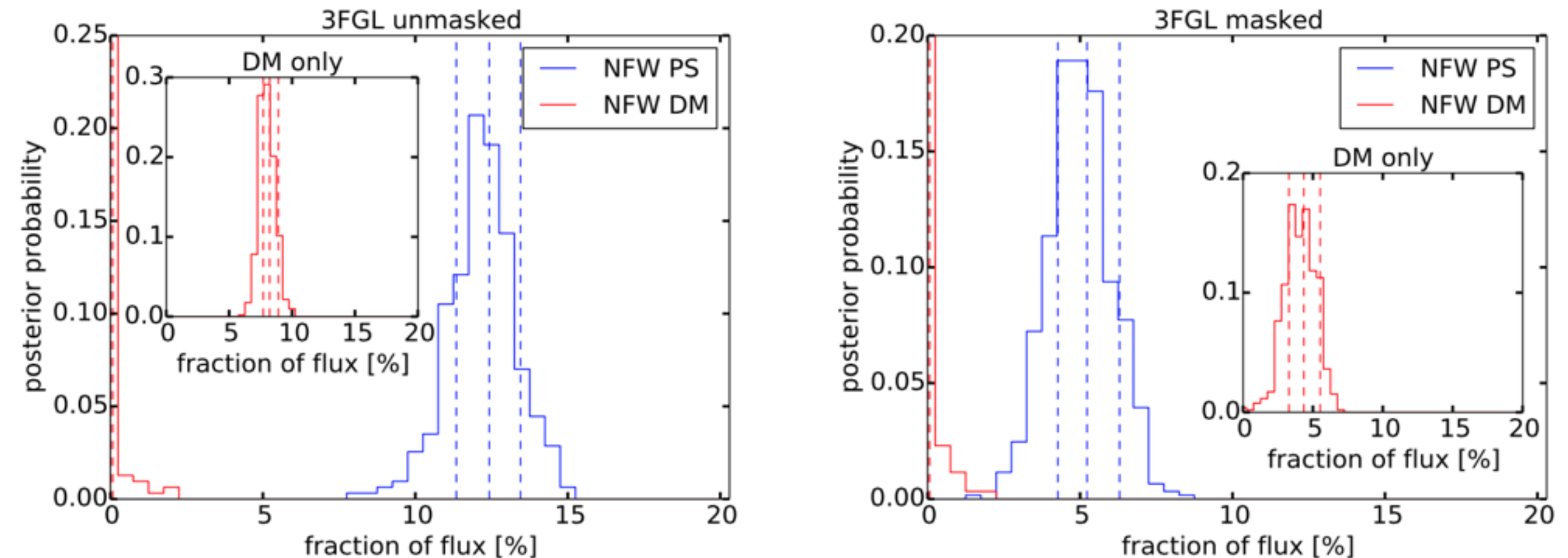
NFW (1)



NFW PS (4)



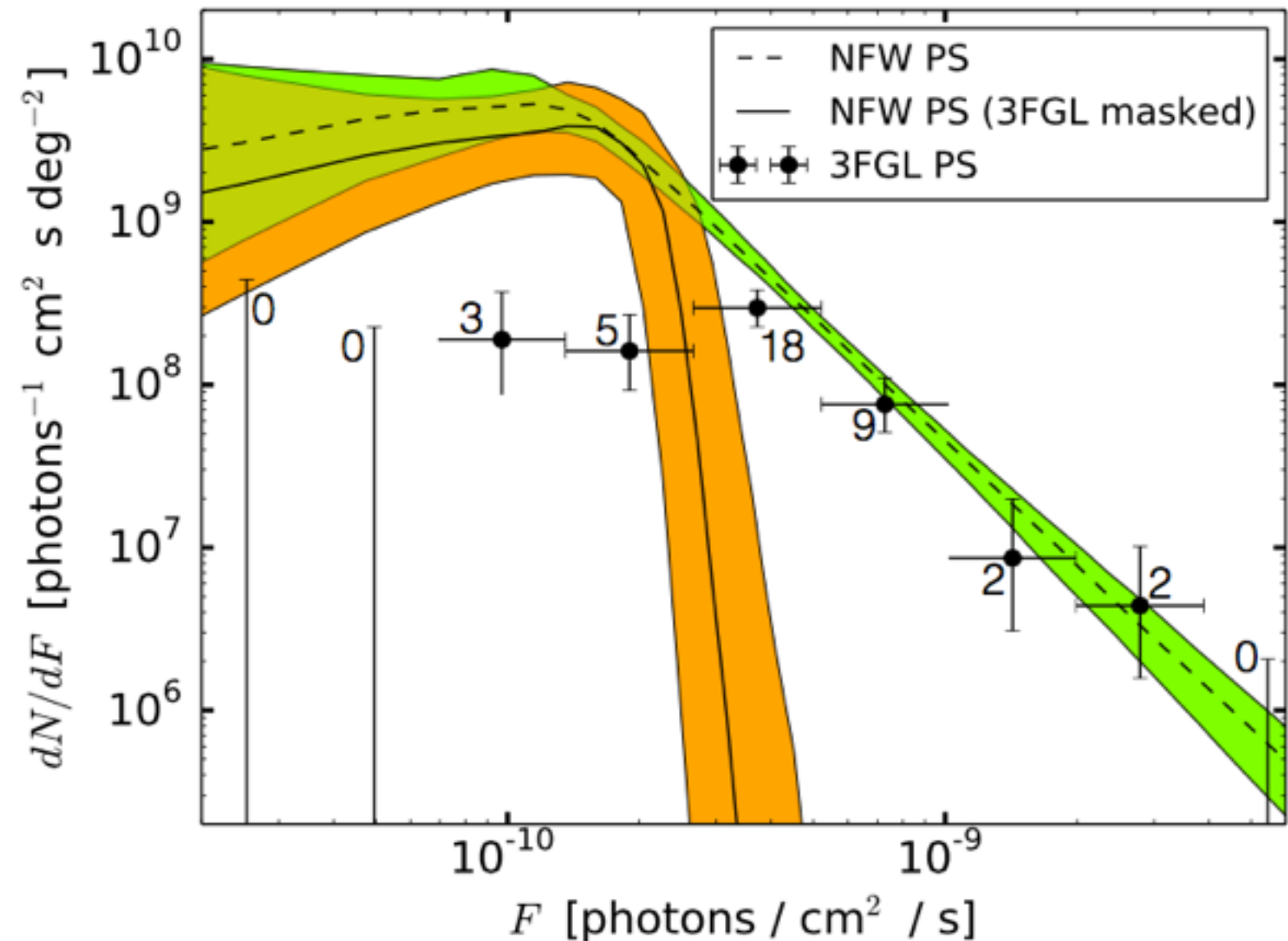
# Inner Galaxy results



- Plots show flux fractions attributed to templates over region within 10 degrees of GC, more than 2 degrees from Galactic plane (including masked areas).
- First: include only NFW DM, not NFW PS - cross-check that we reproduce results from previous studies with Poissonian template fitting.
- Second: include both templates. NFW PS absorbs full flux otherwise attributed to NFW DM.

# The source count function

- High-flux end of reconstructed source count function reproduces 3FGL sources (in unmasked analysis).
- Low-flux end prefers quite flat source count function (in  $dN/dF$ ).
- Due to this flat source-count function, flux is strongly dominated by sources near threshold.
- Excess (in this region) can be explained by  $\sim 203_{-68}^{+109}$  PSs.
- Suggests  $O(1000)$  sources to explain the whole excess.
- Half the flux coming from PSs with above  $\sim 1.7 \times 10^{-10}$  photons/cm<sup>2</sup>/s (in this energy bin) - close to threshold!

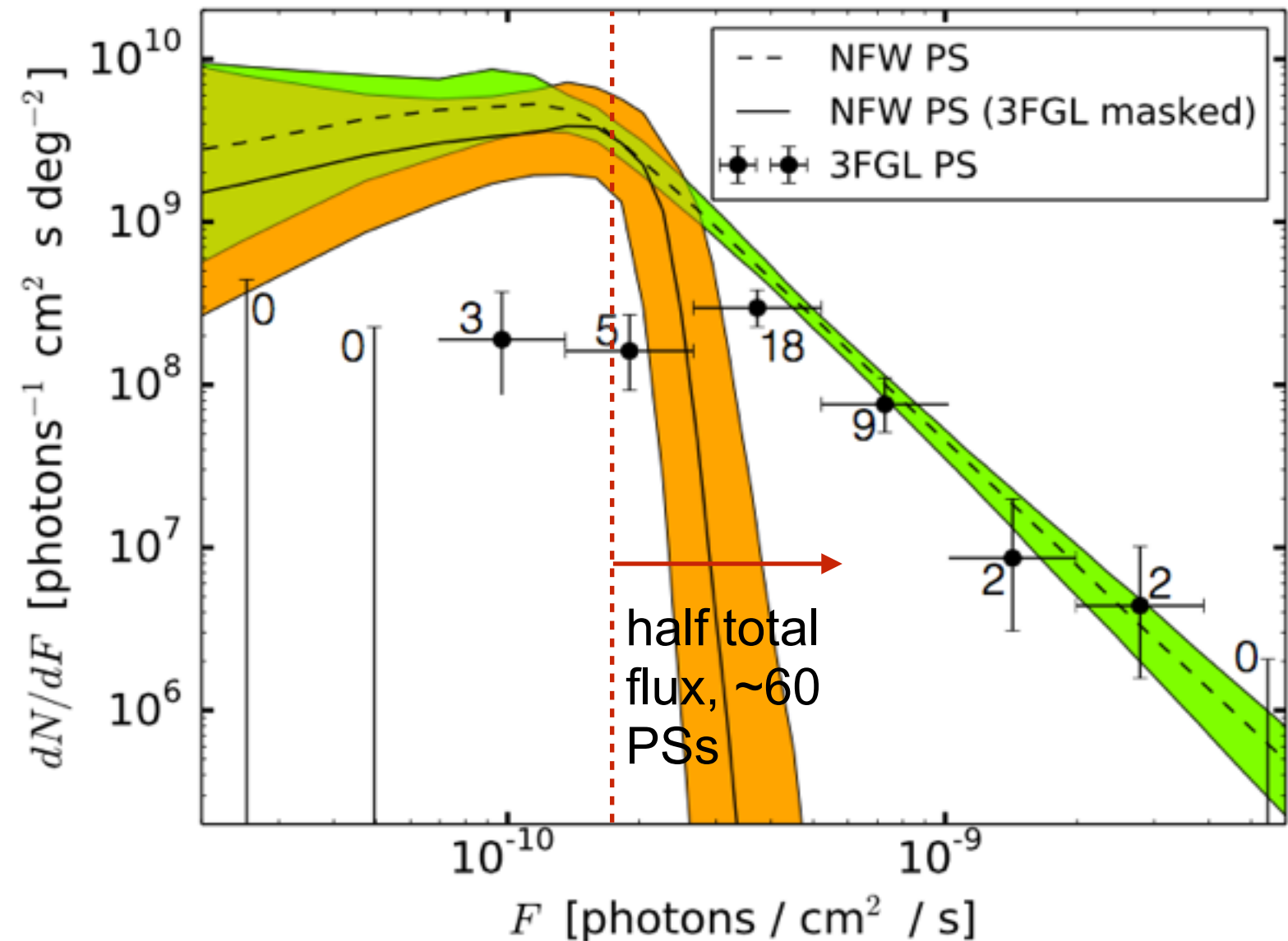


$$F_b = \begin{cases} 1.48_{-0.43}^{+0.41} \text{ unmasked} \\ 2.16_{-0.43}^{+0.64} \text{ masked} \end{cases} \times 10^{-10} \text{ photons/cm}^2/\text{s}.$$

$$n_2 = \begin{cases} -0.57_{-0.85}^{+1.11} \text{ unmasked} \\ -0.47_{-0.93}^{+0.76} \text{ masked} \end{cases}$$

# The source count function

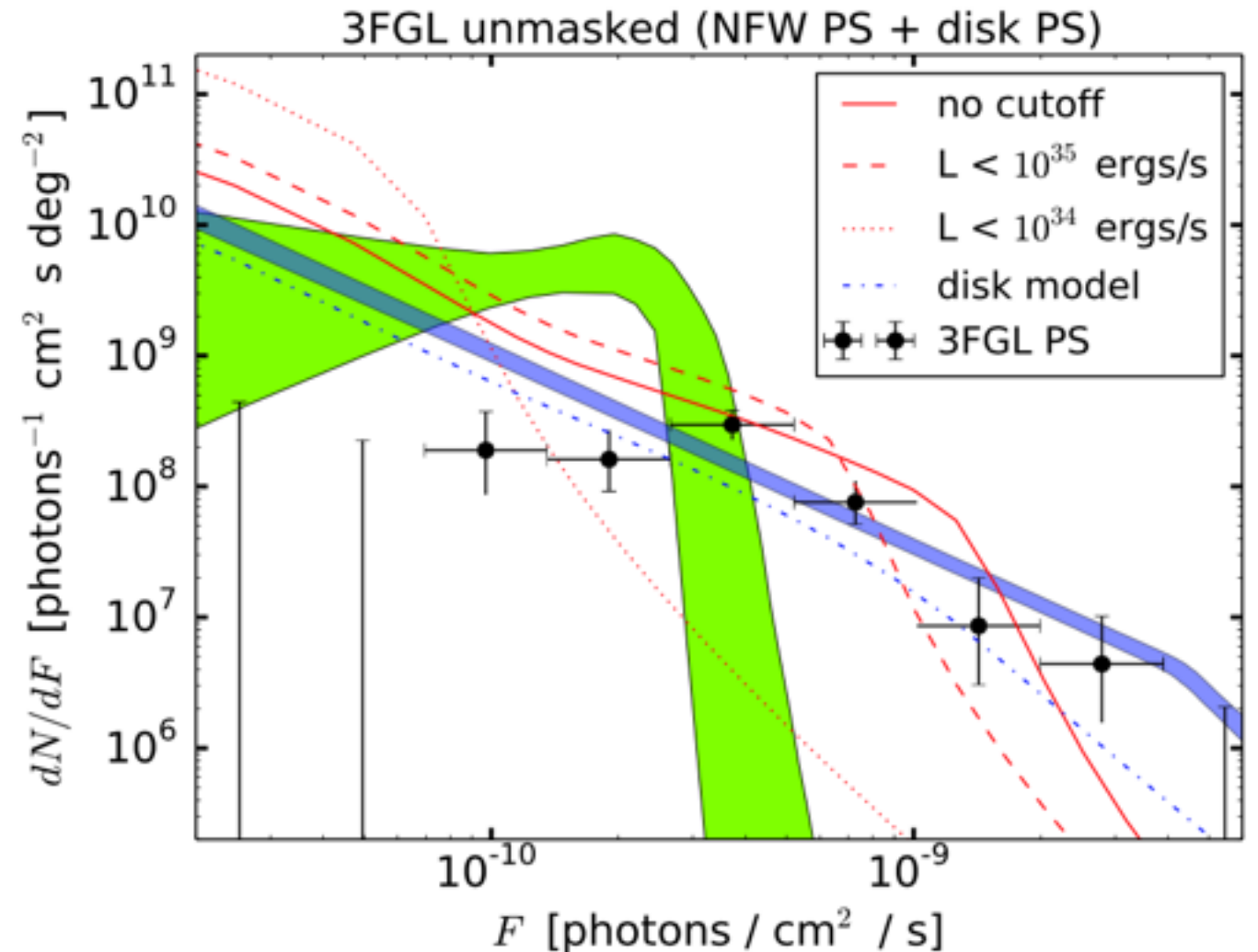
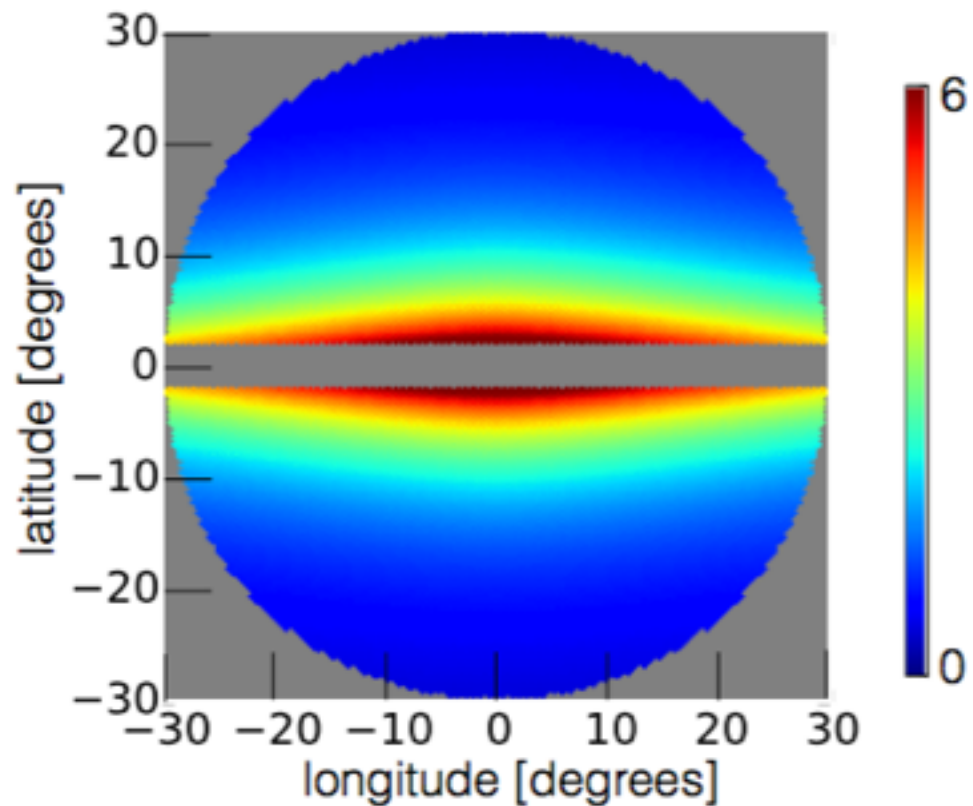
- High-flux end of reconstructed source count function reproduces 3FGL sources (in unmasked analysis).
- Low-flux end prefers quite flat source count function (in  $dN/dF$ ).
- Due to this flat source-count function, flux is strongly dominated by sources near threshold.
- Excess (in this region) can be explained by  $\sim 203^{+109}_{-68}$  PSs.
- Suggests  $O(1000)$  sources to explain the whole excess.
- Half the flux coming from PSs with above  $\sim 1.7 \times 10^{-10}$  photons/cm<sup>2</sup>/s (in this energy bin) - close to threshold!



$$F_b = \begin{cases} 1.48^{+0.41}_{-0.43} & \text{unmasked} \\ 2.16^{+0.64}_{-0.43} & \text{masked} \end{cases} \times 10^{-10} \text{ photons/cm}^2/\text{s}.$$

$$n_2 = \begin{cases} -0.57^{+1.11}_{-0.85} & \text{unmasked} \\ -0.47^{+0.76}_{-0.93} & \text{masked} \end{cases}$$

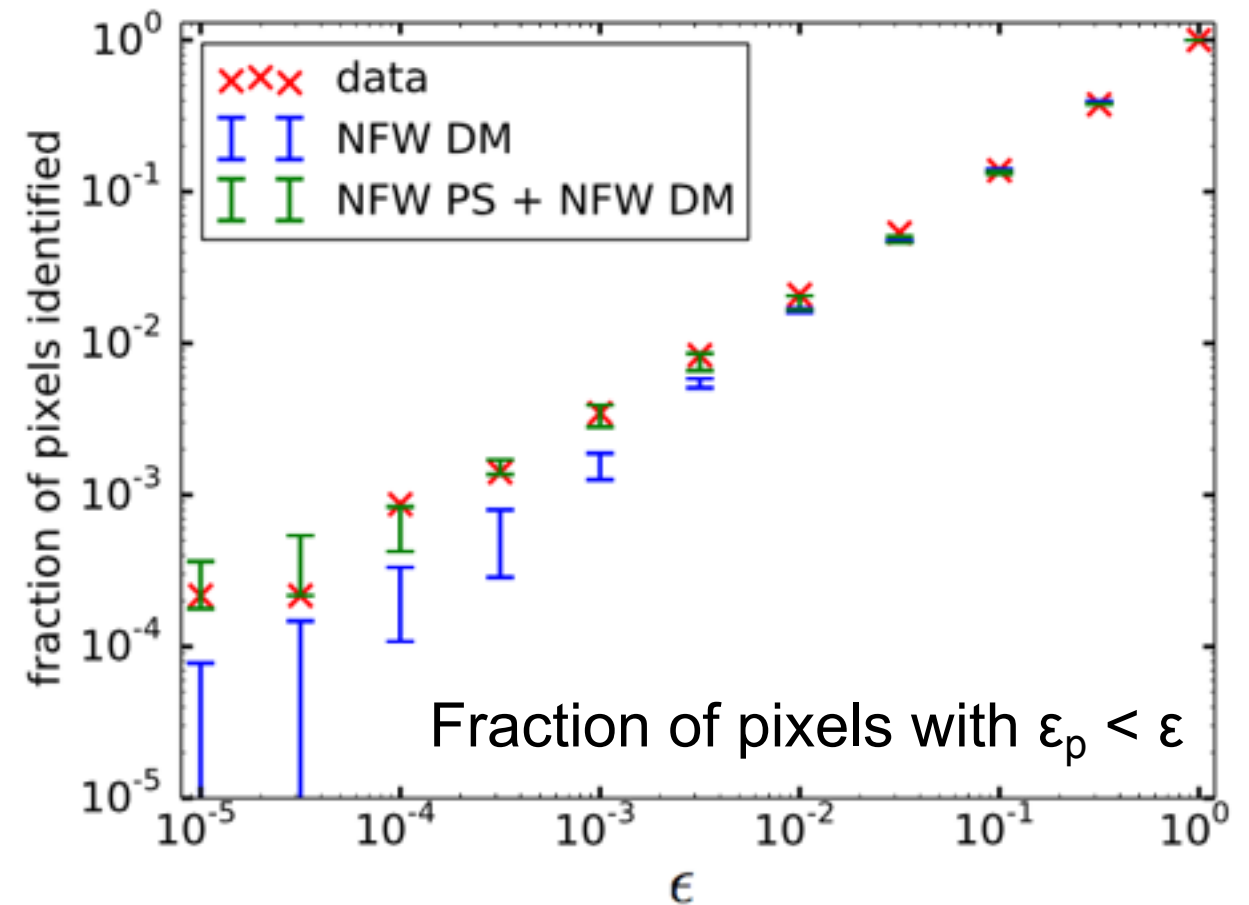
# Adding disk PSs



- Alternative to masking is to model 3FGL sources.
- First simple attempt: add a PS template corresponding to thick-disk distribution, consistent with distribution of observed pulsars.
- Thick-disk distribution largely absorbs known sources - NFW PS template appears to prefer a novel population peaked just below current detection threshold.
- Reconstructed source count function for disk population consistent with luminosity function of observed pulsars (blue line, from Cholis, Hooper & Linden 1407.5583) - new population appears more dominated by bright sources, albeit with large statistical uncertainties.

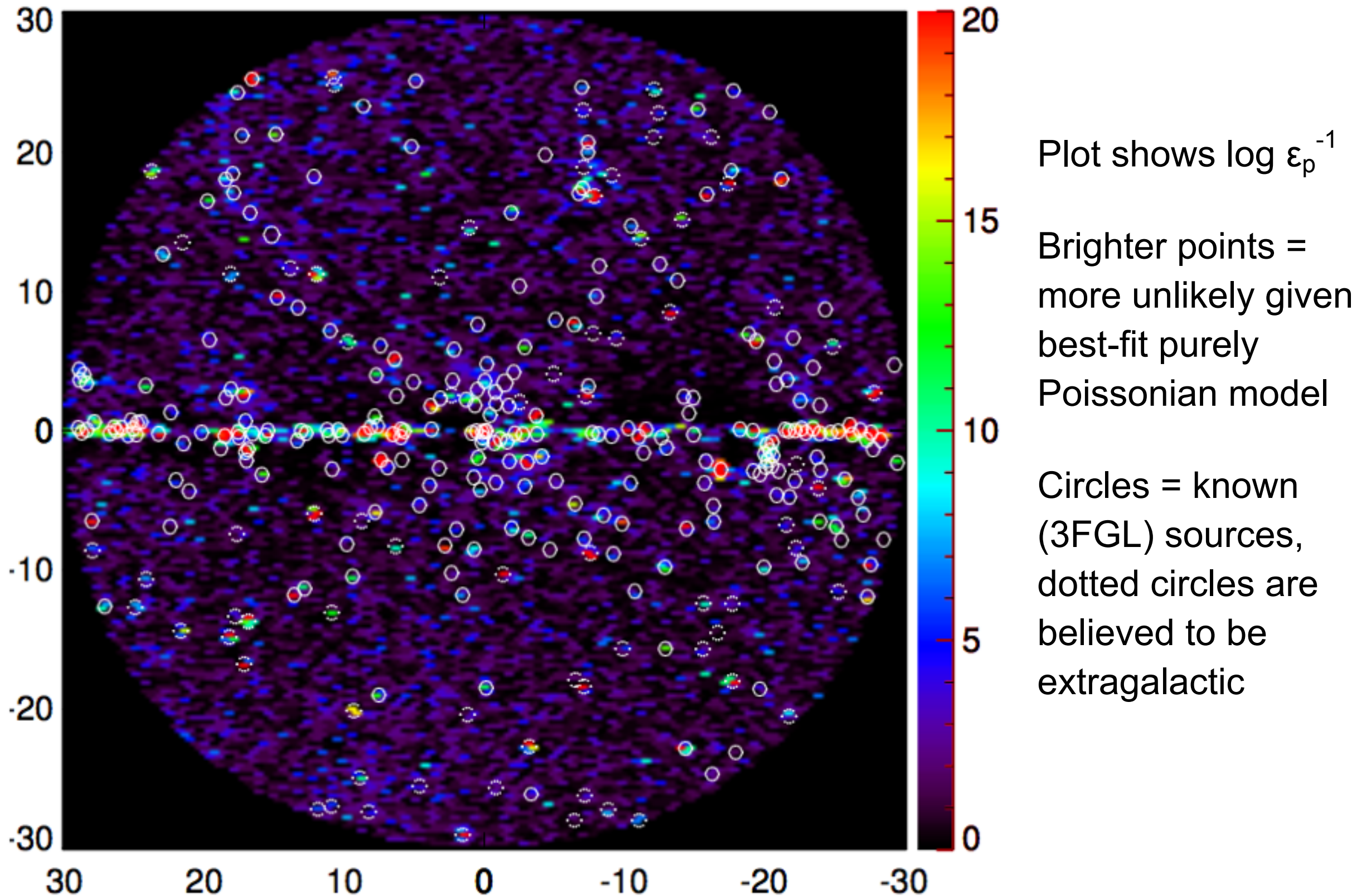
# What drives the PS preference?

- Perform standard Poissonian template fit (including NFW DM) - take best-fit model  $\mu_p$ , make map of  $\varepsilon_p = P(\# \text{ observed photons} > n_p)$  under this model. Here  $n_p$  is the actual observed number of photons in that pixel.
- Small  $\varepsilon_p$  corresponds to “hot pixels” - unusually bright relative to purely diffuse model.
- Fraction of pixels with small  $\varepsilon_p$  is a diagnostic for PS contribution - are there more than are expected from Poisson statistics?



Results shown for mock data with no NFW PSs and best-fit DM model (“NFW DM”), mock data including NFW PSs (“NFW PS + NFW DM”), and real data. In all cases template fit includes NFW DM but not NFW PS, with 3FGL mask.

# Hot pixels and known PSs



# Model comparison

- We use the Bayes factor as our measure of preference for the NFW PS template.
- Bayes factor = ratio of Bayesian evidences for the model with and without including NFW PS:

$$B_{10} = \frac{p(d|\mathcal{M}_1)}{p(d|\mathcal{M}_0)} \quad p(d|\mathcal{M}) = \int_{\Omega_{\mathcal{M}}} d\theta p(d|\theta, \mathcal{M})p(\theta|\mathcal{M})$$

- In our masked analysis, non-zero NFW PS contribution is preferred with a Bayes factor  $\sim 10^7$ .
- Agrees reasonably well (within systematic uncertainties due to modeling of diffuse emission) with mock data created using best-fit reconstructed model.

# Systematics

“There is no systematic way to address systematic uncertainties” - Licia Verde

- Spatially mismodeled background ..... Can affect source count function, flux fraction, but preference for PSs is consistent
- Spatially mismodeled signal ..... No effect
- Mismodeled angular resolution ..... Can change details of source count function
- Mismodeled source count function ..... Add more freedom - results consistent within uncertainties
- Simple “look elsewhere” - study of bright excess 30 degrees away from GC ..... No robust preference for point sources, i.e. this preference is not inevitable
- Halving the dataset - northern hemisphere vs southern hemisphere ..... Source count function and flux fraction consistent within uncertainties
- Increased dataset (from ~5.5 years to 7 years Pass 7 to 7 years Pass 8) ..... Bayes factor increases, results consistent within uncertainties

# In progress

- Include multiple energy bins - more careful study of energy spectra.
- In-depth studies of NPTF method sensitivity and possible biases, using mock data.
- “Hot pixels” provide candidate point source locations, so:
  - Can new Pass 8 Fermi LAT data allow us to (significantly) detect the individual sources contributing to the excess?
  - Can we search for counterparts or correlations at other wavelengths or with other messengers (e.g. ICECUBE neutrinos), either in archival or new data?
  - What is the energy spectrum in these pixels, as a function of the  $\epsilon$  parameter?
  - If new sources are detected, can we constrain the underlying spatial distribution from which these sources are drawn? (requires careful modeling of point source sensitivity as a function of position)

# Conclusions

- Template fitting with non-Poissonian statistics provides a model-independent probe of pointlike structure in photon data.
- We estimate that point sources (resolved and unresolved) contribute roughly half the isotropic gamma-ray background at 2-12 GeV.
- We find a strong statistical preference for a novel unresolved point source population in the inner Galaxy, with a source count function dominated by sources near Fermi's current detection threshold.
- In the presence of such a population, a dominant contribution to the GeV excess from annihilation of a smooth dark matter component (or any similar smooth diffuse source) is disfavored.

**BACKUP SLIDES**

# Generating functions

- Can express the probabilities in terms of generating functions:

$$p_k^{(p)} = \frac{1}{k!} \left. \frac{d^k \mathcal{P}^{(p)}}{dt^k} \right|_{t=0}$$

- For the Poisson case, generating function is simple:

$$\mathcal{P}^{(p)}(t) = \exp[\mu_p(t - 1)]$$

- More generally, the total generating function for Poissonian + non-Poissonian templates is simply the product of the components:

$$\mathcal{P}^{(p)}(t) = \mathcal{D}^{(p)}(t) \cdot \mathcal{G}^{(p)}(t)$$

# Generating functions (II)

- PSF can be included at the level of the generating function (Malyshev & Hogg 1104.0010).
- Effect is to reduce number of very bright and faint pixels, more pixels with intermediate brightness.

expected number of  
m-photon sources

$$x_m = \frac{\Omega_{\text{pix}}}{4\pi} \int_0^\infty dS \frac{dN}{dS}(S) \int df \rho(f) \frac{(fS)^m}{m!} e^{-fS}.$$

determined by Monte Carlo, accounts for PSF

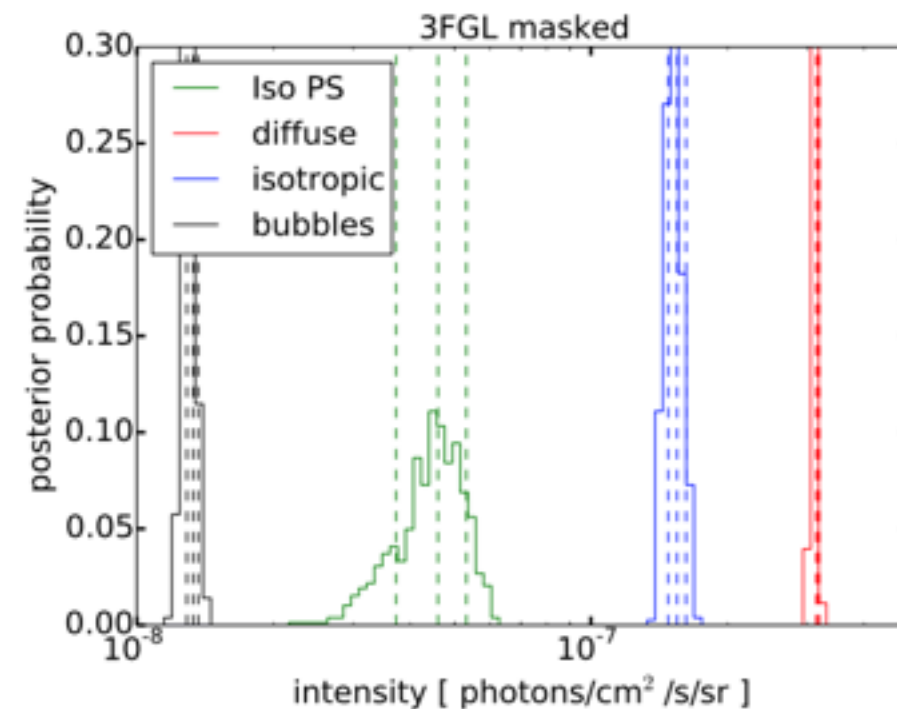
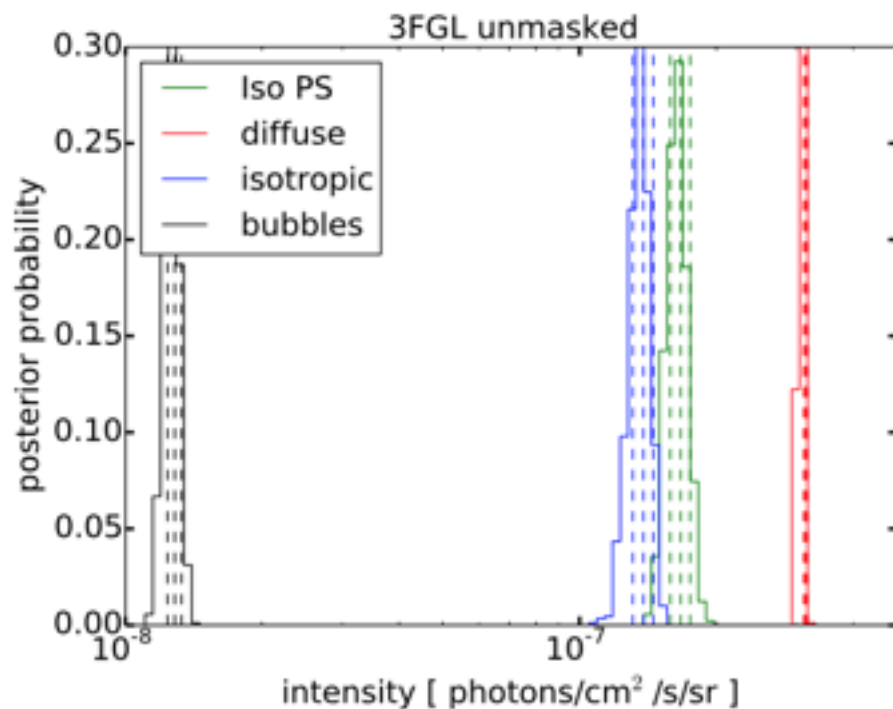
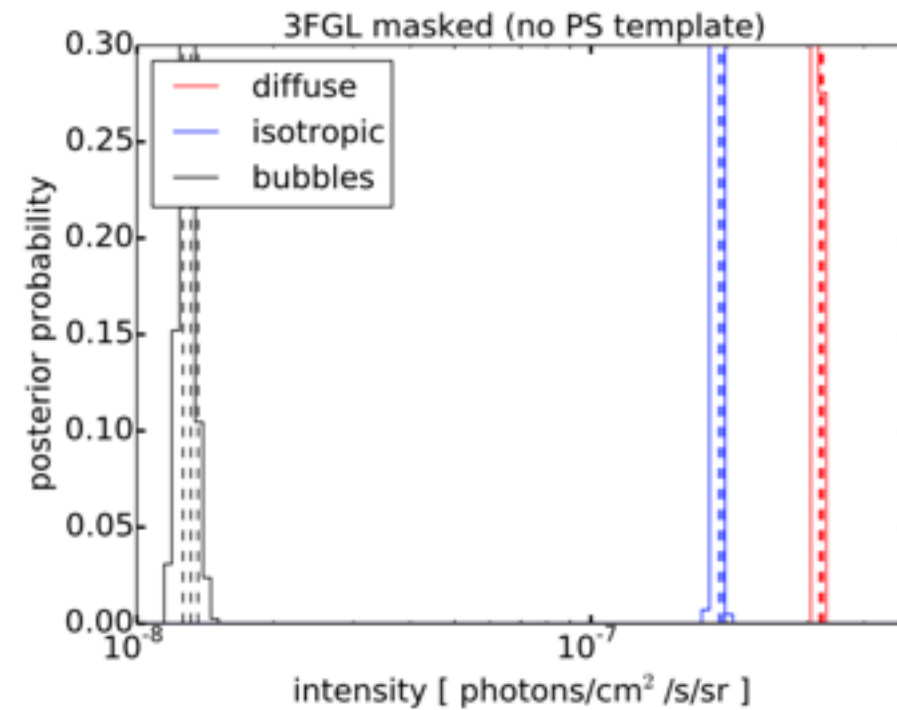
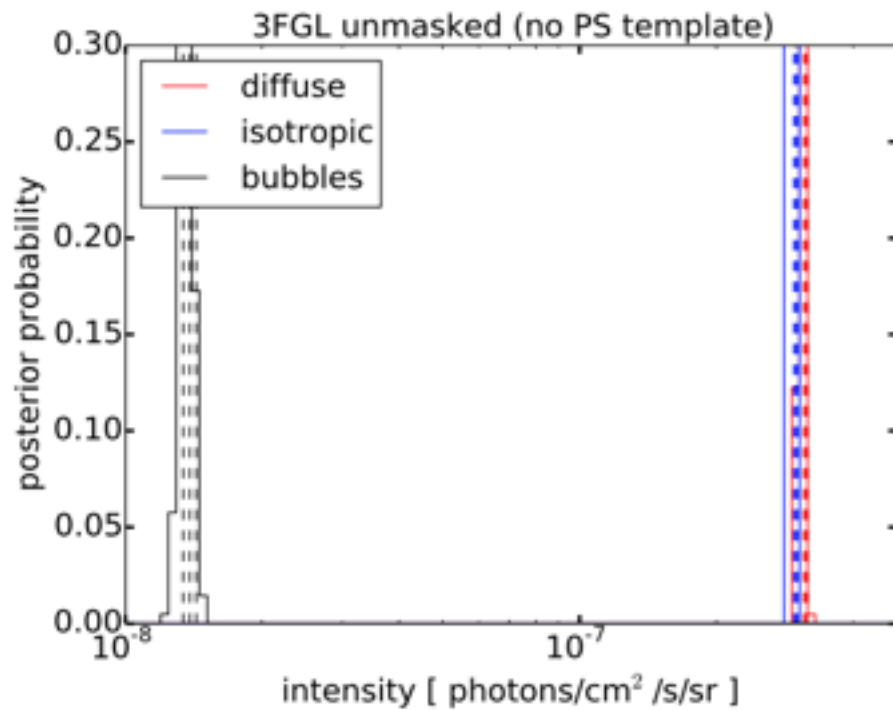
$$\sum_{k=0}^{\infty} p_k t^k = \exp \left[ \sum_{m=1}^{\infty} x_m (t^m - 1) \right] \equiv P(t)$$

generating function for  
point source population

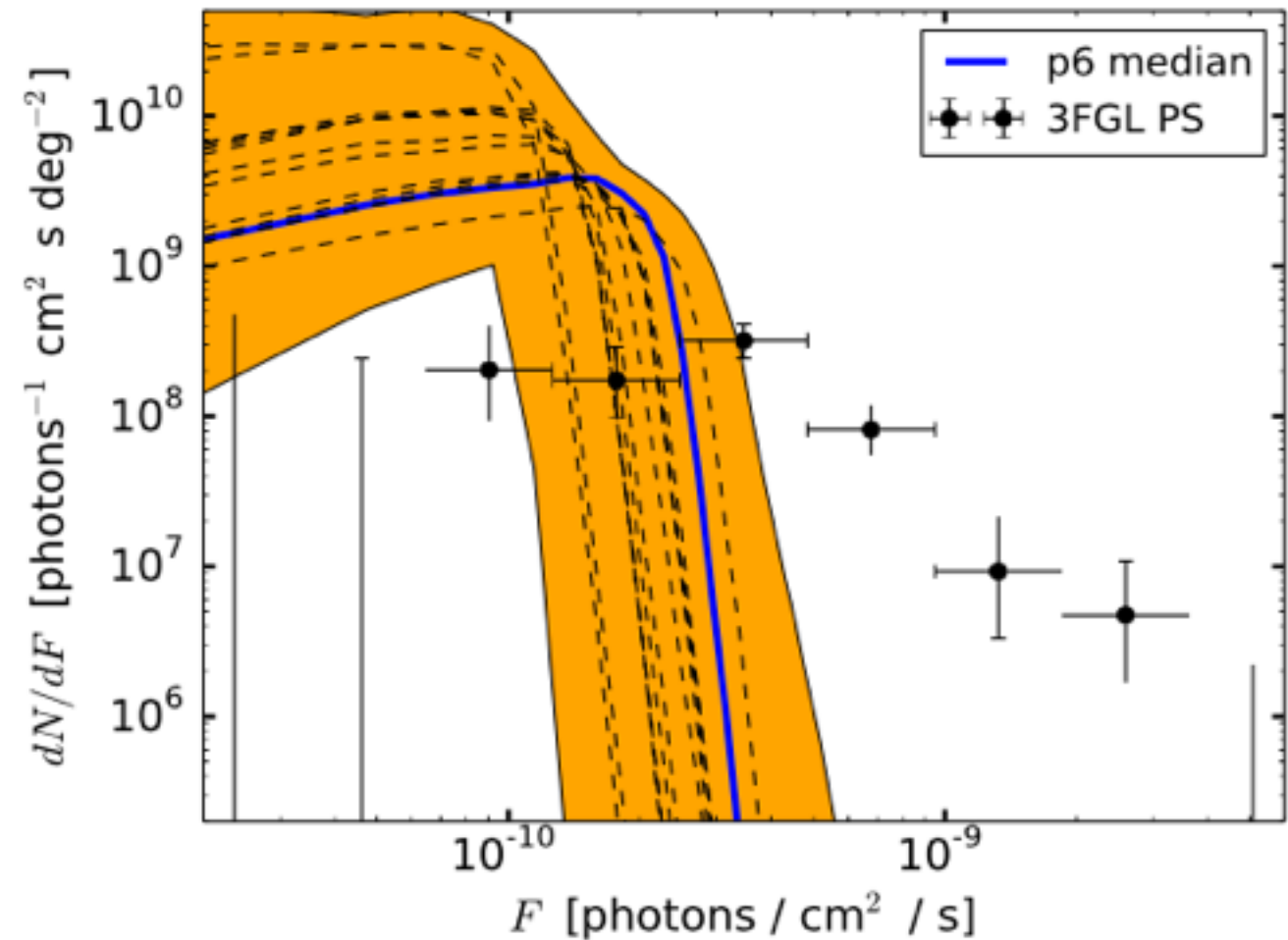
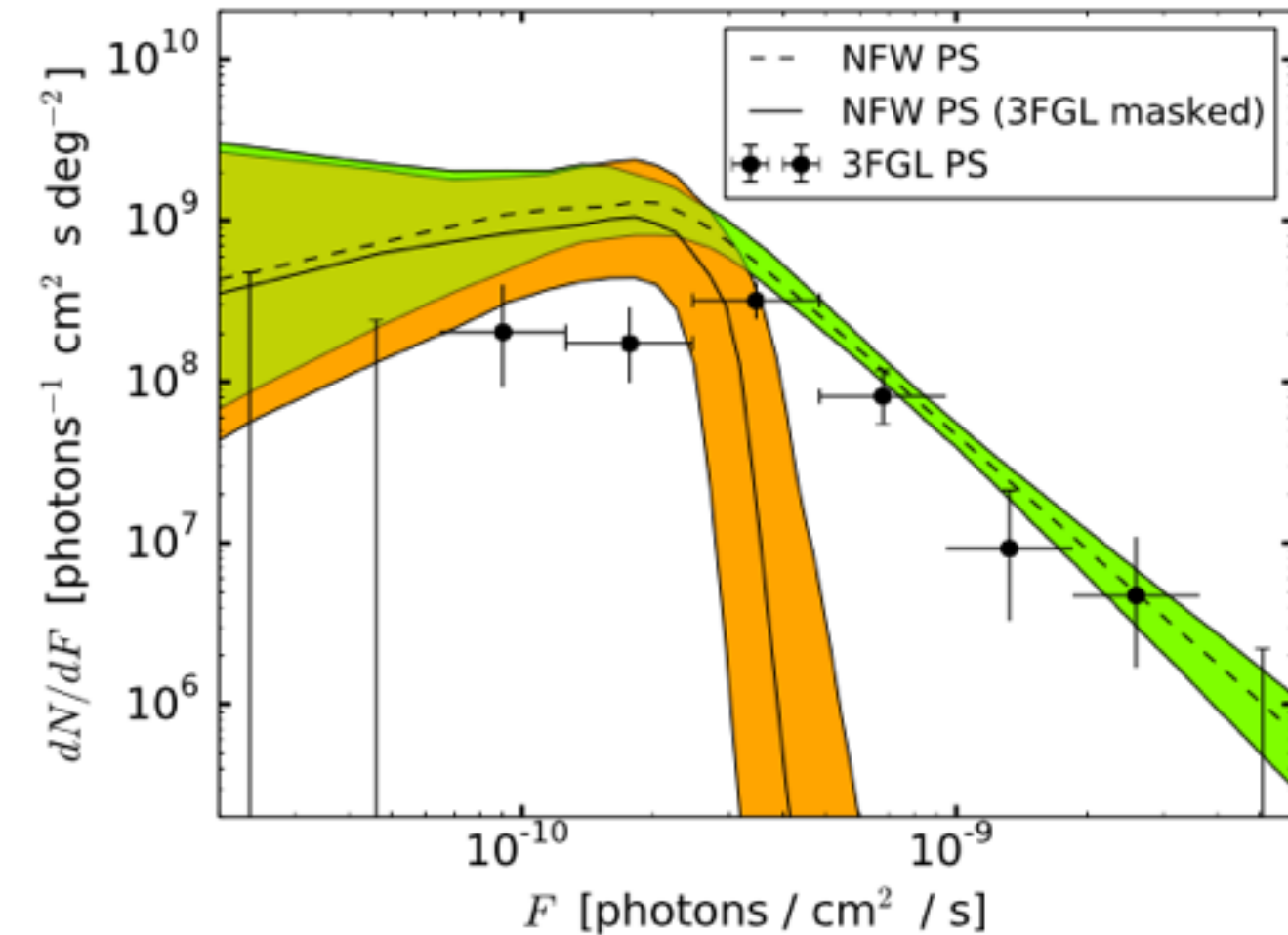
# Priors

Parameter	Prior Ranges	
	High Latitude	Inner Galaxy
$A_{\text{iso}}$	[0, 10]	20% of $A_{\text{iso}}^{\text{HL}}$
$A_{\text{diff}}$	[0, 10]	20% of $A_{\text{diff}}^{\text{HL}}$
$A_{\text{bub}}$	[0, 10]	20% of $A_{\text{bub}}^{\text{HL}}$
$\log_{10} A_{\text{NFW}}$	[-6, 6]	[-6, 6]
$\log_{10} A_{\text{PS}}$	[-6, 6]	[-6, 6]
$S_b$	[0, $k_{\text{max}}$ ]	[0, $k_{\text{max}}$ ]
$n_1$	[2.05, 50]	[2.05, 50]
$n_2$	[-2, 1.95]	[-2, 1.95]

# Additional results for the high-latitude analysis



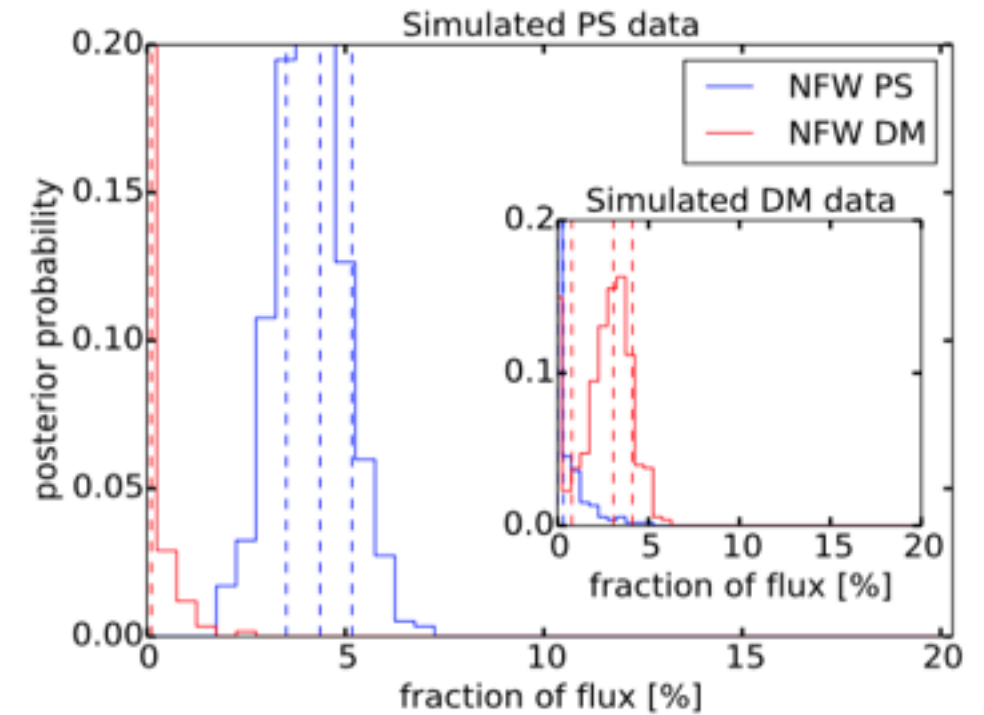
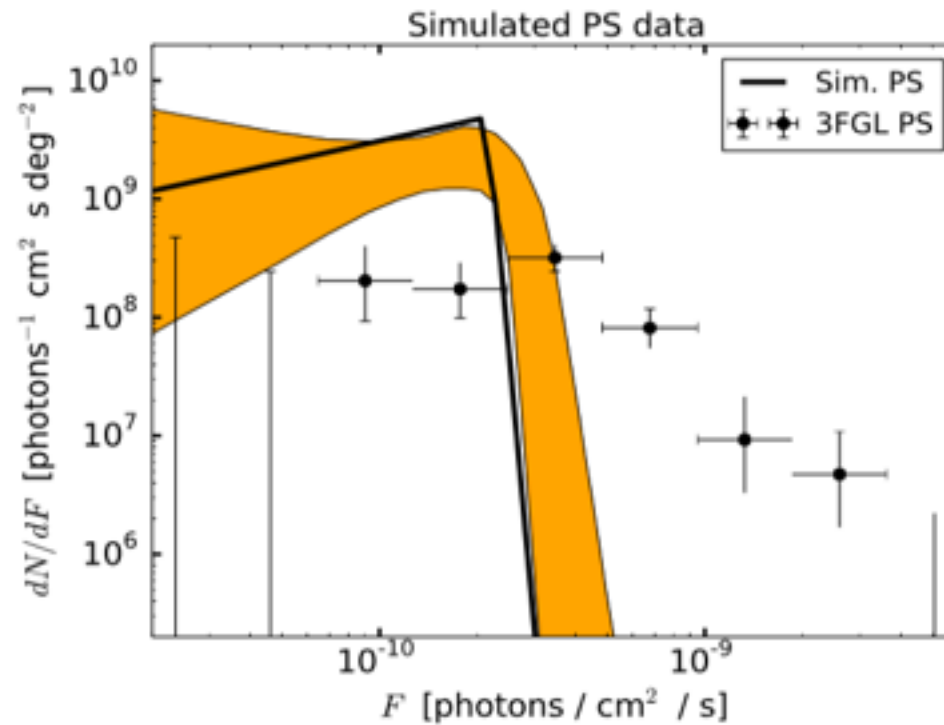
# A different background model



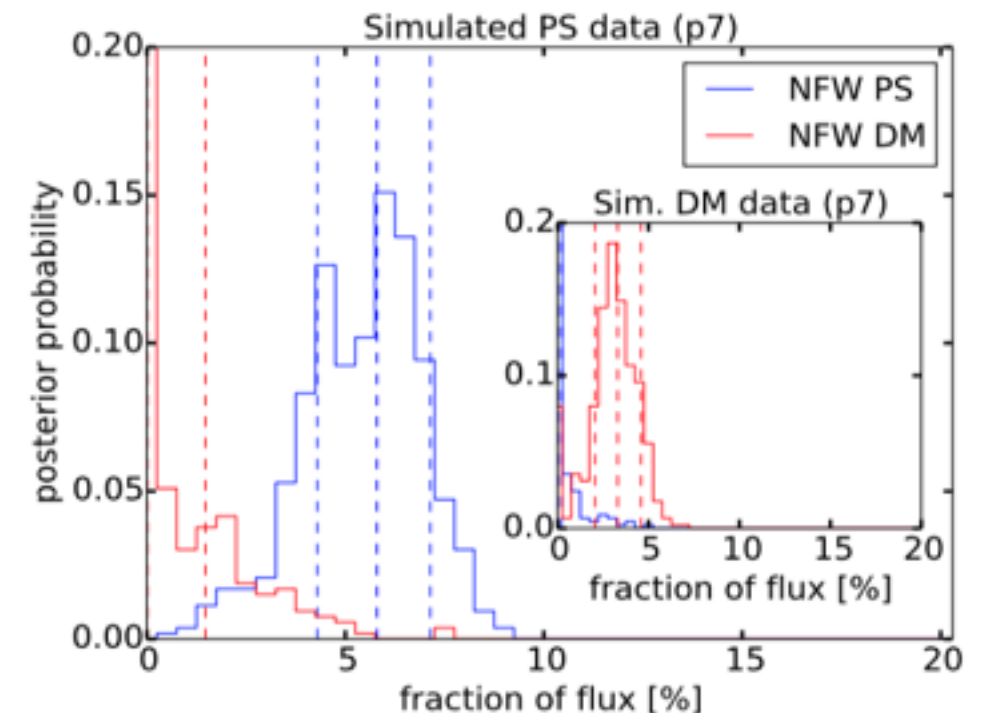
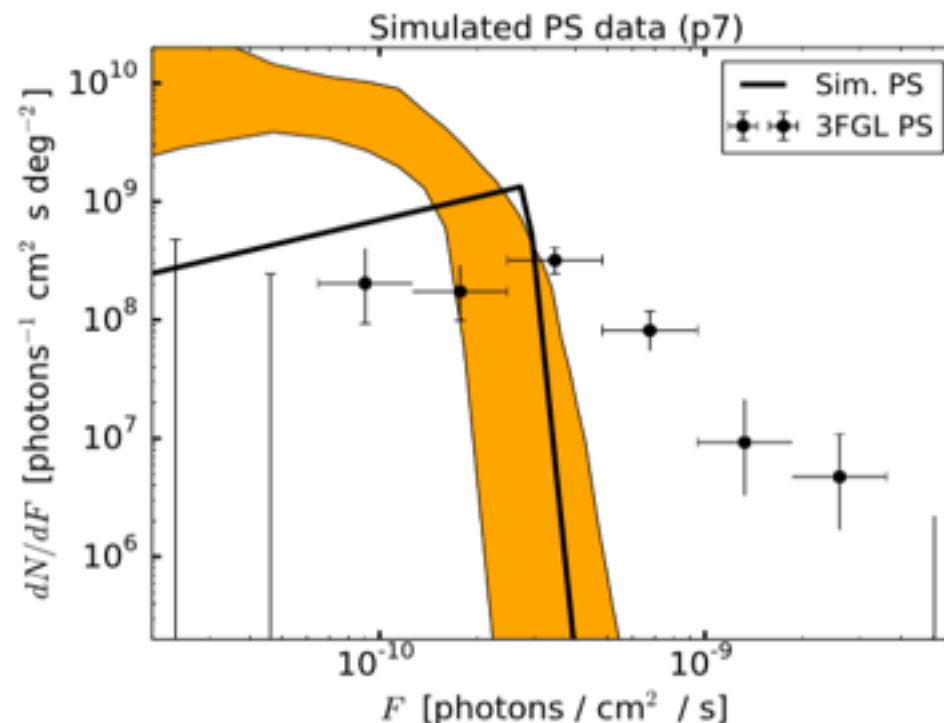
- Left panel: reconstructed source-count function for p7v6 Fermi diffuse model.
- Right panel: reconstructed source-count functions for 13 GALPROP-based diffuse models, with the 3FGL point sources masked.

# Mock data tests

- Upper panels: mock data generated and fitted with p6 model (and best-fit contributions from other templates).



- Lower panels: mock data generated with p7 model, fitted with p6 model.

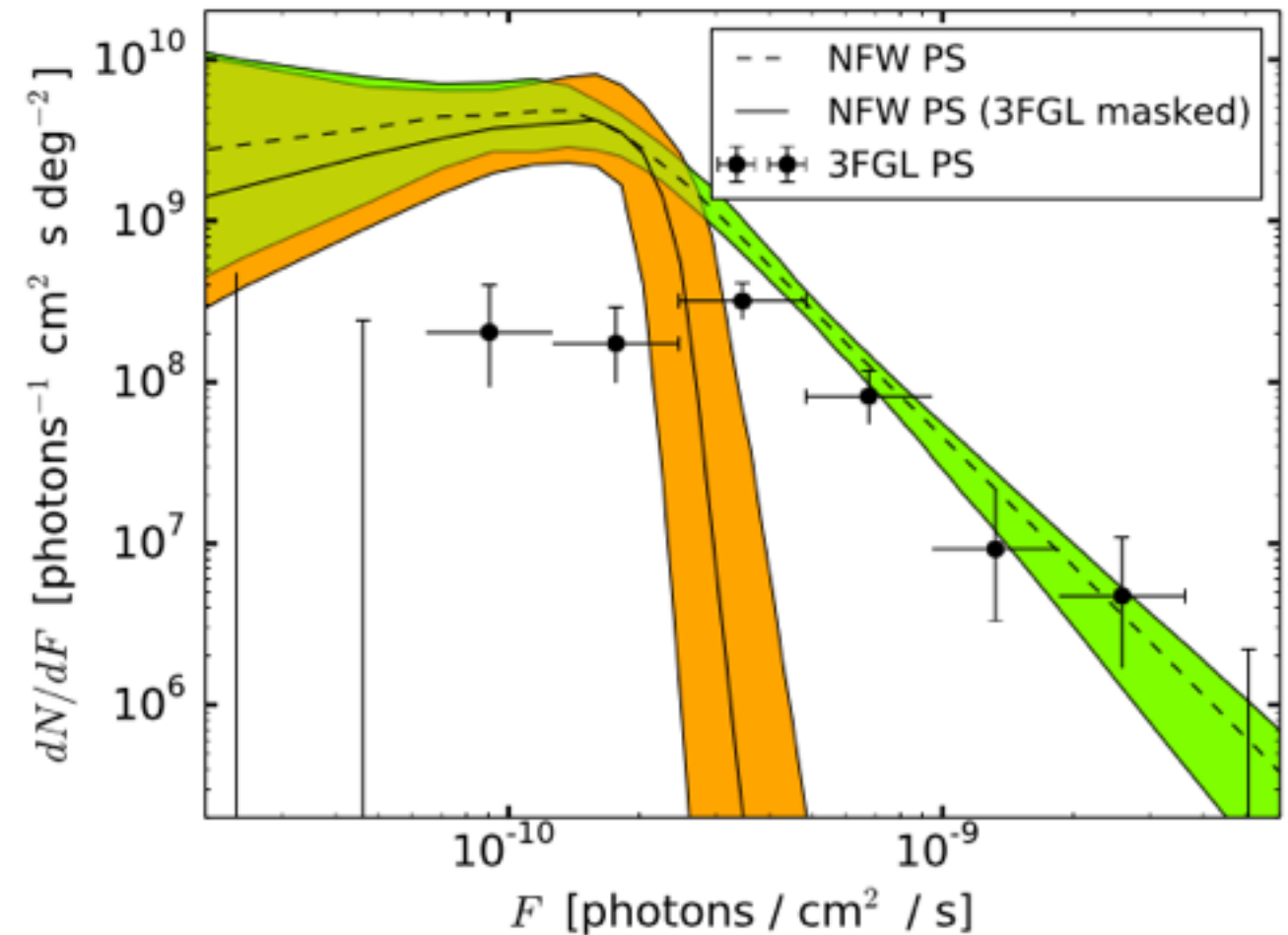
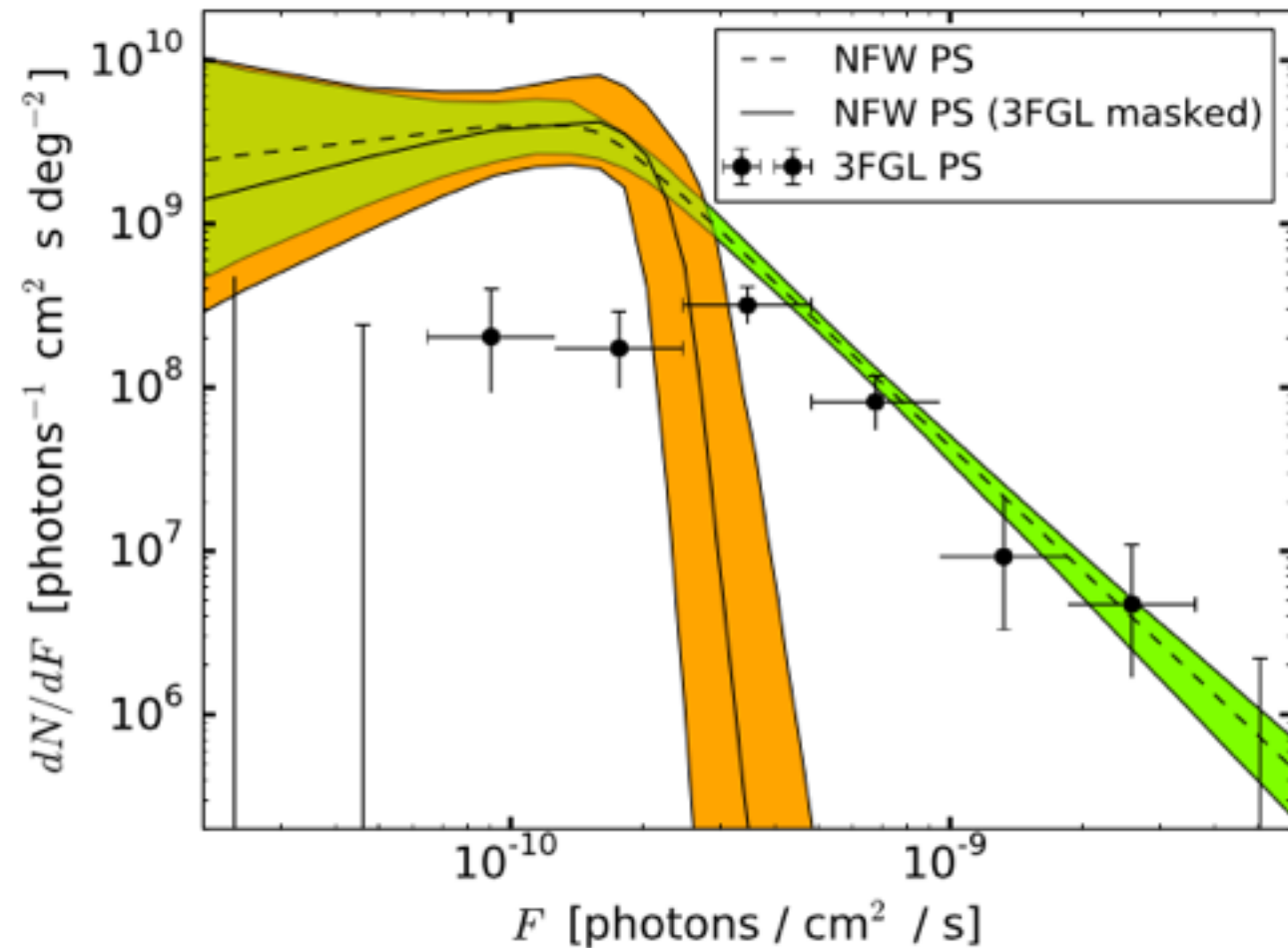


- Insets: data generated with only DM component, no PSs.

# Mock data tests (II)

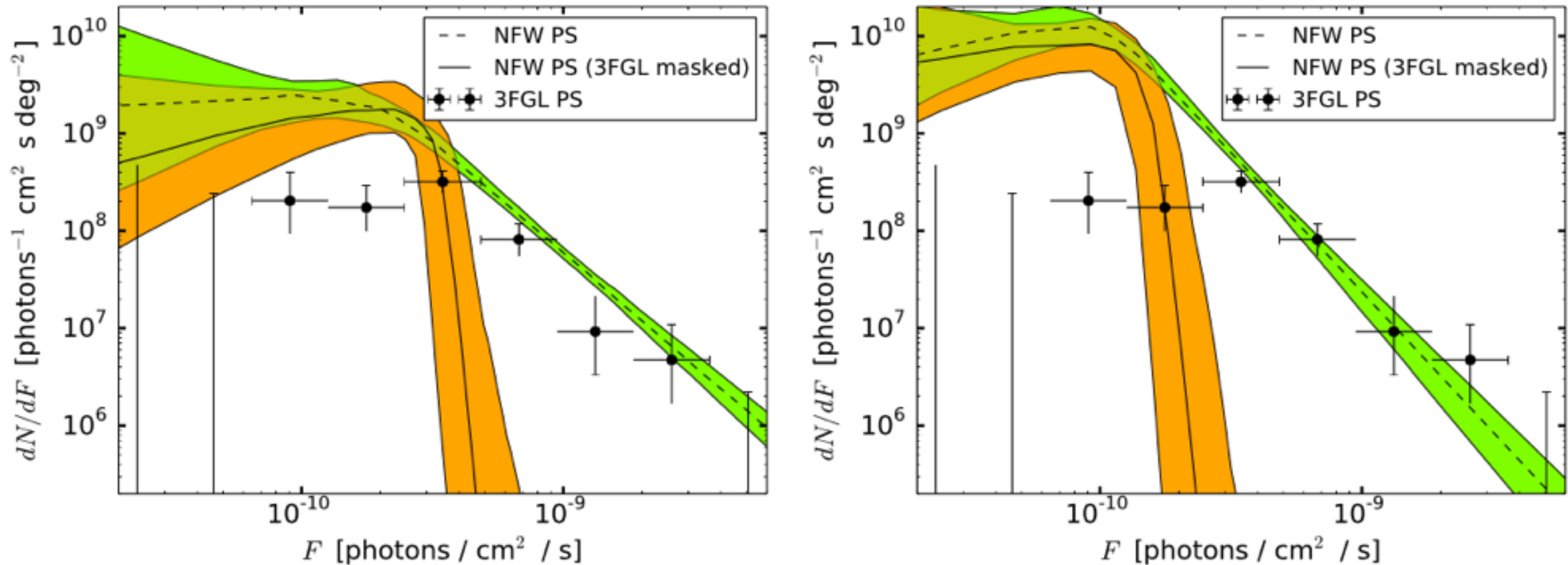
- Bayes factor in mock data (including PSs) is  $\sim 10^{10}$ , somewhat larger than in real data.
- Pipeline run again using 13 GALPROP-based diffuse models and p7 diffuse model to generate the simulated data; in all case fit is performed using default (p6) diffuse model. There is always a preference for PSs with Bayes factor  $\sim 10^5 - 10^9$ .
- That is, mismodeling the diffuse emission tends (if anything) to reduce the preference for point sources.
- We also tested mock data with half the excess attributed to PSs and half to DM - in this case, a non-zero PS contribution was favored with a Bayes factor of  $O(100)$ , but the source count function could not be reliably reconstructed.

# Changing the signal template

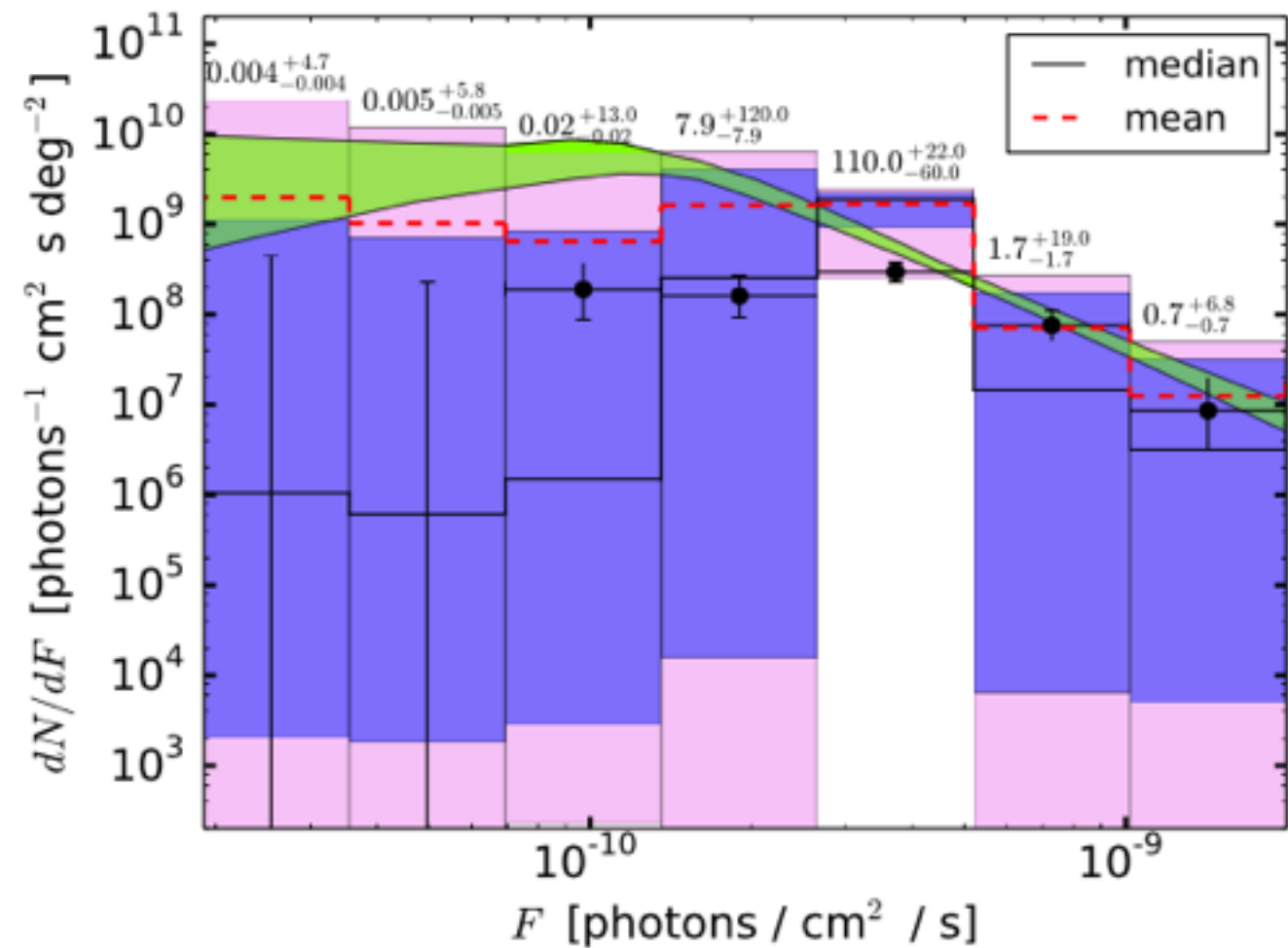
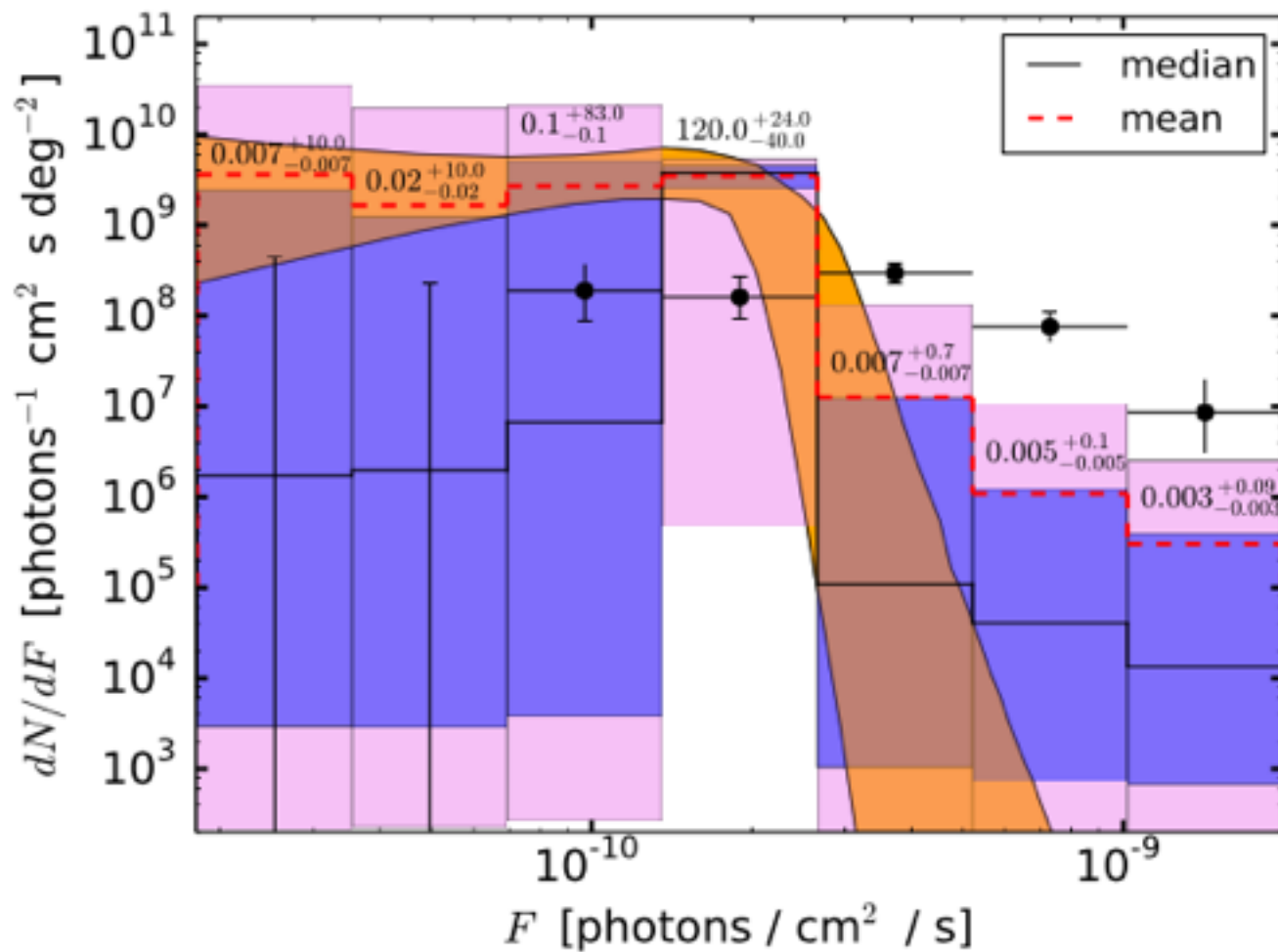


- Effect of changing the power-law slope of the NFW profile at small  $r$  to 1.1 (left) or 1.4 (right), rather than the default value of 1.25.

# Mismodeling the PSF

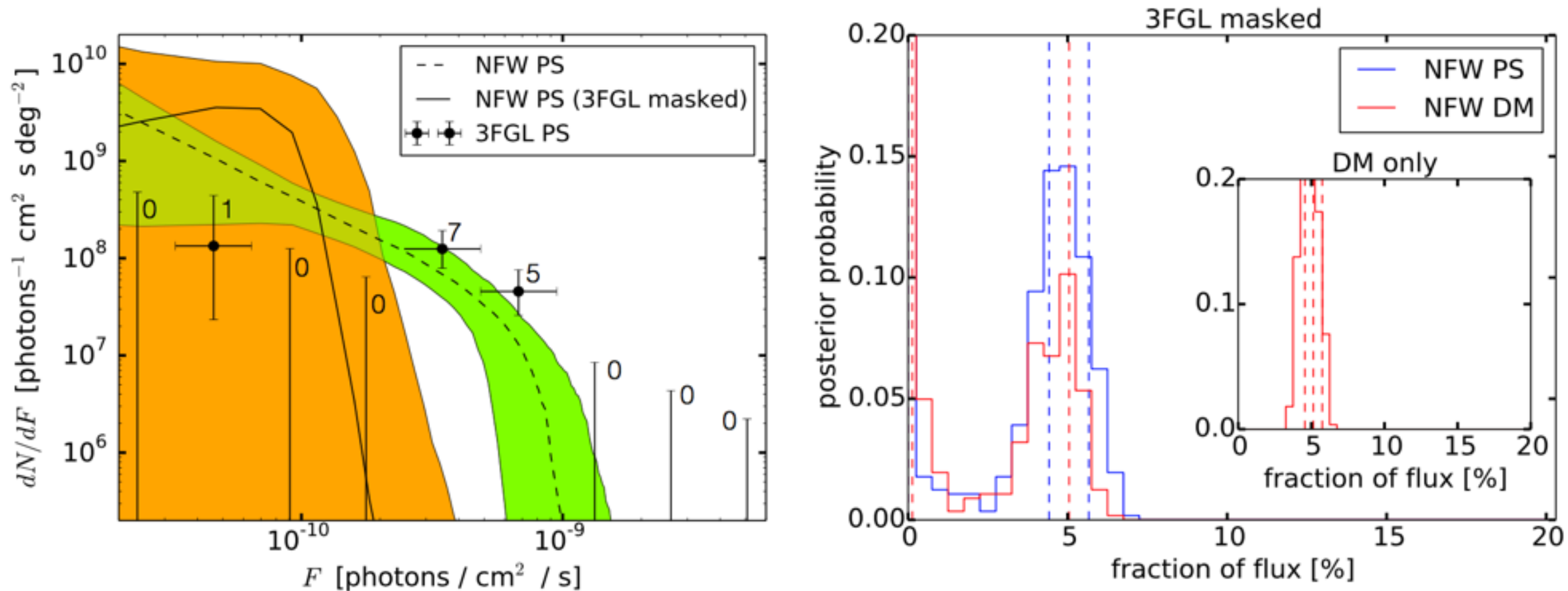


- Gaussian sigma for PSF set to 0.198 degrees (left) or 0.0492 degrees (right), in generating function formalism - these correspond to the estimated PSF at the lowest and highest energies in our bin.
- We neglect non-Gaussian PSF tails in the generating function formalism (but include them properly in smoothing the diffuse background), but taking a much broader Gaussian PSF should largely capture the impact of mismodeled tails.



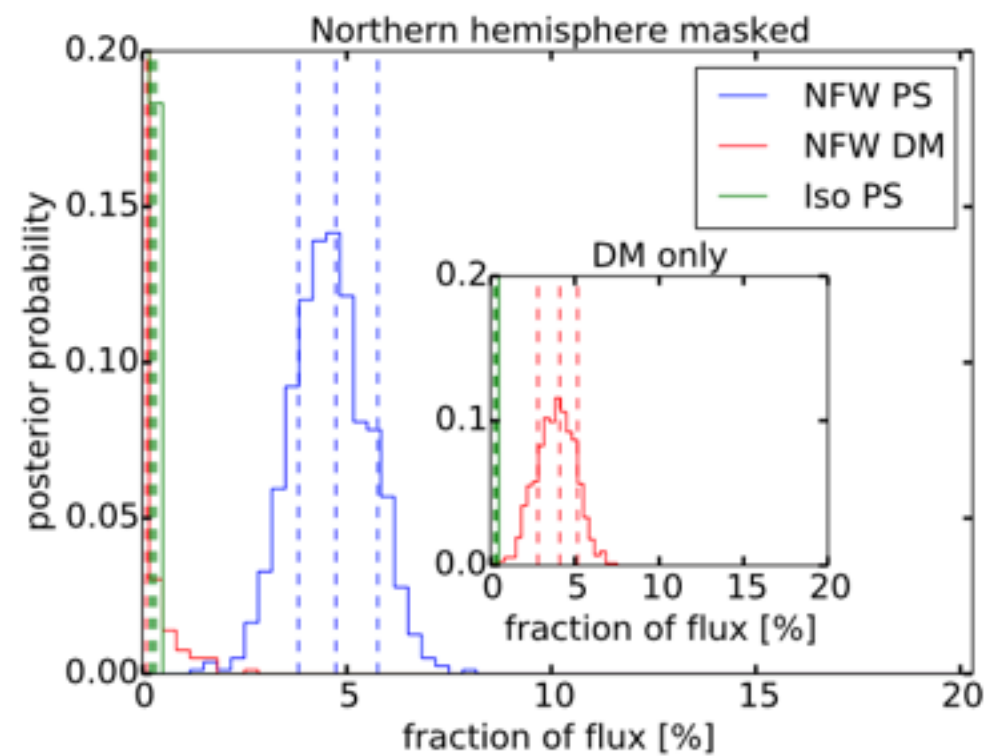
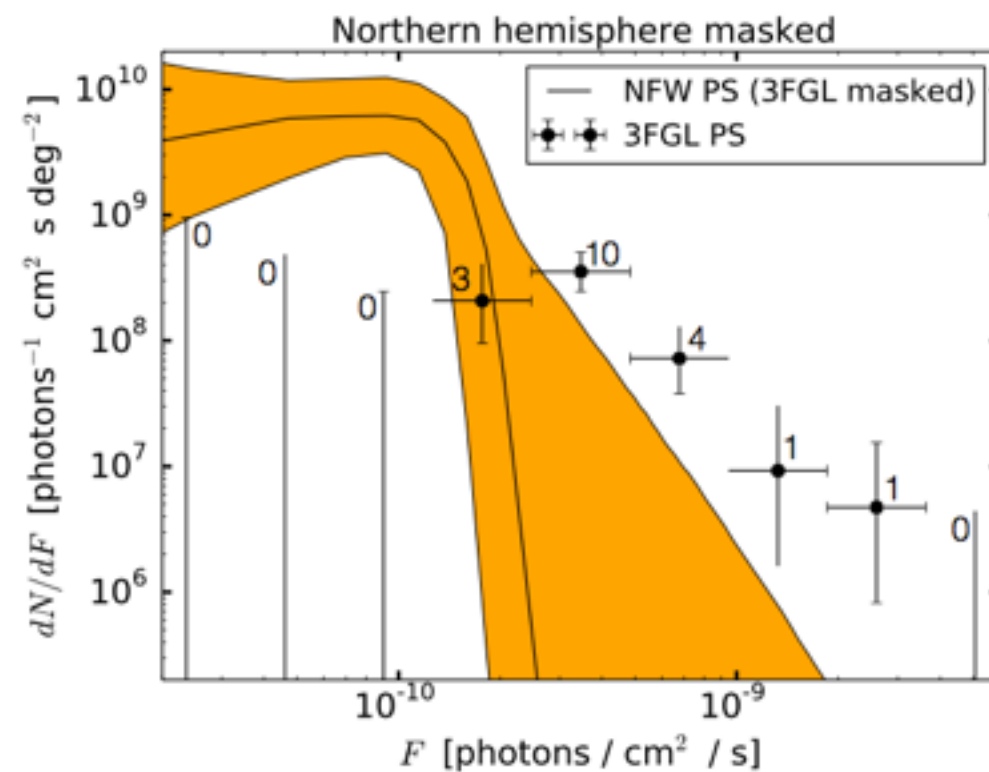
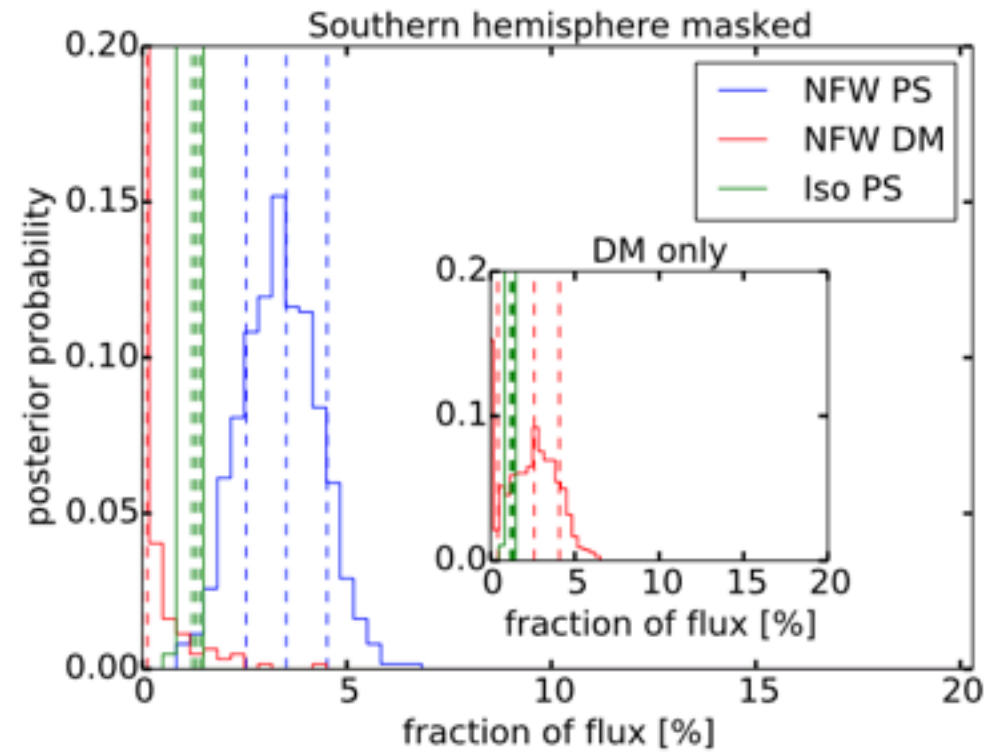
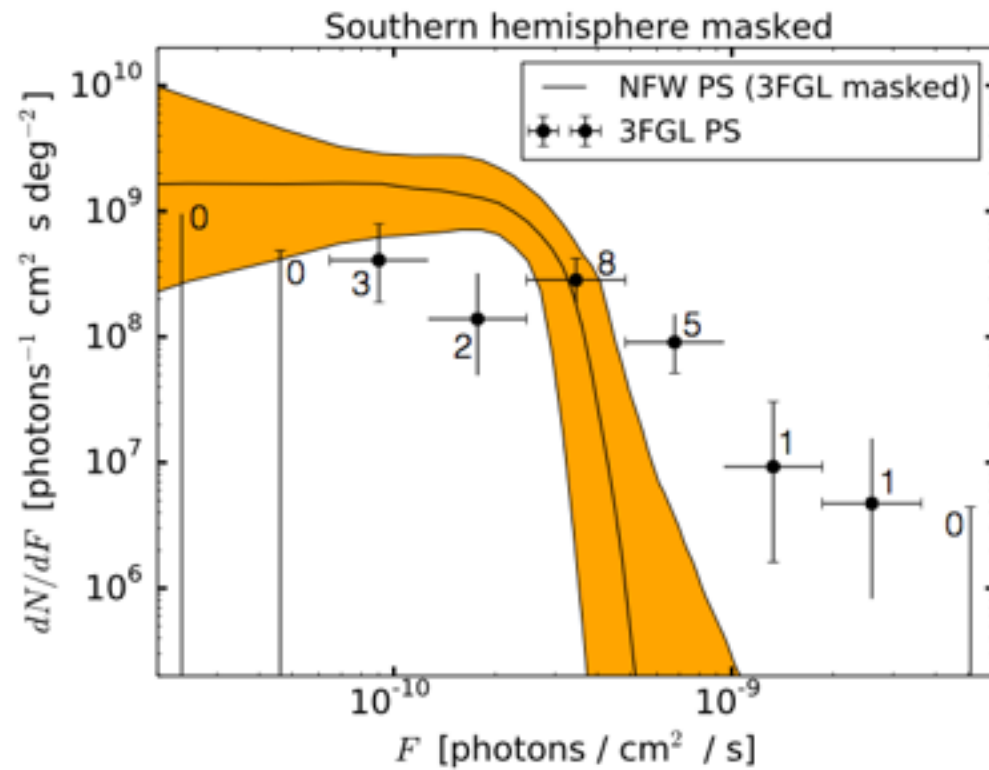
- Rather than modeling the source-count function as a broken power law, we can allow it to float independently bin-by-bin.
- Uncertainties are large (and highly correlated - not shown by error bars above), but results are consistent.
- Purple region shows 68% containment, pink region shows 95% containment, orange (green) regions are those attributed to NFW PS template in masked (unmasked) analyses.

# An alternate region

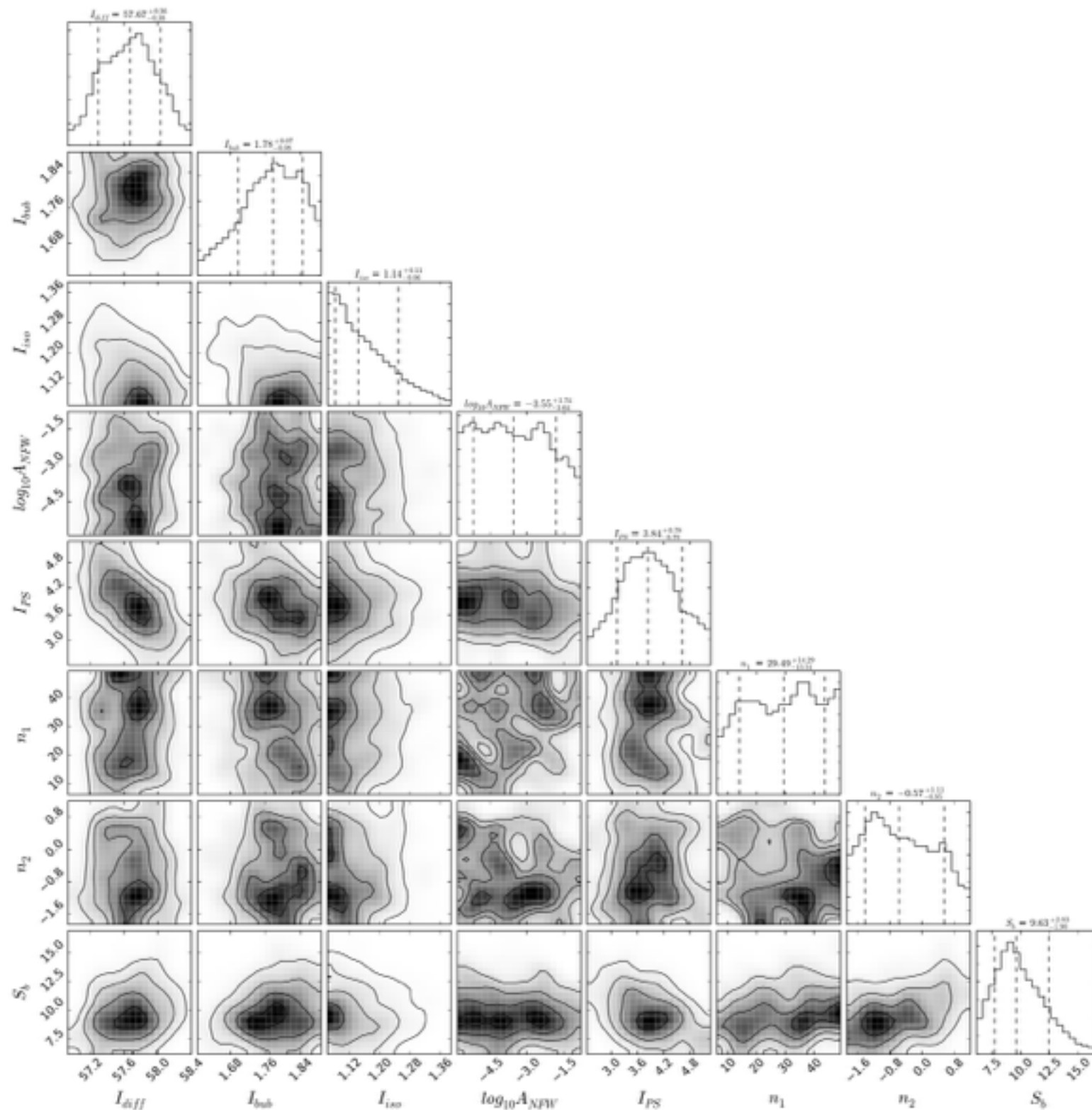


- There is a bright excess 30 degrees along the Galactic Plane from the Galactic Center, albeit with a soft spectrum.
- When the same analysis is repeated on this region in masked data, there is no significant preference for PSs over a diffuse signal.

# North vs south

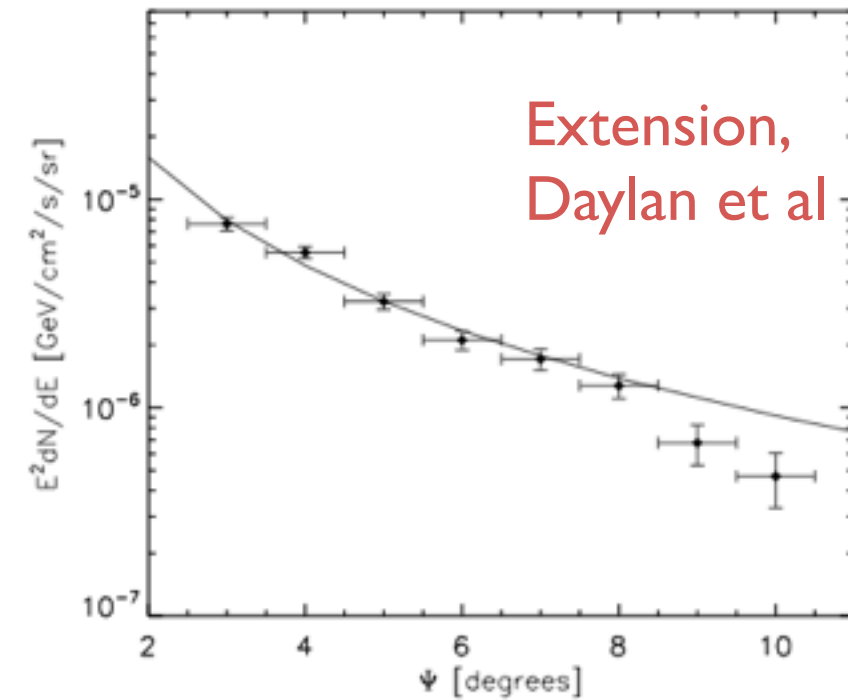
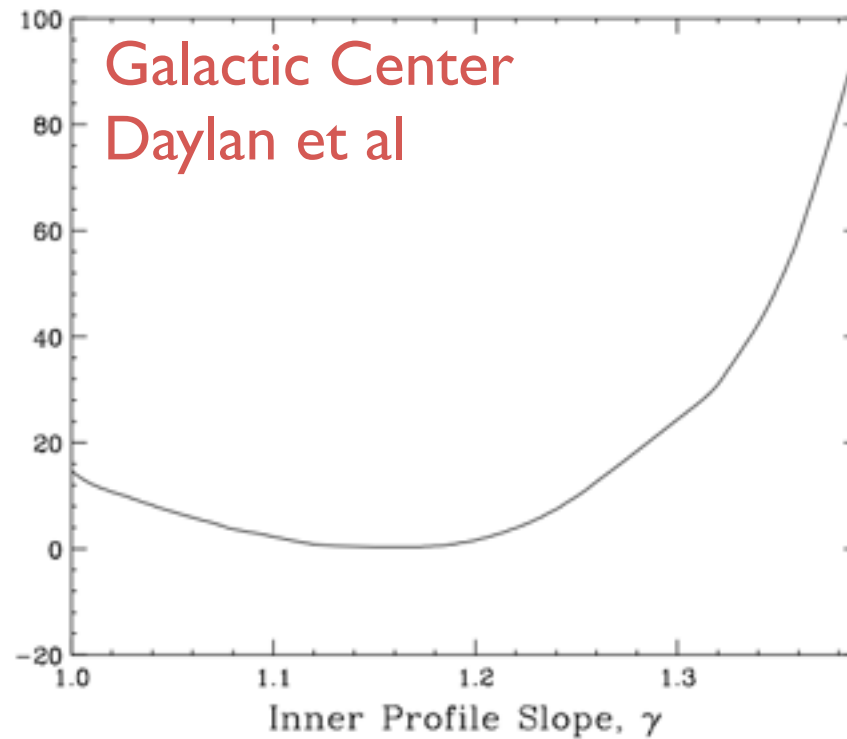
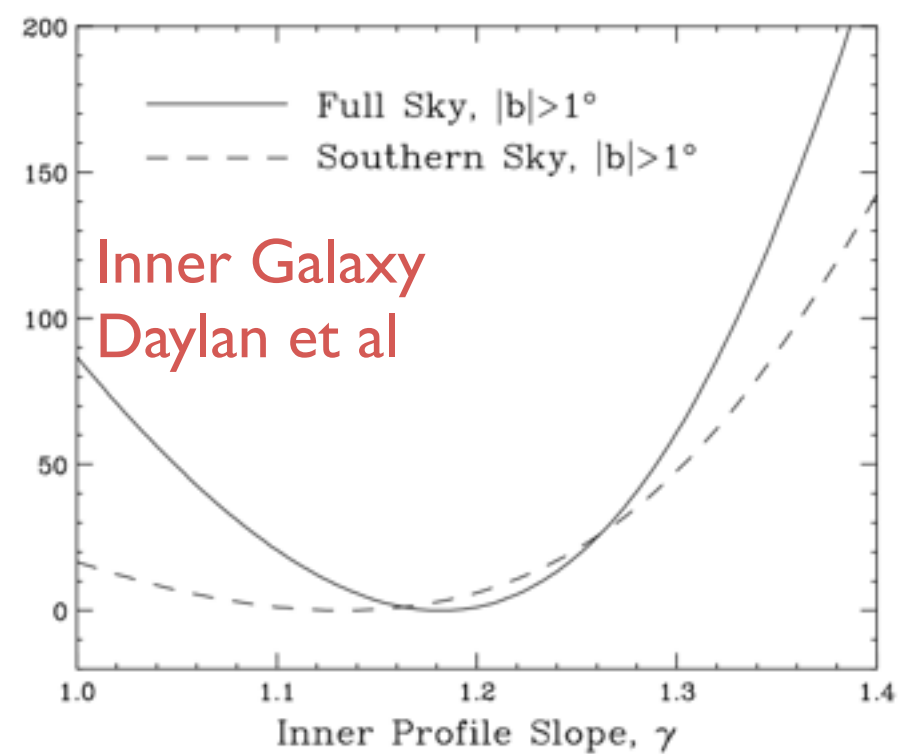


# Triangle plot (masked IG)



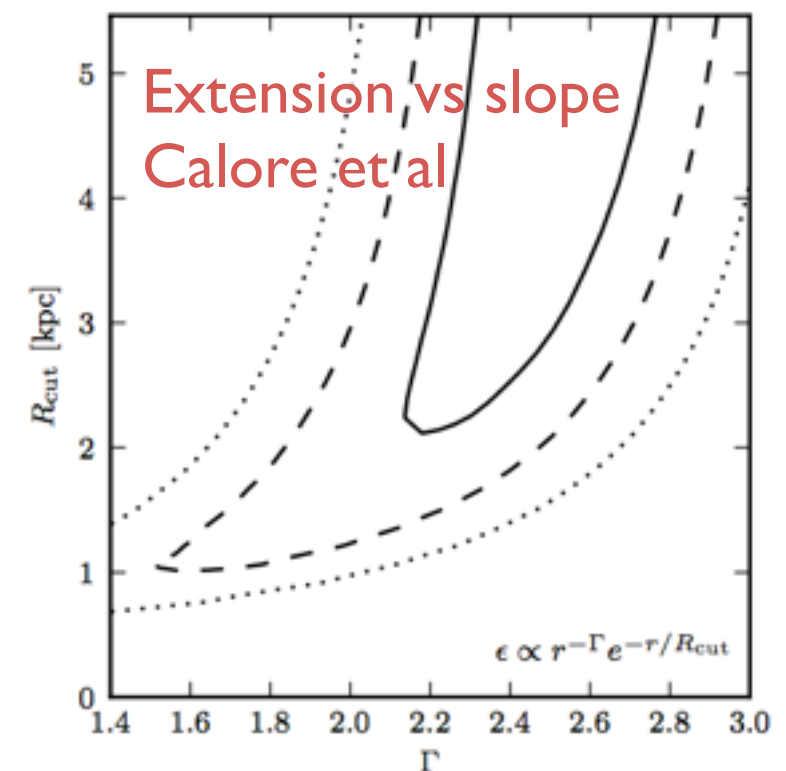
# Properties of the GeV excess

# Slope and extension



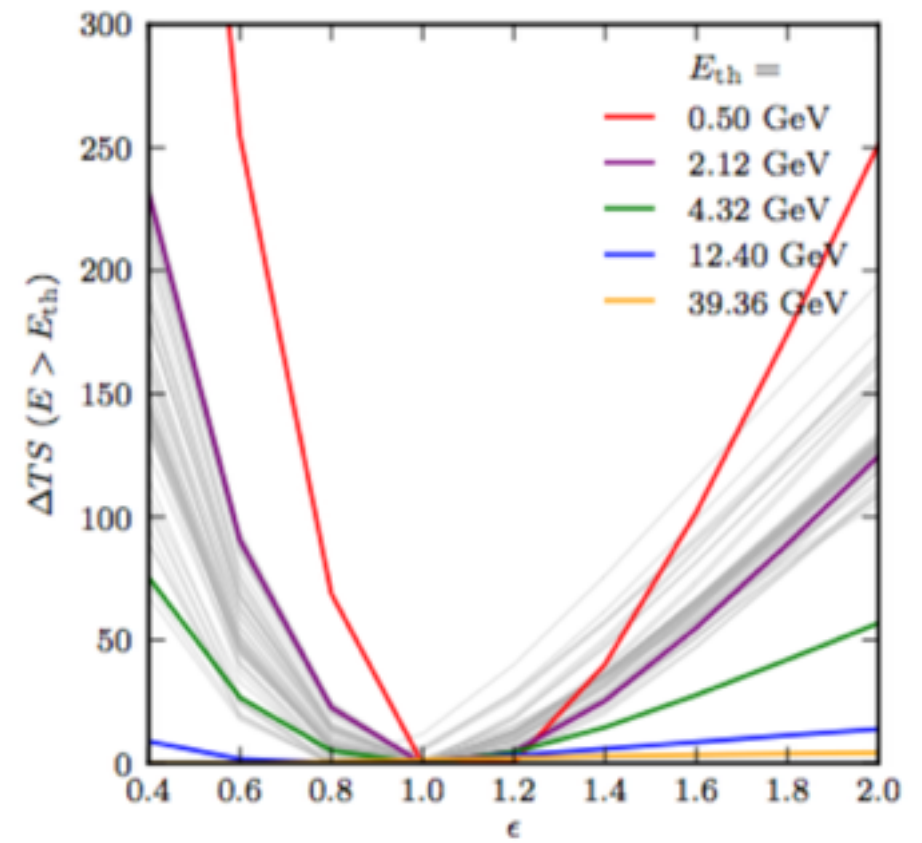
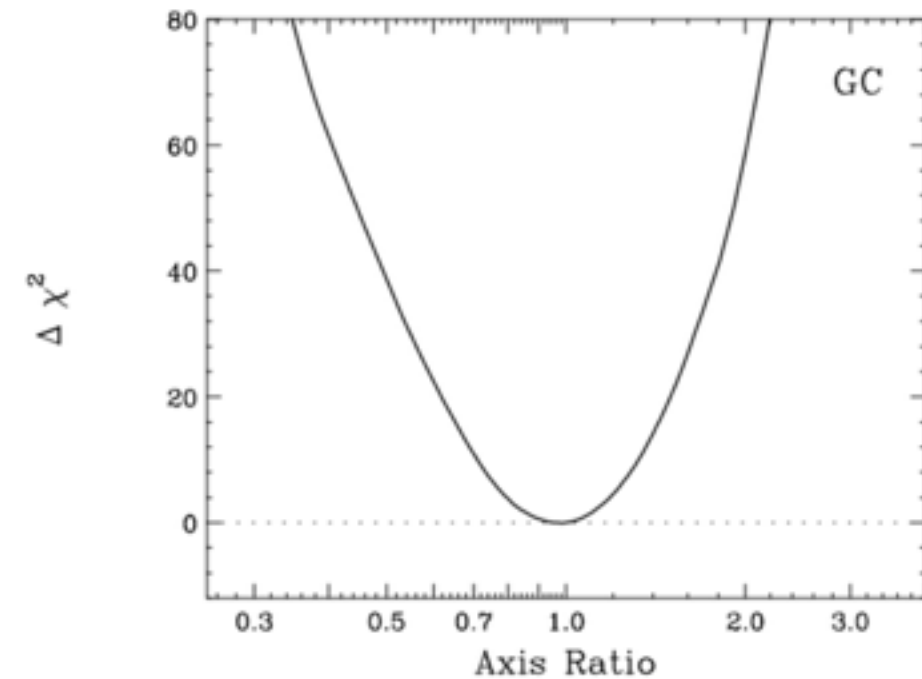
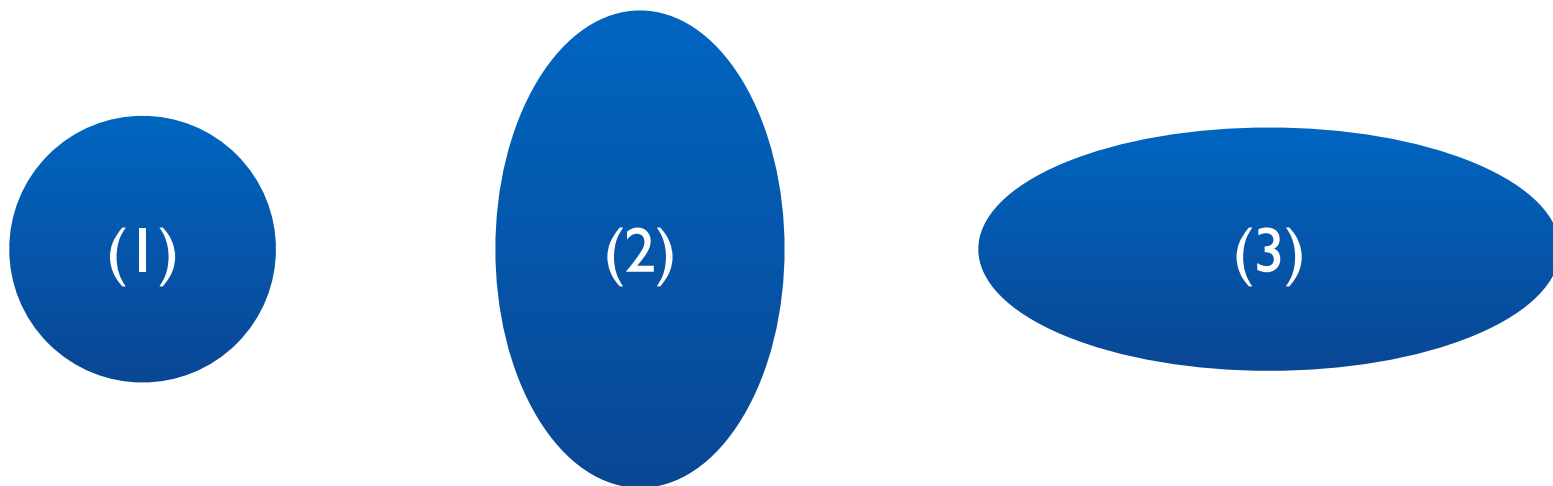
- Preferred power-law slope for power per unit volume (i.e.  $2\gamma$  for annihilation from an NFW profile):  $\sim 2.2-2.4$  (Galactic Center, Paper 1),  $\sim 2.2-2.6$  (Inner Galaxy, Paper I),  $\sim 2.2-2.8$  (CCW, syst. errors included)

- Extends to  $\sim 10$  degrees / 1.5 kpc.



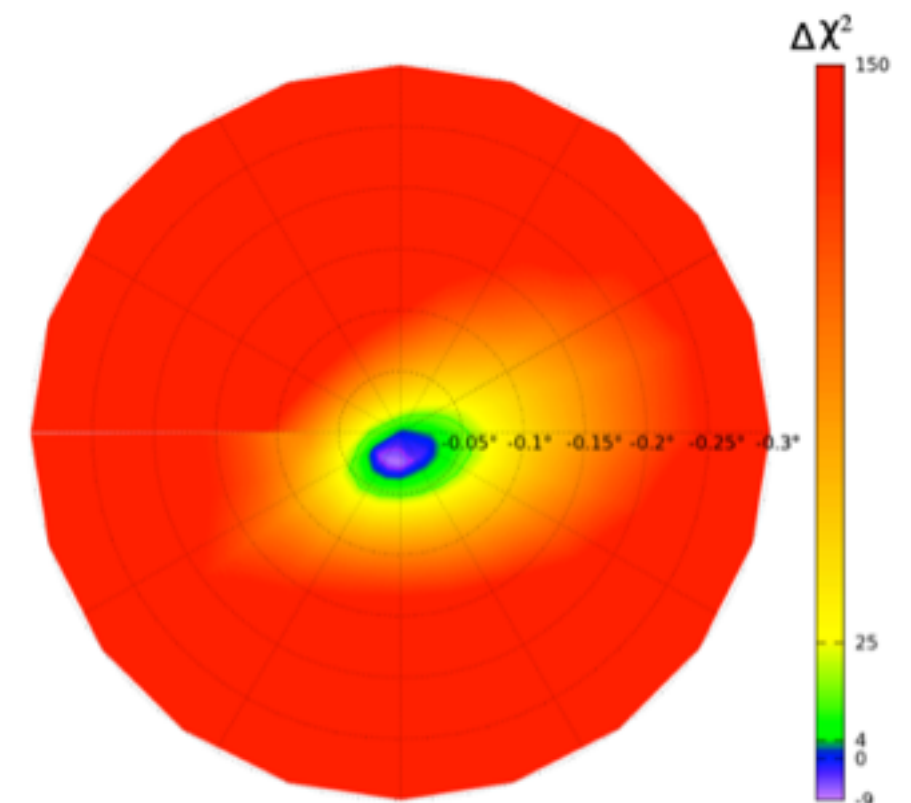
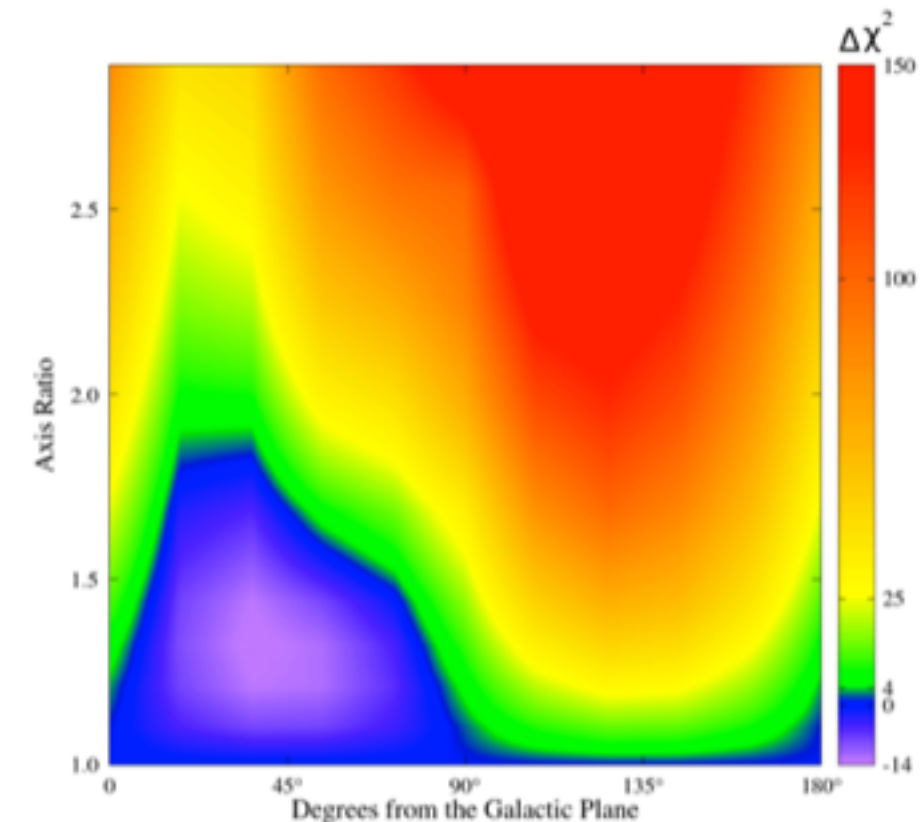
# Sphericity

- Test: which provides a better fit to the data? (1) Circular template, (2) template stretched perpendicular to the Galactic plane, (3) template stretched along the Galactic plane?
- (3) would be a strong hint at an astrophysical origin. But data seem to prefer (1), disfavoring a stretch by a factor of more than 1.2.
- Top - Daylan et al, bottom - Calore et al.



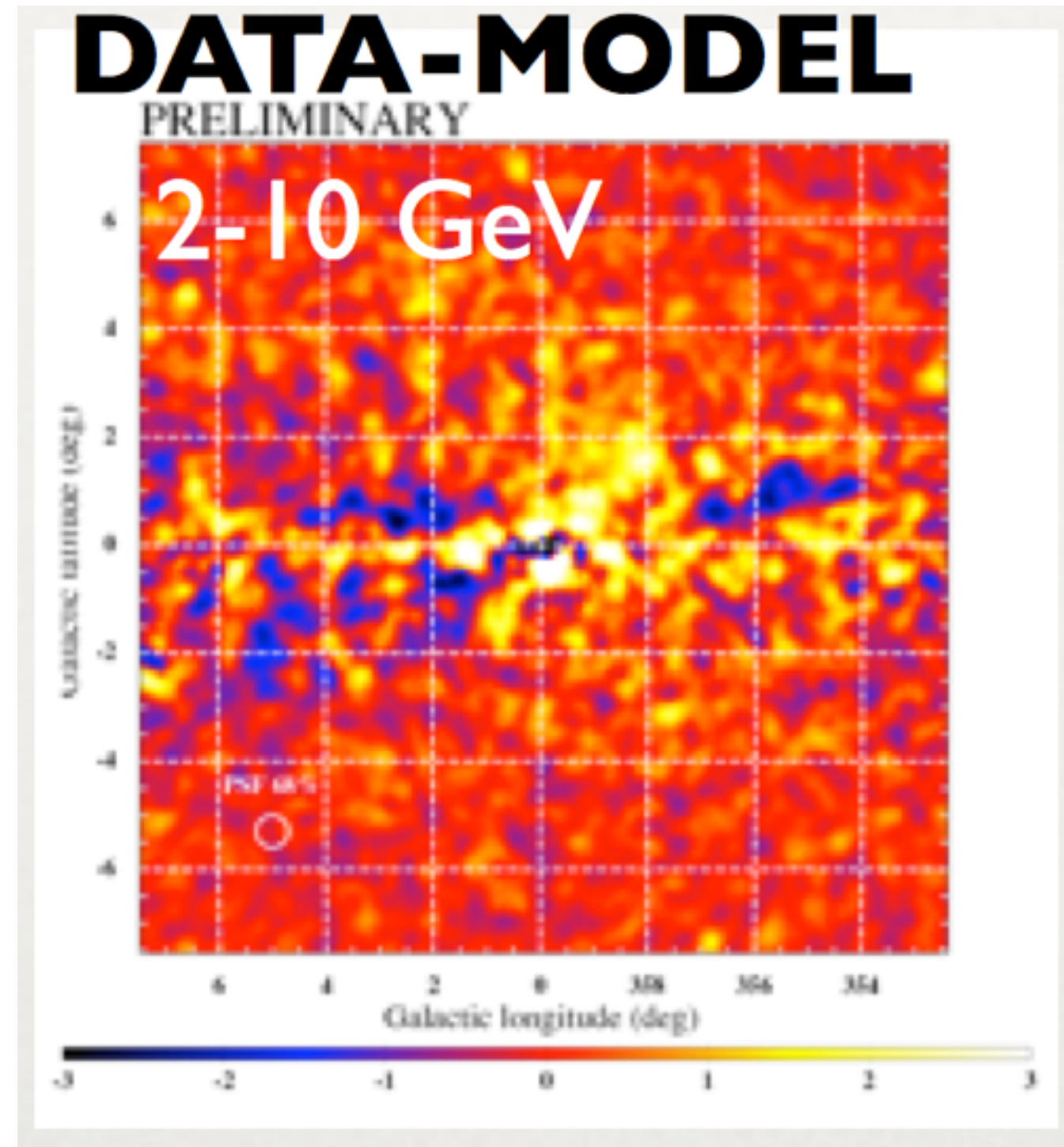
# Orientation & centering

- More spatial tests (from Daylan et al):
- Stretch signal template along arbitrary angles to the Galactic plane.
- Move template so it is not centered on Galactic Center.
- Results: shift more than 0.05 degrees from the GC is disfavored at 95% confidence (from GC analysis - inner Galaxy analysis less sensitive).
- Mild preference for stretch factor of 1.3-1.4 at an angle  $\sim 35$  degrees from the Galactic Plane, but not significant.



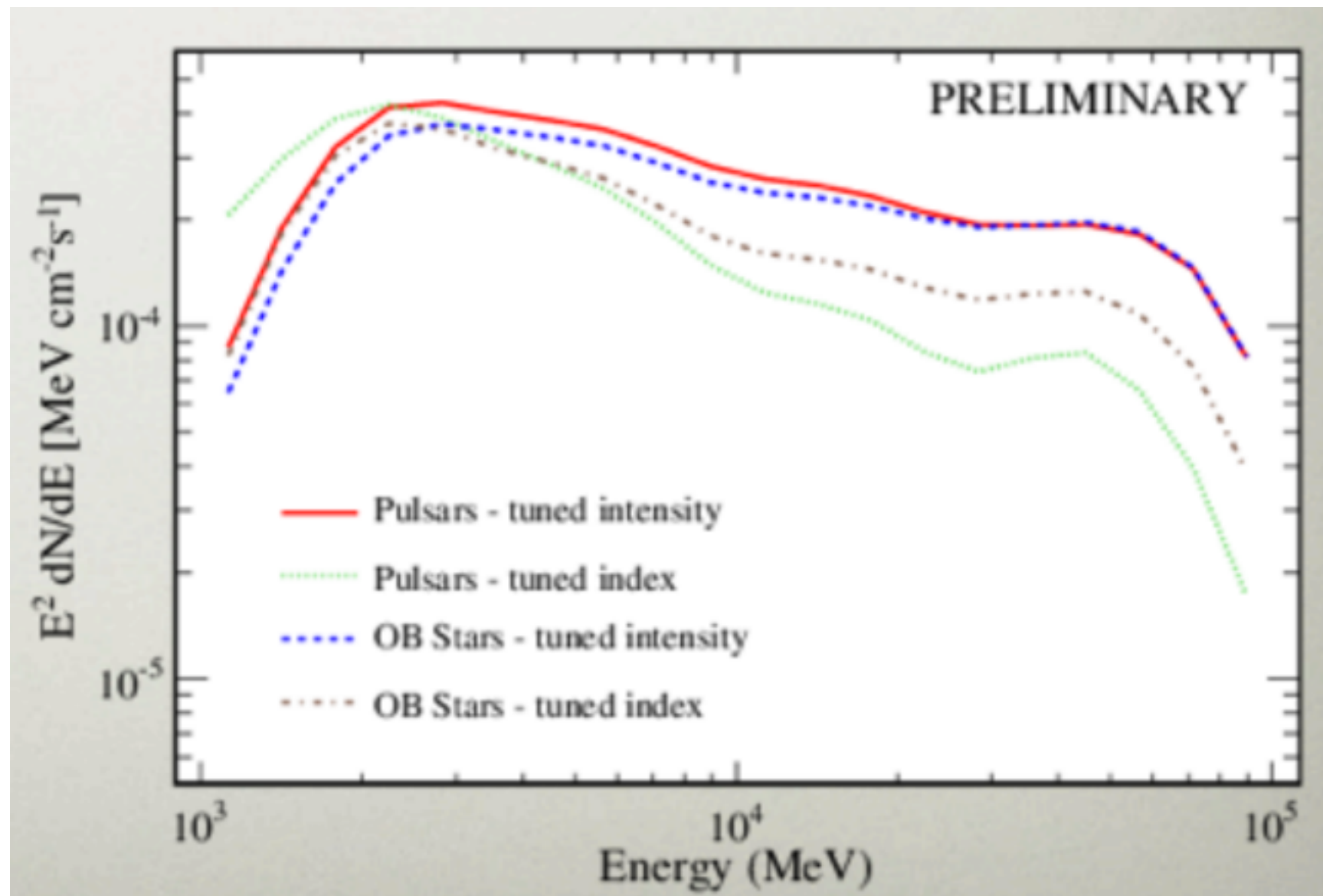
# What does the Fermi Collaboration say?

- Talk presented by Simona Murgia at Fermi Symposium 20-24 October.
- “We find an enhancement approximately centered on the Galactic center with a spectrum that peaks in the GeV range, that persists across the models we have employed”
- “Peaked profiles with long tails (NFW, NFW contracted) yield the most significant improvements in the data- model agreement”



# The spectrum from the Fermi Collaboration

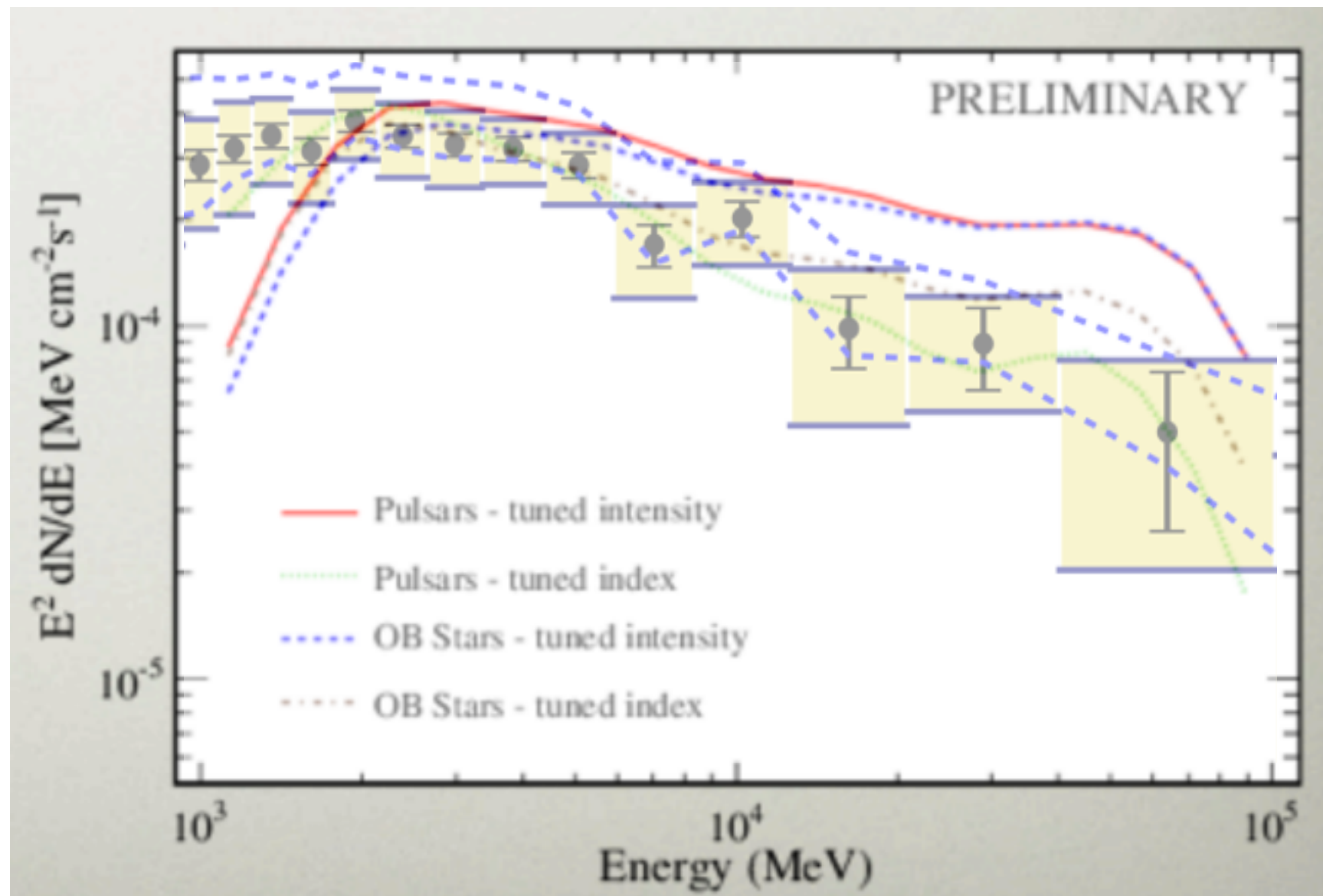
- Two sets of source distributions (“pulsars” and “OB stars”). “Tuned index” models allow spectral indices of background to vary (rather than just intensity), provide better agreement with data.
- Spectrum of excess seems broadly consistent with other results (lower at  $\sim 1$  GeV); tuned-intensity models lead to higher “signal” tails at large E, but are known to generically undersubtract data at high energies.



Talk presented by Simona Murgia at Fermi Symposium

# The spectrum from the Fermi Collaboration

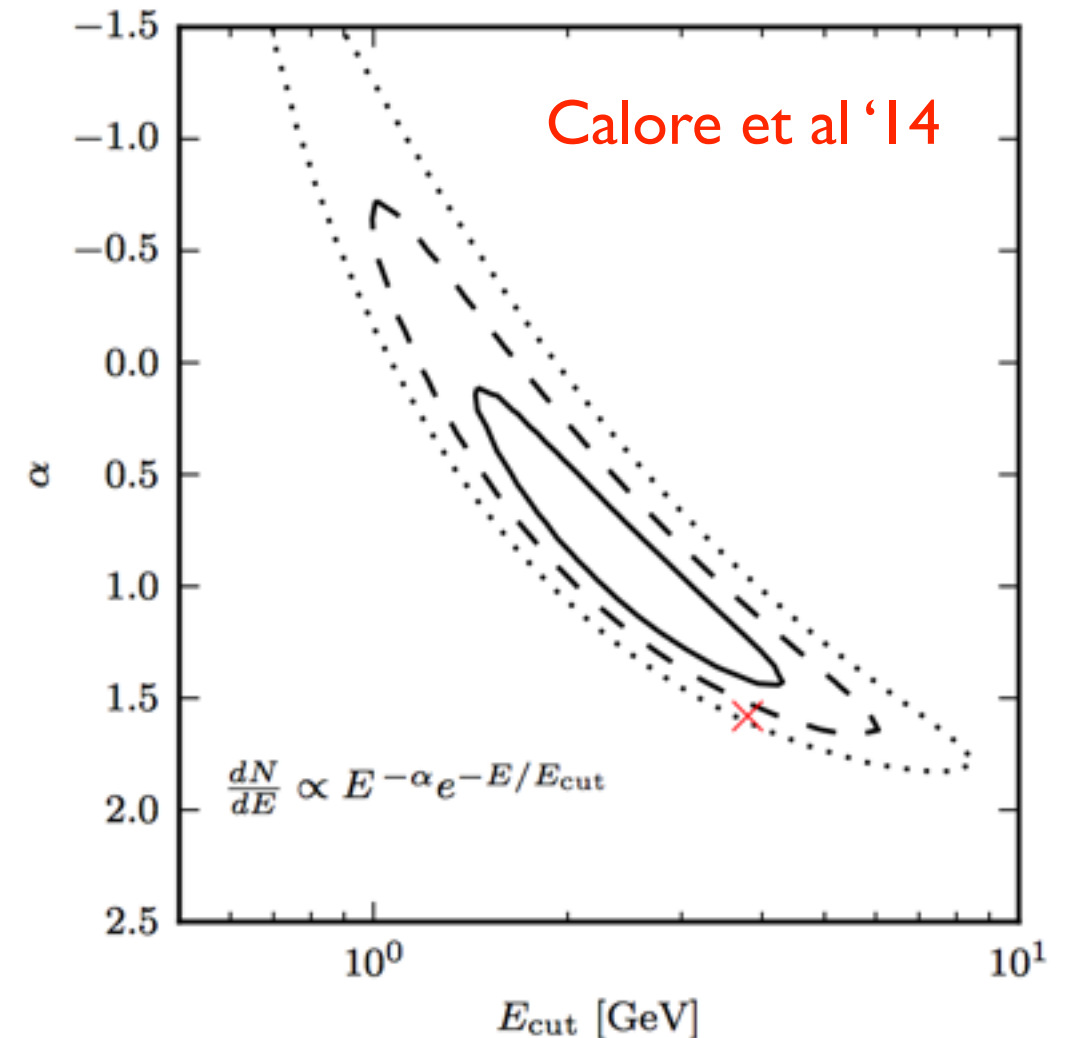
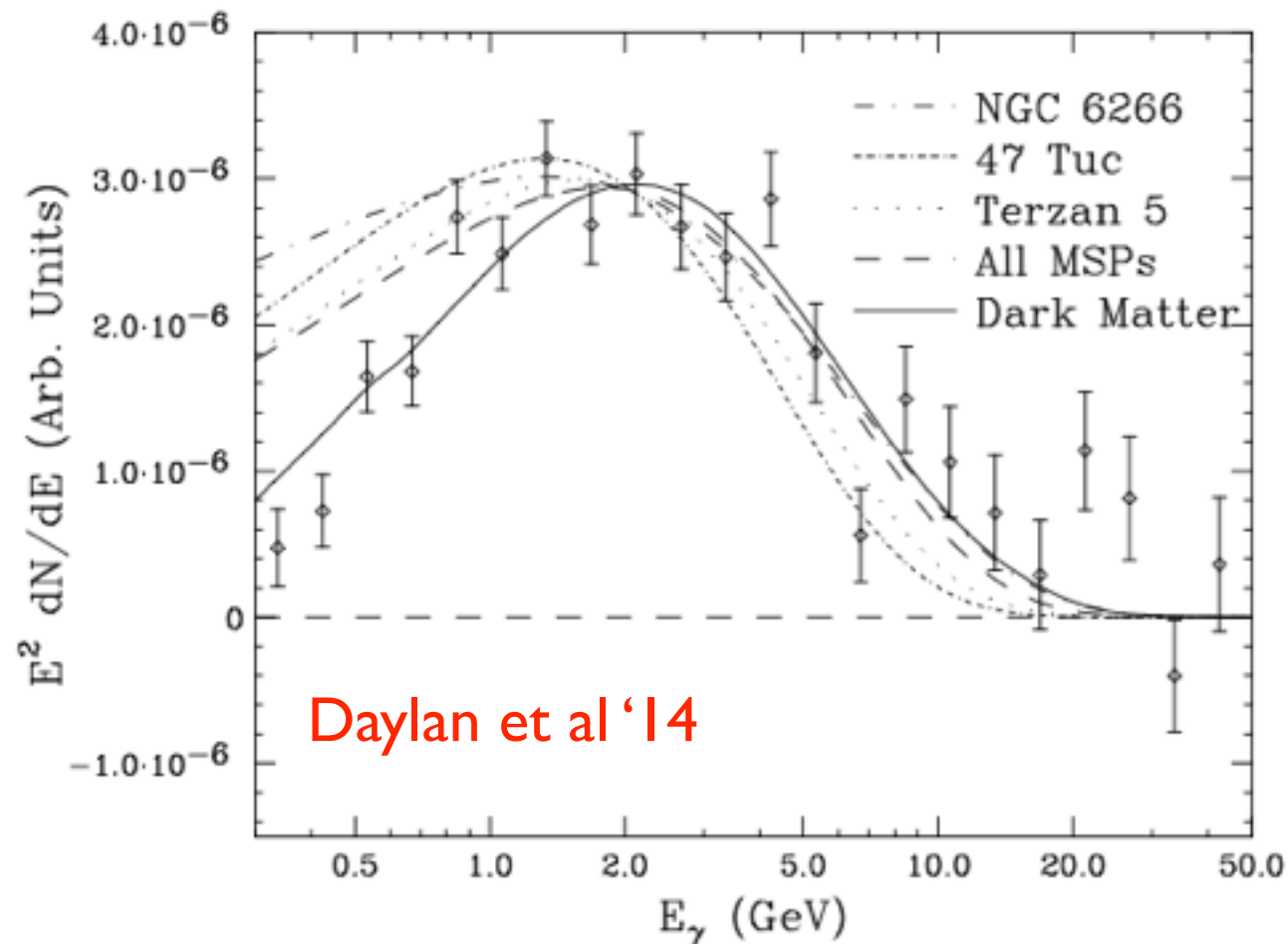
- Two sets of source distributions (“pulsars” and “OB stars”). “Tuned index” models allow spectral indices of background to vary (rather than just intensity), provide better agreement with data.
- Spectrum of excess seems broadly consistent with other results (lower at  $\sim 1$  GeV); tuned-intensity models lead to higher “signal” tails at large  $E$ , but are known to generically undersubtract data at high energies.



Talk presented by Simona Murgia at Fermi Symposium

# The pulsar interpretation for the GeV excess

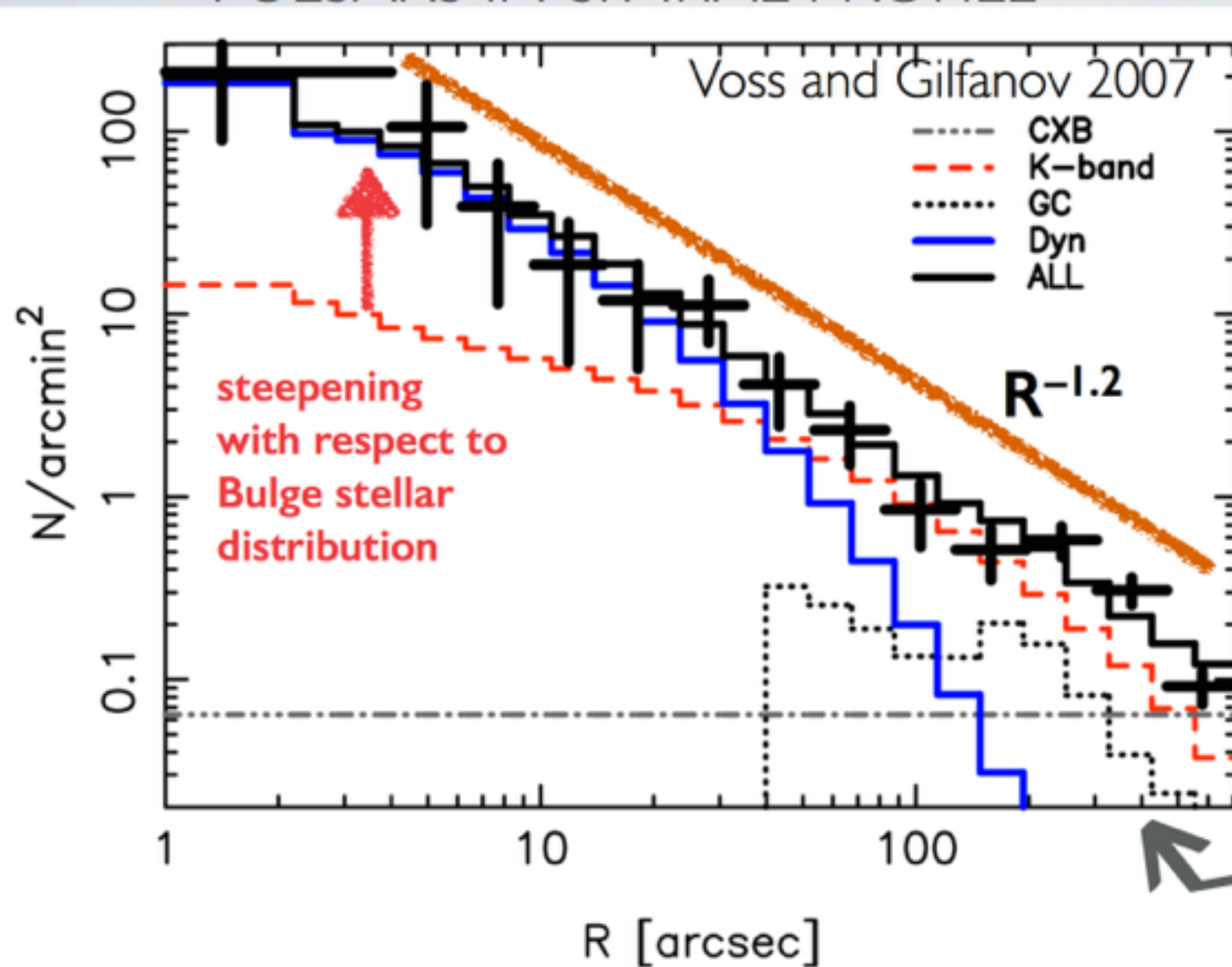
# The pulsar spectrum



- Millisecond pulsars (MSPs) have an (observed) spectral cutoff at approximately the correct energy ( $\sim 5$ - $10$  GeV).
- Low-energy spectrum of MSPs seems somewhat softer than signal (marginally compatible given CCW estimates on systematic uncertainties).
- Abundance estimates seem to predict fewer MSPs than required (e.g. 1305.0830, 1407.5625).

# Spatial distribution of MSPs

DEGENERACY WITH MILLI-SECOND PULSARS IN SPATIAL PROFILE



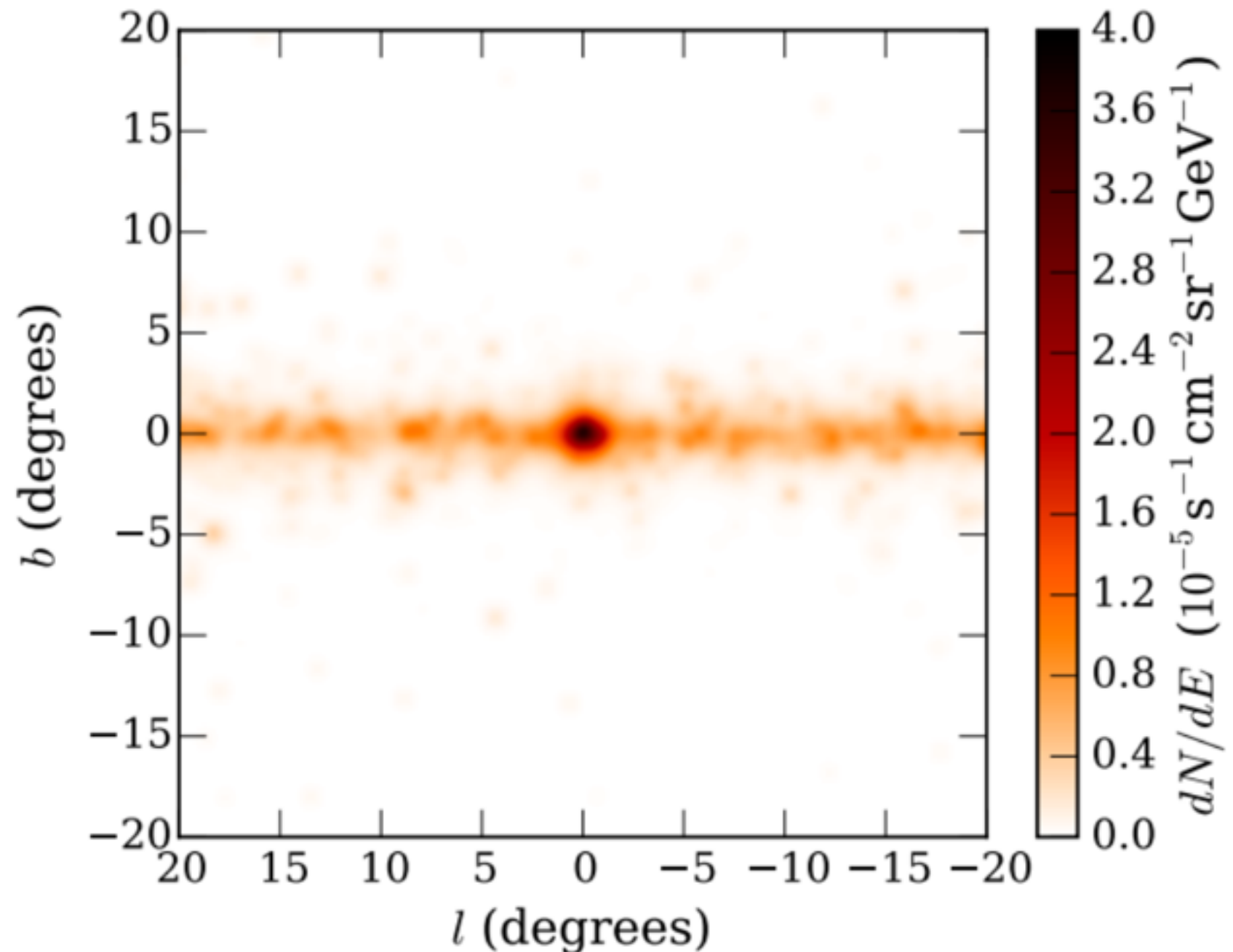
We make the reasonable assumption that Low-Mass X-ray Binaries have the same spatial distribution as MSPs

400'' towards M31 center = 1.5 kpc distance from center = 10 degrees towards MW center

Orange line is same as best-fit excess template ( $R^{-1.2}$  in projection implies  $r^{-2.2}$  de-projected)!

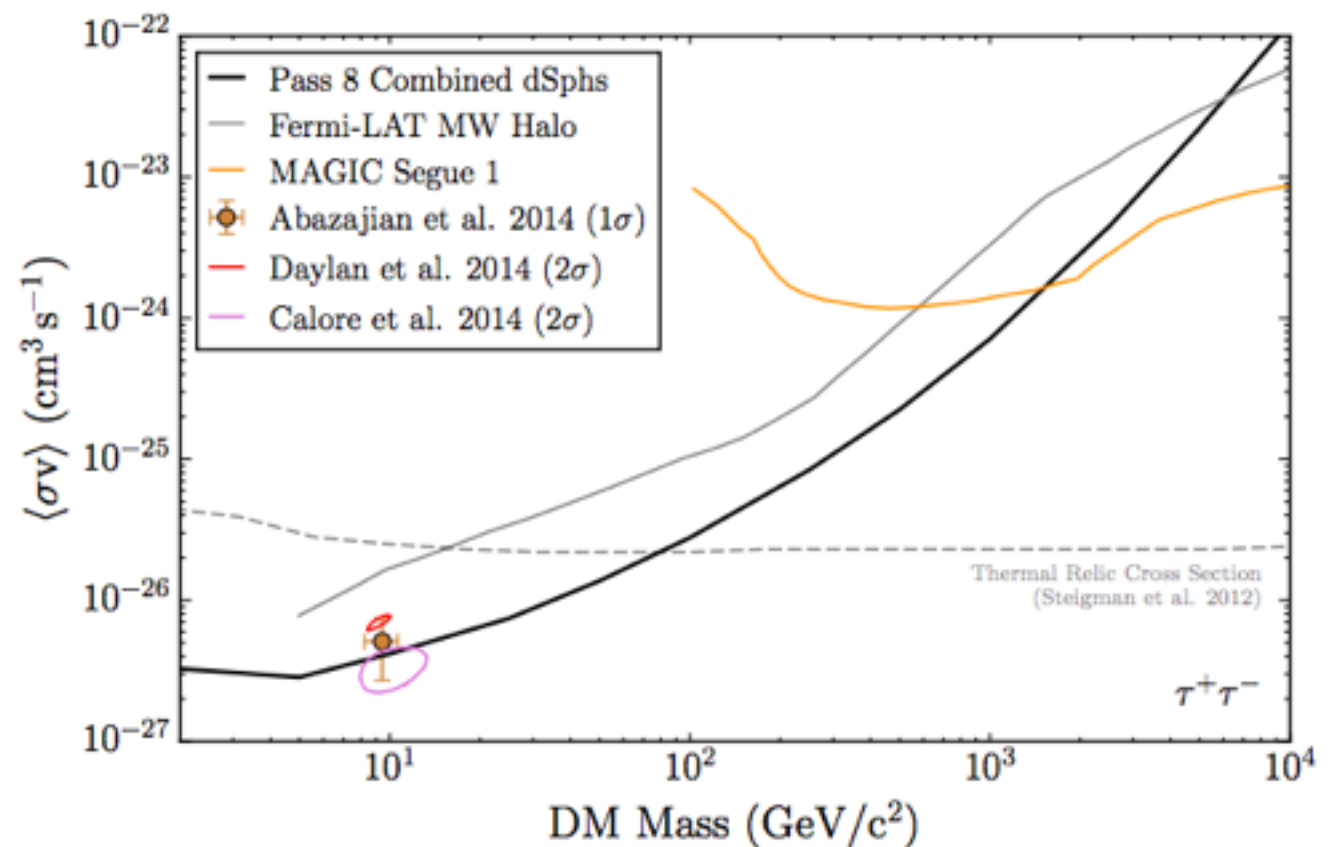
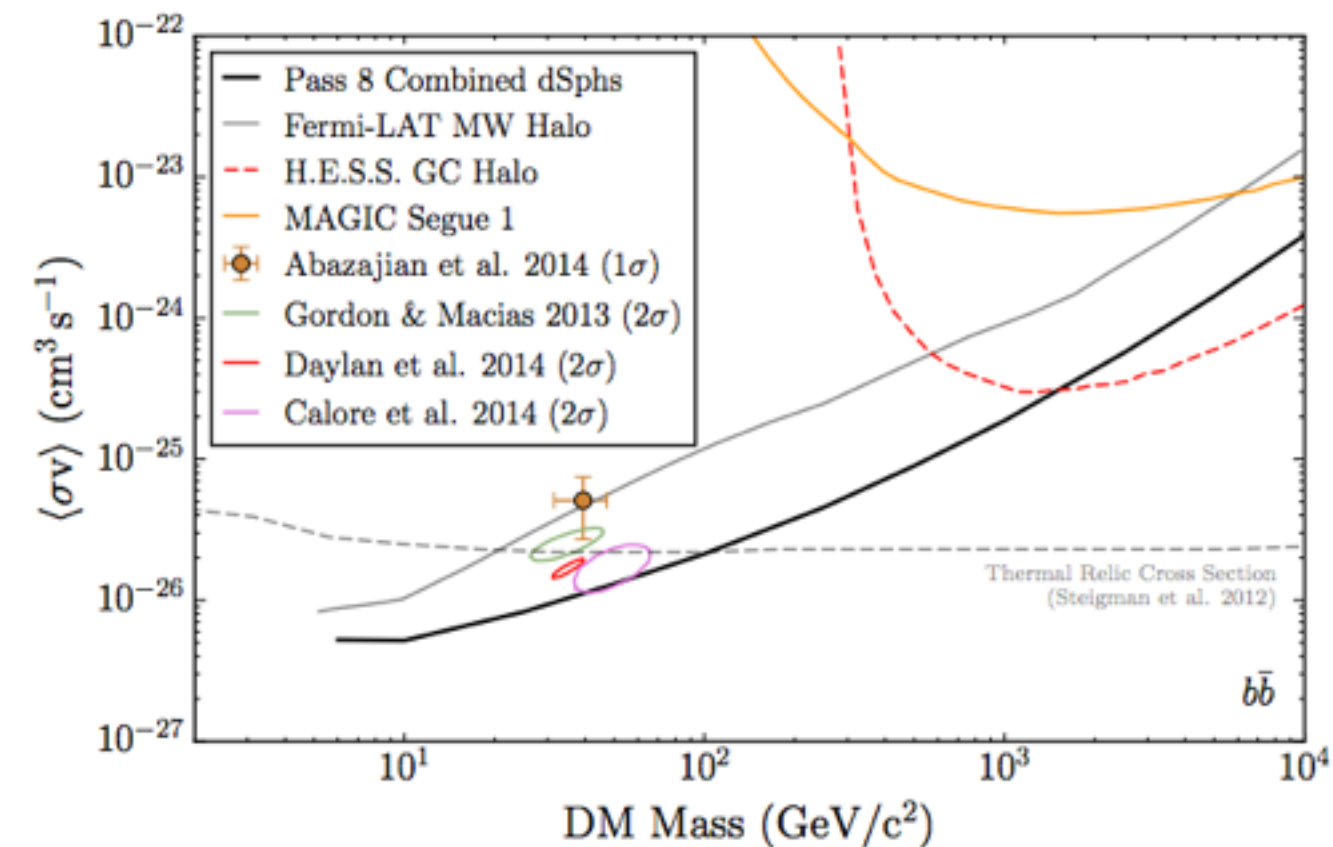
# Sphericity?

- Study of young pulsars by O'Leary, Kistler, Kerr and Dexter 1504.02477 - claims to reproduce morphology of excess.
- However, only angle-averaged profile is shown, sphericity is not tested explicitly.
- By eye, morphology appears much more disk-like than spherical, and disk pulsars are said to dominate outside inner few degrees.
- As found in earlier studies and confirmed in our current analysis, excess is absorbed by spherical population rather than a thick disk.



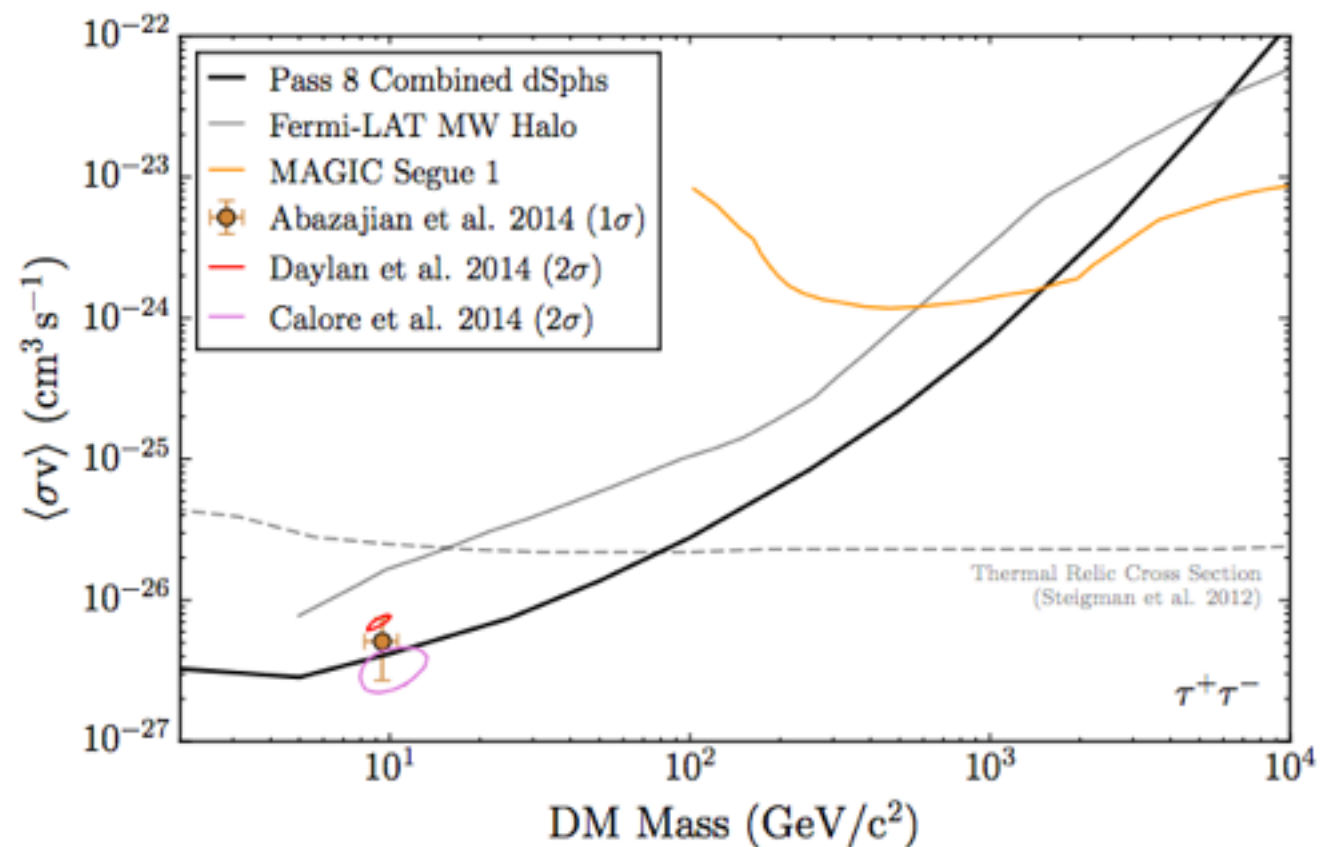
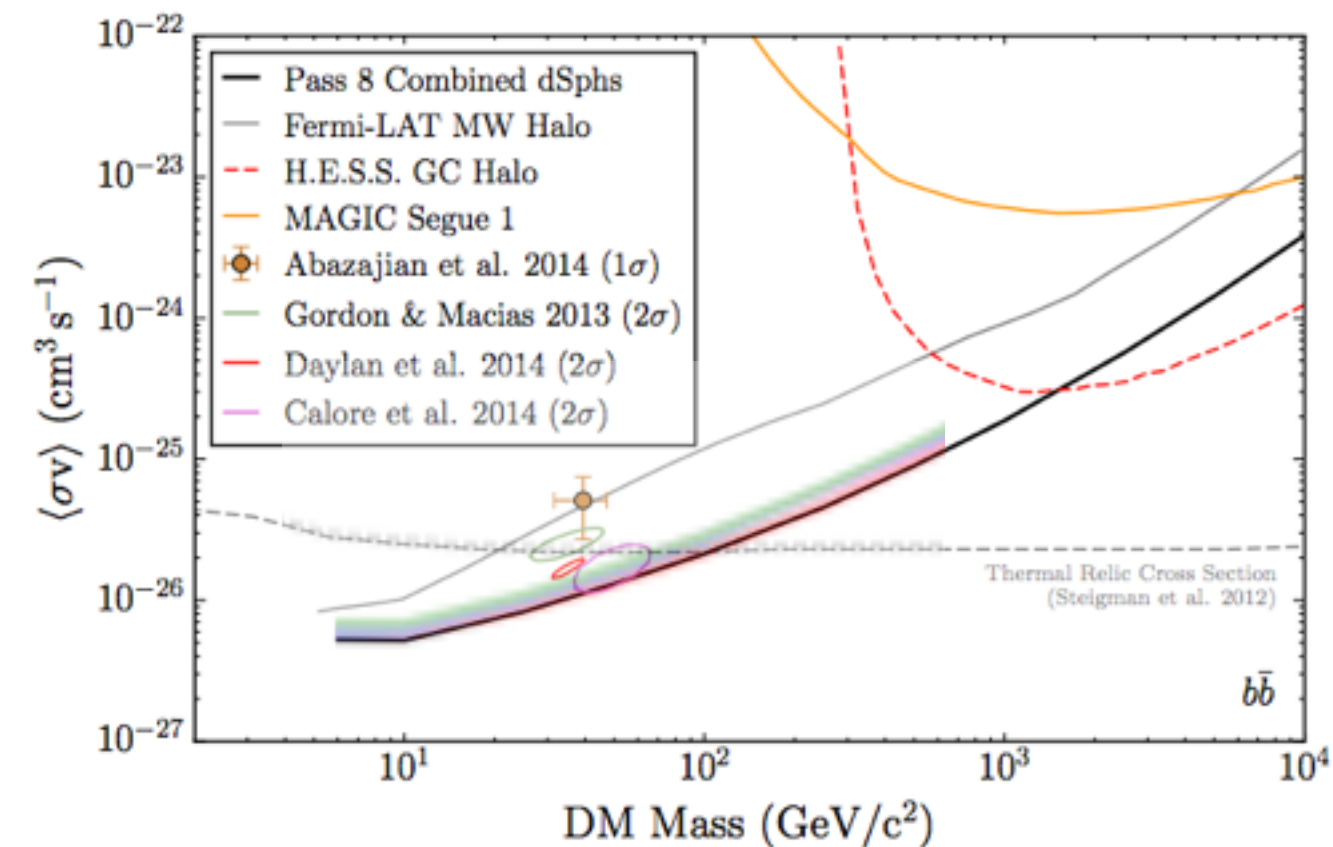
# Indirect constraints on the GeV excess

# Dwarf galaxies



- Dwarf galaxies: DM-dominated systems, provide a clean independent test of DM-annihilation hypothesis.
- Currently provide best current limits on sub-TeV DM annihilating through most channels (Fermi Collaboration, 1503.02641).

# Dwarf galaxies



- Dwarf galaxies: DM-dominated systems, provide a clean independent test of DM-annihilation hypothesis.
- Currently provide best current limits on sub-TeV DM annihilating through most channels (Fermi Collaboration, 1503.02641).

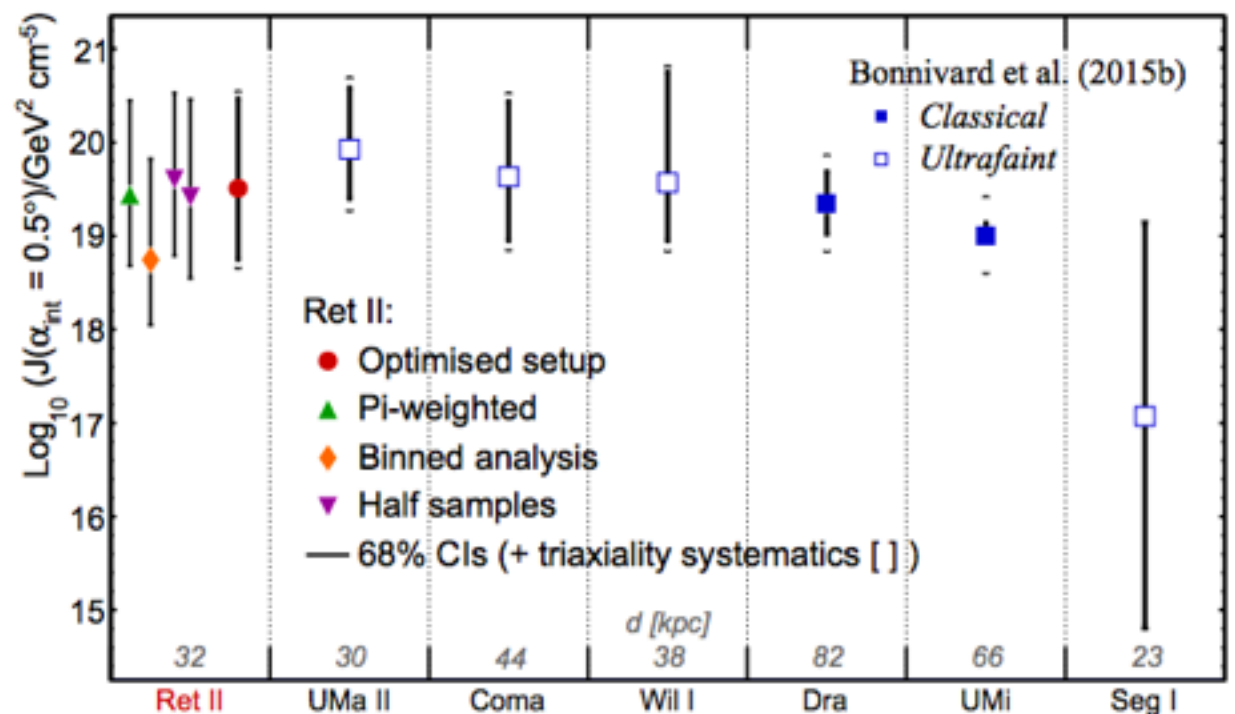
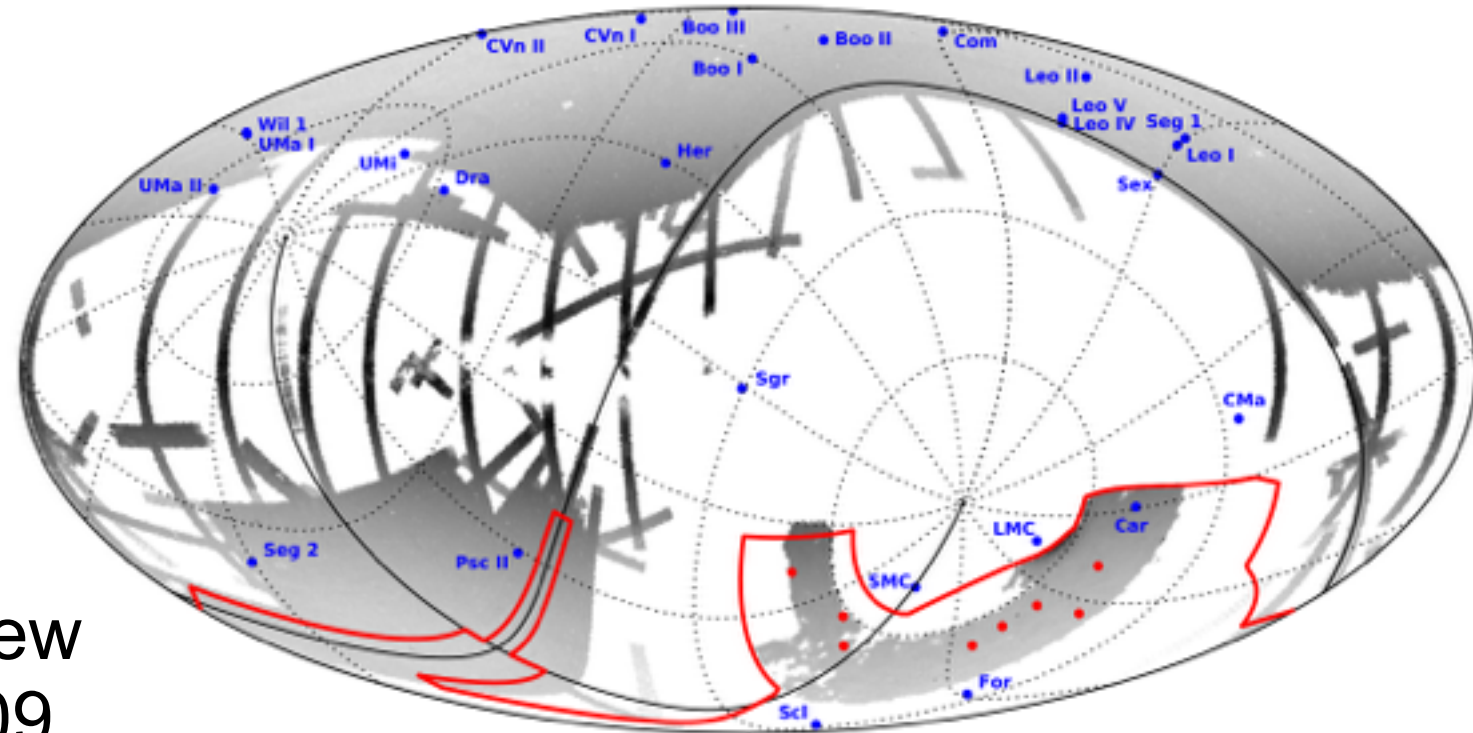
# DES discovers new dwarf galaxies

- Discovery of 8-9 new dwarf candidates in DES data in March (1503.02079, 1503.02584).

- More recently, kinematic studies were made of the DM content of “Reticulum II”, the closest of the new dwarfs (Bonnivard et al 1504.03309, Simon et al 1504.02889).

- Want to estimate “J-factor”, figure of merit for DM annihilation.

- Results are consistent within the (large) error bars, but Simon et al prefer a somewhat smaller value.





# Reticulum II

- Recently discovered in DES data, ~30 kpc away. A gamma-ray excess is consistently seen, in the 2-10 GeV energy range.
- Significance debated, various groups find 2.2-3.7 $\sigma$  local significance depending on background modeling. (See talk by K. Bechtol for detailed discussion.)
- Global significance depends on J-factors for dwarves, and whether one scans over DM mass + annihilation channel.
- Within uncertainties, consistent with Galactic Center excess - but uncertainties are large.

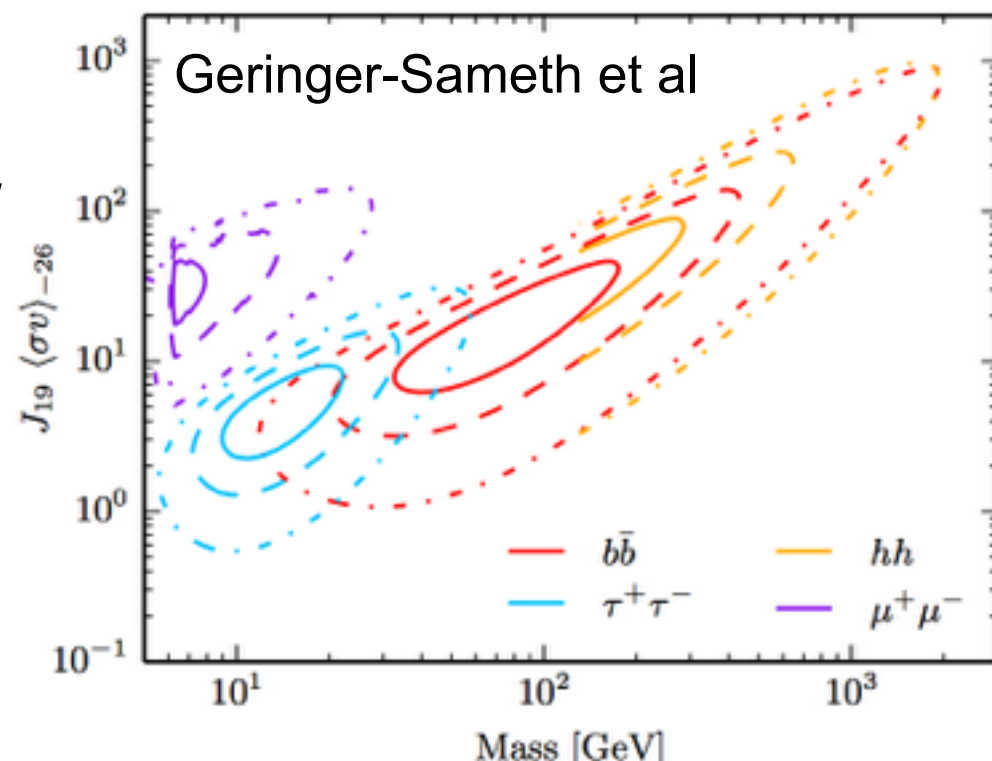
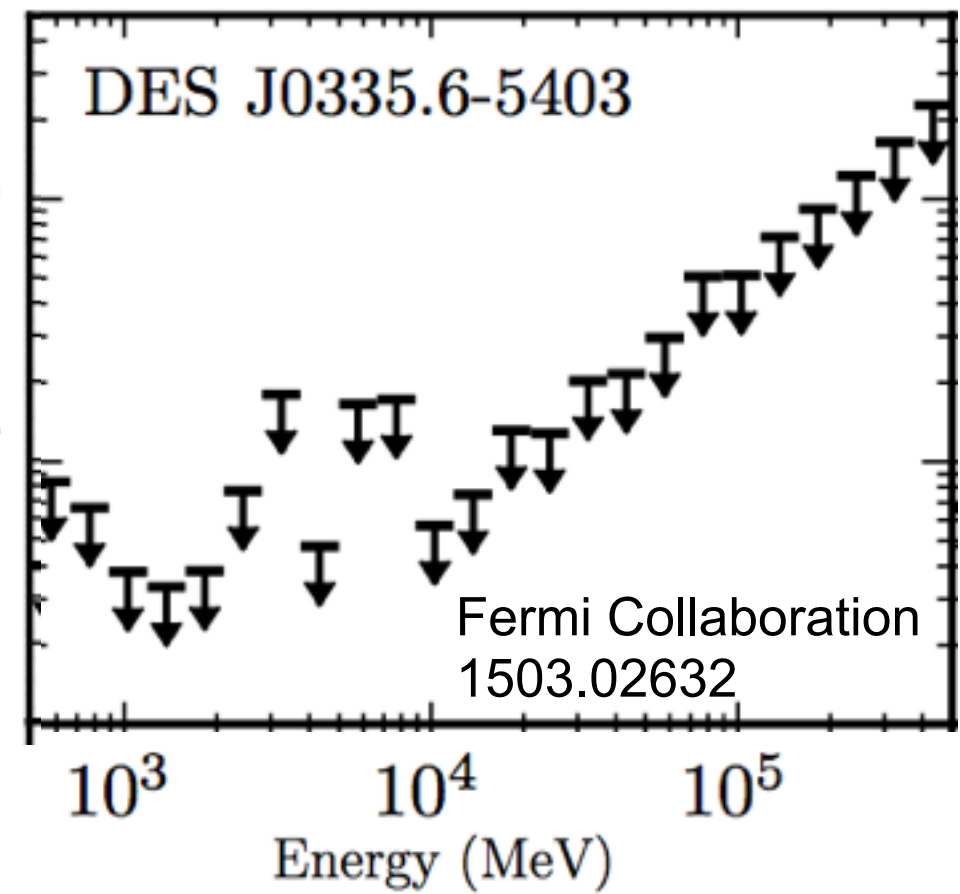
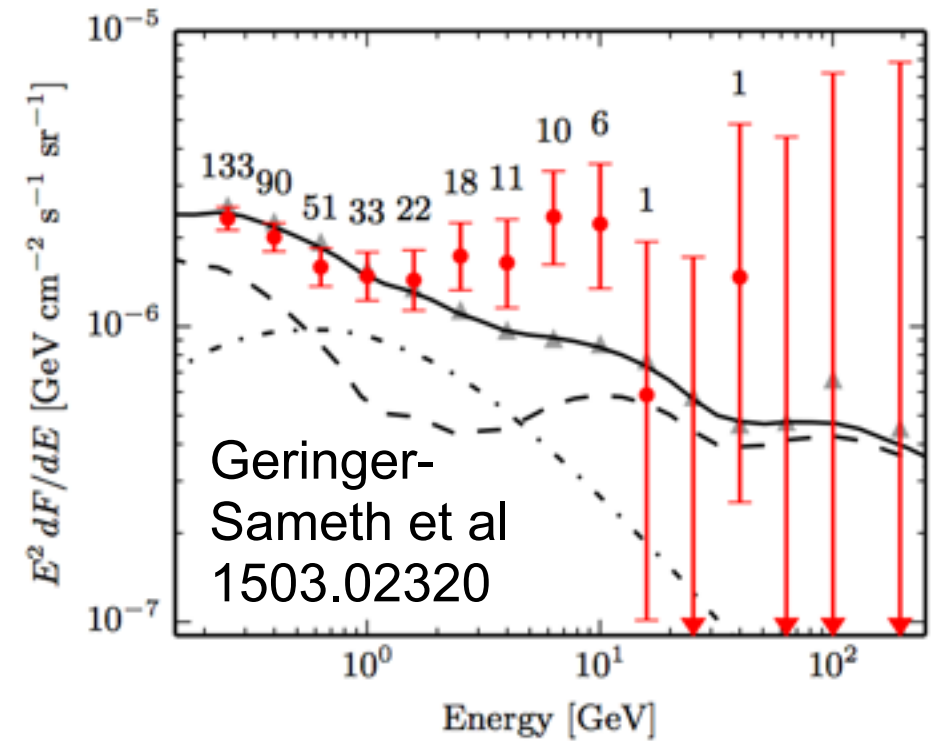


Figure takes a J-factor of  $10^{19.5} \text{ GeV}^2/\text{cm}^5$  as found by 1504.03309\*.

\*Note however that this value has a 1-order-of-magnitude error bar.

# Reticulum II

- Recently discovered in DES data, ~30 kpc away. A gamma-ray excess is consistently seen, in the 2-10 GeV energy range.
- Significance debated, various groups find 2.2-3.7 $\sigma$  local significance depending on background modeling. (See talk by K. Bechtol for detailed discussion.)
- Global significance depends on J-factors for dwarves, and whether one scans over DM mass + annihilation channel.
- Within uncertainties, consistent with Galactic Center excess - but uncertainties are large.

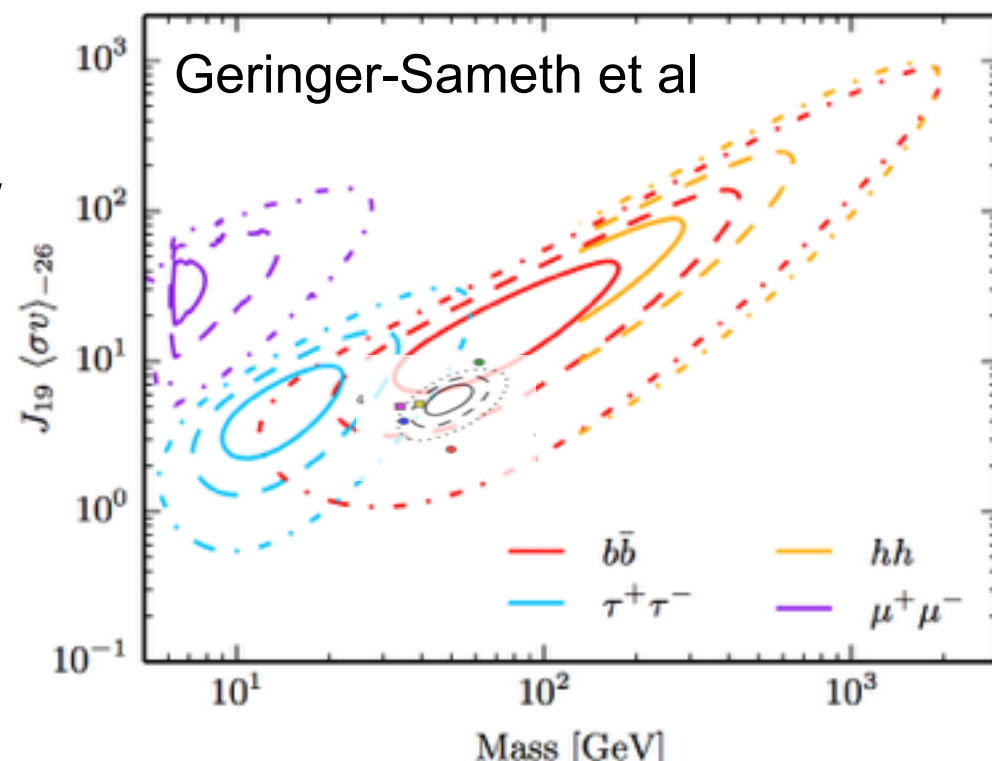
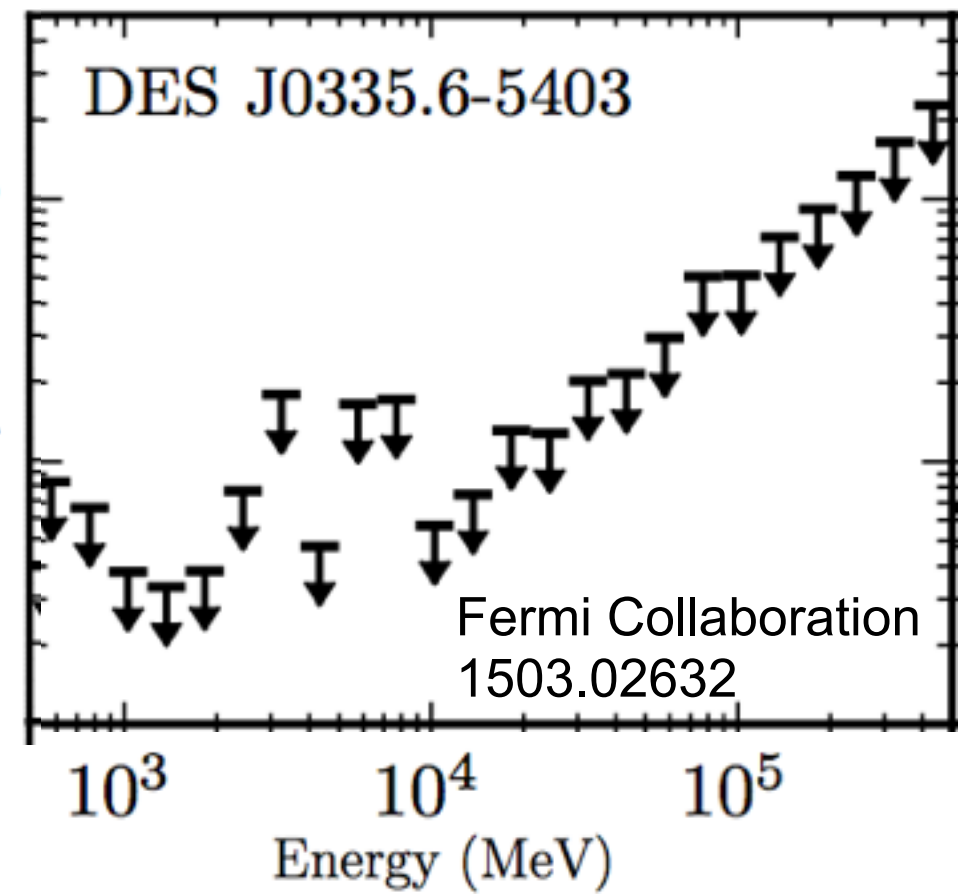
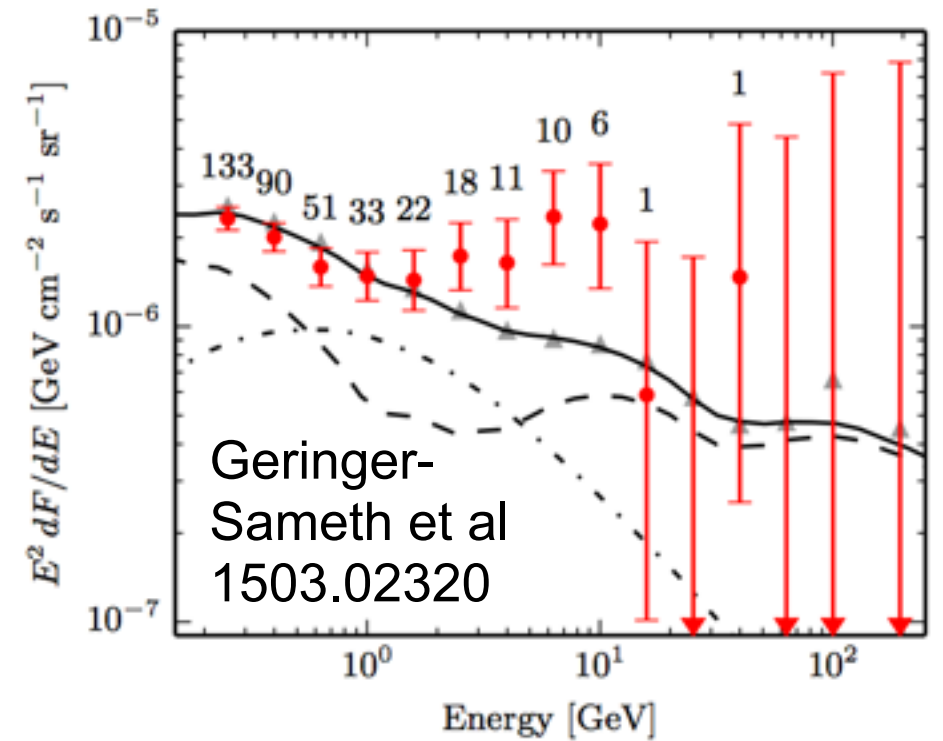
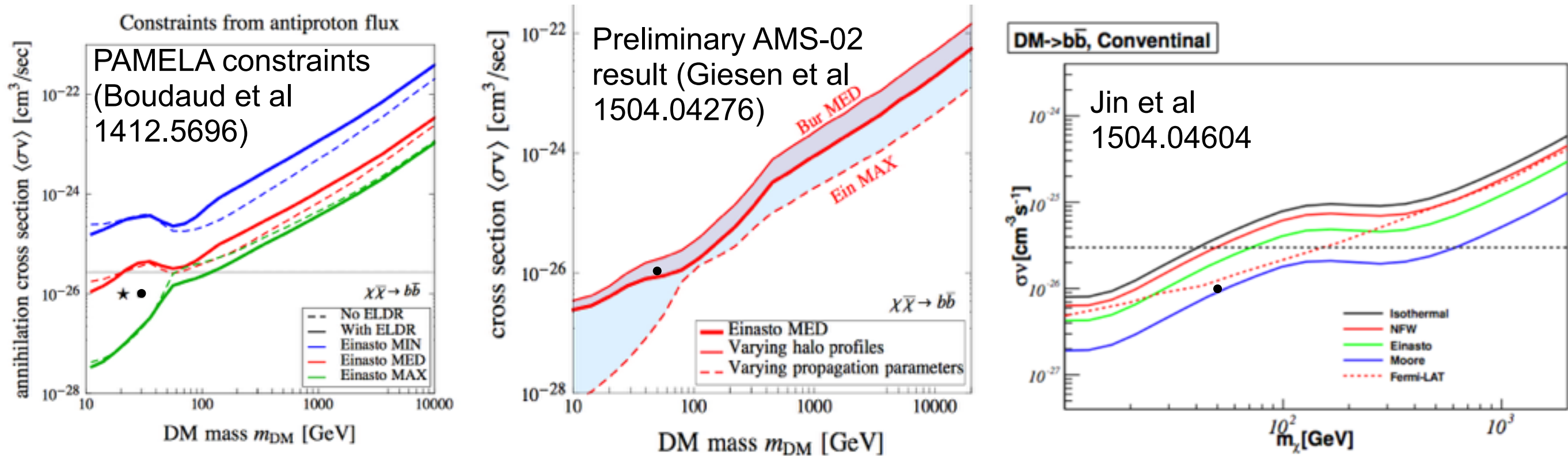


Figure takes a J-factor of  $10^{19.5} \text{ GeV}^2/\text{cm}^5$  as found by 1504.03309\*.

\*Note however that this value has a 1-order-of-magnitude error bar.

# Constraining light dark matter with AMS-02



- Precision antiproton measurements give the hope of sensitivity to DM annihilating into hadronic channels.
- Large systematic uncertainties due to complex propagation effects (e.g. solar modulation, energy loss from tertiary particles, diffusive reacceleration). Incorporating all AMS-02 data may help constrain propagation models.
- Current estimates constrain thermal relic DM annihilating to b quarks below (very roughly)  $\sim 30$ -200 GeV, depending on DM density profile and propagation model.
- Also stringent limits from positron data on light DM annihilating to leptonic channels.